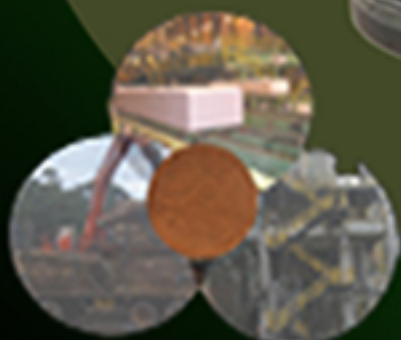# Synthesis of polyols of different lignocellulosic residues to obtain greener products

Silvia Helena Fuentes da Silva

Universidad
del País Vasco

Euskal Herriko
Unibertsitatea

Synthesis of polyols of different lignocellulosic residues to obtain greener products

Doctoral thesis presented by
SILVIA HELENA FUENTES DA SILVA

In fulfillment to the Requirements for the
Degree of Doctor of Philosophy in Renewable Materials Engineering by
the University of the Basque Country UPV/EHU

Under the supervision of
Dr. Jalel Labidi

Chemical and Environmental Engineering Department
Faculty of Engineering of Gipuzkoa

Donostia - San Sebastián, 2019

Acknowledgment

I would like to thank my director, Dr. Jalel Labidi, for giving me the opportunity to carry out my PhD studies under his supervision and to have been part of his research group.

In addition, I would like to thank the working group on the Biorefinery Process and all those who have contributed in some way to my work during this period. In particular, I would like to thank Itziar for all her help from the outset, Rene, who always believed in me and encouraged me in difficult times, my angel of computing Asier, as well as like Oihana, Eduardo and Pedro. And a special thanks to my friend Patricia, who has always encouraged me to do my doctorate in this wonderful group.

I can not forget to thank Dr. Tomasz Krystofiak who kindly received me at Poznan University of Life Sciences, Poznan/Poland for a Short Term Scientific Mission (Cost Action FP1407).

I would also like to thank my husband for listening my doubts and anxieties and comfort me in difficult times and for having made the cover of my thesis. My son for his love and understanding. And my mother, for her love, trust and complicity. You are my "safe harbour". Finally, thanks to my cousin Junior and my godfather Cesar for all the support to my mother.

PREFACE

This thesis aims to contribute to the production of greener products through the revaluation of lignocellulosic residues. In this sense, these residues were converted to polyol, that is, a liquid rich in hydroxyl groups, which makes it extremely reactive. Thus, Kraft lignin, almonds shells, sugarcane bagasse, pecan shells, pine sawdust and oak sawdust were chosen as the raw material for the production of polyol.

The reaction conditions of the liquefied products were optimized for a higher yield with good properties. In addition, some organic acids were evaluated as a lignin precipitating agent and as a liquefaction catalyst.

The optimized polyol were used as partial substitute to phenol in formulations of resol resins and assessed as wood adhesive.

To achieve these goals the following specific objectives have been established:

- Characterization of the different lignocellulosic residues;

- Development of an experimental design for polyols;

- Characterization of the obtained polyols;

- Determination of optimum conditions for polyols;

- Production of optimized polyols;

- Characterization of the optimized polyol;

- Development of an experimental design for resol resins;

- Characterization of the obtained resins;

- Determination of optimum conditions for resins;

- Production of optimized resins;

- Characterization of the resins;

- Evaluation of the resins as wood adhesive;

This research is described throughout five chapters, which are summarized as follows.

Chapter 1 gives a brief background about the need to change to a biomass-based economy, the role biorefinery in this context and lignocellulosic biomass as well as its thermochemical conversion with special approach to the liquefaction with polyhydric alcohols.

Chapter 2 focused on the liquefaction of Kraft lignin. Throughout this chapter, lignin has been extensively characterized and thermal converted. The liquefied lignin was investigated using two different heat sources under reflux and under microwave, in addition, the optimal conditions were determined. Thereafter, a comparison between the two techniques was described.

Chapter 3 was dedicated to the production of polyols from some lignocellulosic residues under optimal conditions. After the characterization of agricultural and forest wastes, the optimized polyols were discussed in two parts. One on the liquefaction of lignin and the other on liquefied agroforestry wastes.

At first, the influence of organic acids as a precipitating agent (compared to sulfuric acid) and the liquefaction catalyst on the properties of the polyols was investigated. In the second part, the influence of the liquefied agricultural and forest residue was studied.

Chapter 4 was devoted to the synthesis of resol resins using the obtained polyols to replace part of the phenol. However, initially, an experimental design was carried out with the objective of determining the optimal reaction conditions for the resin. Under optimum conditions, the resins were synthesized and characterized. Then,

the resins using 60% liquefied Kraft lignin or liquefied pine sawdust were studied as wood adhesive and the mechanical properties of the produced plywood were evaluated.

Chapter 5 finally describes the general conclusions about the results obtained throughout this thesis. Moreover, some lines of research are proposed for future work.

Contents

Chapter **1**

Introduction

1.1   Background

During the last decades, the world population has been growing rapidly, with the global growth rate around 2% per year, reaching 7 billion people in 2011[1]. In consequence, the consumption of commodities (energy, gas, coal, wood and chemicals) and the demand of synthetic polymers (resins, paints and varnishes, plastics, fertilizer, detergents and clothes) has also been growing, not only to meet the needs, but also to provide more comfortable life. The commodity services and synthetic polymers are often based on fossil resource, and this dependence is reflecting on the world economy, which is mainly based on petrochemical resources. It is known that the extraction process, the pathway of synthesis and transport involving fossil resources are usually very expensive and in some cases, could result toxic and dangerous to health and pollutes the environment. It is the case of the diesel engine exhaust which is an environmental polluter and on 12th of June (2012) was classified as carcinogenic to humans (Group 1) by WHO[2] during the International Agency for Research on Cancer - IARC in Lyon/France. Thus, concerns about climate change and global warming are often related to the side effects of the petrochemical process.

At the end of the 1990s, the Kyoto Protocol was created with the aim of reducing the emission of gases, mainly by developed countries, to minimize the global warming. This international treaty came into force after ratification by member countries in 2005. Spain and Brazil ratified on April 11th and August 23th of 2002, respectively.[3][4] According to these sources, both Spain and Brazil are committed to the Kyoto Protocol guidelines until 2020 with the ratification of the Doha Amendment. Another international conference held to reaffirm countries' commitment to environmental aspects and how to achieve those goals was the United Nations Conference on Sustainable Development, Rio+20, celebrated in June 2012 in Brazil. In this event,
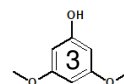
a series of measures were adopted "with the potential to contribute to a more equitable, cleaner, greener and more prosperous world - recognizing the important linkages between health and development".[5]

These actions, among others, have demonstrated a gradual governmental and social awareness about the global climate, which, coupled with oil price fluctuations, have encouraged the researchers to seek alternatives that would minimize these effects.

In this sense, lignocellulosic materials have been widely investigated as an alternative option to replace fuels and chemicals based on fossil resources.

The lignocellulosic material is a renewable resource, mainly made up of cellulose, hemicellulose, and lignin, which have different chemical functionalities (see section 1.3). Therefore, this raw material presents huge opportunities to be used in several applications. Furthermore, it is widely available in nature, as well as industrial, agricultural and forestry waste, that increases daily in a proportion higher than population growth. These residues, are generally generated in large quantities, causing serious space problems and sometimes concerns about environmental pollution. Besides that, these residues can increase the production costs because must be treated as a waste before disposal.

With regard to industrial waste, it can be mentioned the pulp and paper industry that generates millions of tons of black liquor as waste from pulp and paper production. The black liquor is burned in the boiler to recover the chemicals and to provide energy for the mill. However, this liquor contains dissolved lignin, which can be recovered and converted into valuable products such as polyol.

The sawmill is another important segment of the woody forest sector, where wood is dismembered producing a large amount of
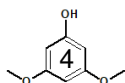
wood waste in the form of sawdust, bark, or wood shaving, which can be valued through thermal conversion.

In terms of agricultural residues, nut crops, such as almond and pecan, are one of the most harvested in the world and generate a large amount of shells as residue, which can be used to produce added value products.

Sugarcane is another crop of the agricultural segment that is mainly exploited for the production of sugar and bioethanol. Thus, sugar cane bagasse is the main waste generated in these two processes. It is used for power generation from distilleries and mills, however it can be used as value product.

The great advantage of using these kind of wastes is that they do not form part of human diet, are available in large quantities and are renewable source. In addition, these residues can add value to its production chains.

1.2   Biorefinery

As consequence of some events that took place over the last few years, as the instability of the oil price that resulted in a recession 1990s, the energy crisis in the 2000s, speculation about the decline in oil reserves and a growing concern about the emission of greenhouse gases boosted the emergence of the biorefinery concept. Among the definitions, very similar to each other, the IEA Bioenergy Task 42[6] defines biorefinery as "sustainable processing of biomass into a spectrum of biobased products (chemicals, materials, human food and animal feed) and bioenergy (fuels, power and/or heat)".[7] Since then, numerous scientific, governmental and social efforts have been made to have a more environmentally friendly world and to impulse more sustainable development, that is, development
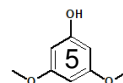
that meets the needs of the present without compromising the ability of future generations to meet their own needs.

In 1975, Brazil started the Pro-alcohol Program, which had as goal to ensure the energy supply, in addition to boosting the sugar industry through the diversification of production. At that time, distilleries were built, with government incentives, to process the excess production of sugarcane and transform it into anhydrous ethanol to be incorporated, without any modification, as an additive (24%) in the gasoline to be used in the engines of the vehicles.[8] In 2002, Brazil launched the first flex-fuel vehicle to encourage the resumption of bioethanol production after some problems and discredit of the Pro-alcohol Program. Today, more than 92% of the national fleet of cars has a flex engine. Throughout that time, environmental development was possible, mitigating more than 480 million tons of CO_2, promoting millions of jobs in the countryside and cities. In addition, the country has one of the world's cleanest energy matrices, being an international benchmark in sustainability.[9]

European Bioeconomy Strategy 2012[10], is one of the recent efforts at the governmental level towards an environmentally friendly and sustainable economy. In this strategy and its action plans Europe intends "strengthening the connection between economy, society and the environment" improving the bioeconomy, unlocking new potentials resources and ensuring food security. The bioeconomy accounting 8.2% of the European Union workforce and, turnover is expected to increase from €2.09 billion in 2008 to €2.29 billion in 2015.[10][11] According to Bio-based Industries Consortium[12] there were 224 biorefineries throughout Europe, most of them were "first-generation" facilities producing mainly bioethanol, but also products to be used in food or feed or biochemicals, and only 43 are so-called "second-generation" facilities. However, as mentioned above, the European Union has been encouraging the growth of new biorefiner-

ies using non-food and non-energy crops and bio-waste to produce biofuels, electricity, heat, bio-based chemicals and biomaterials.
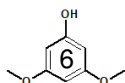
Analogous to the refinery, the biomass can be separated into small fragments and, from these fractions valuable goods as fuel, polymers, chemicals and gas can be obtained in a biorefinery (Fig. 1.1). However, a biorefinery can provide more classes of products because the input feedstocks is widely diversified compared to the conventional refineries. This represents many possibilities to use a great variety of renewable raw materials as an alternative to replace fossil resources. However, the implementation of biorefineries is challenging and require to overcome some difficulties, such as the development and/or adaptation of technologies and equipment required to process the heterogeneous constitution of the lignocellulosic material.[13] In addition, aspects such as the input/output transport logistics and annual supply need to be taken into account.
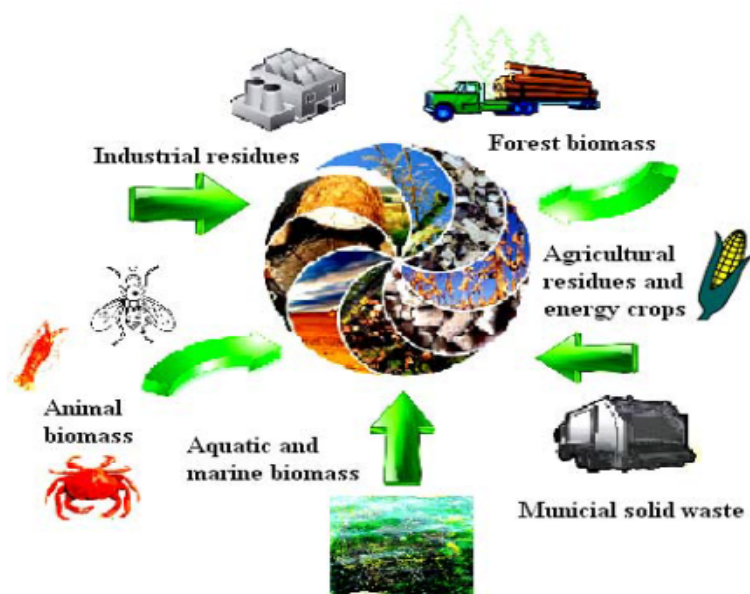

Fig. 1.1: Biomass sources in biorefinery process. Image courtesy of Itziar Egües
.

The basic parameters in a biorefinery are feedstock, platform,

7
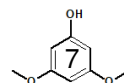
products, and process. Some process can be applied to more than one platform and it is possible to implement many routes in a biorefinery to obtain a wide range of products.[14] Depending on the applied technology biorefineries can treat different feedstocks and can be classified into three different generations.

► The first generation of biorefineries is characterized by the use of sugar, starch, animal fats or vegetable oil extracted from edible grains to produce mainly biofuels like bioethanol and biodiesel using conventional technologies.[13] Brazil is the second largest producer of bioethanol in the world after the United States (Fig. 1.2). Brazil is located in a privileged zone, between the tropical and subtropical strip of the planet, has great agricultural potential, infrastructure and demand for bioethanol. These factors probably make of Brazil the best region of the world to produce biofuels.[15] In 2017, the production was about 7060 million gallons[16] and will grow due to an increase for sugarcane production in the coming years (Table 1.1).[17] In addition, since 2014 the used of enzymatic technology, developed by Danish company Novozymes, to produce bioethanol second generation was introduced. This technology enables the production of cellulosic biofuels even more sustainable since it takes advantage of agricultural residues, straw, and sugarcane bagasse. The two commercial-scale plants, one in São Miguel dos Campos (AL) and another in Piracicaba (SP) belonging to Granbio and the Raízen Group, respectively, both have a capacity to produce together 182 million liters of 2G ethanol per year.[15]

► In second generation biorefinery, the raw material can be based on residues, non-edible crops, and side or waste streams from the production process, such as black liquor and sawdust.[19] This approach enables a wide variety of products, such as biofuels, polymer precursors and chemicals, to be produced in a single facility due to the possibility of combining process and platform like
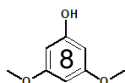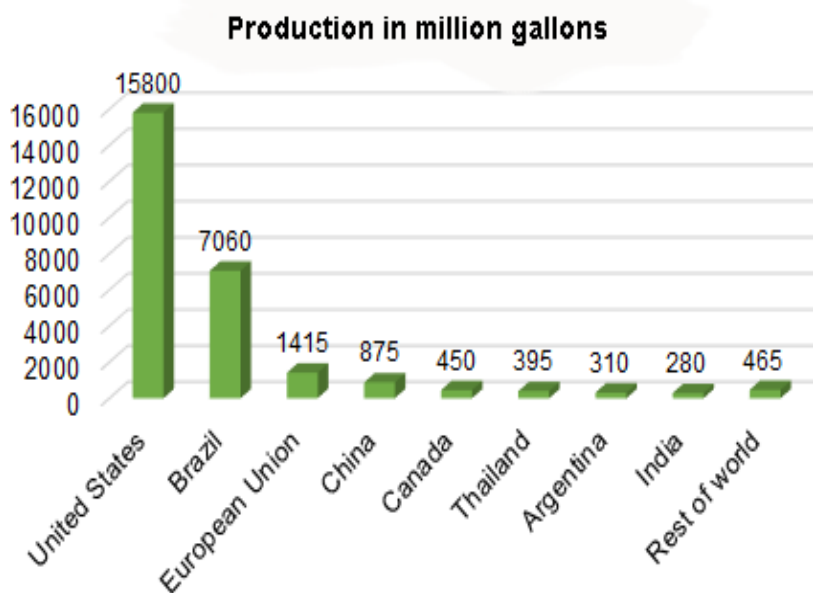
Fig. 1.2: Fuel ethanol production worldwide in 2017.[16]

biochemical and thermochemical and the variety of lignocellulosic material used.

The modern pulp mills based on the Kraft process, currently already operating in a biorefinery concept, producing electric and thermal energy through the use of industrial and forest residues that would be destined to landfills.[14] Nevertheless, due to declining printing and writing paper segment and market competitiveness, pulp mills are looking for alternatives in biorefinery approaches to improve the efficiency of their chain.[14][20] One of the bottlenecks of this segment is the black liquor which, although part is used to generate energy and steam for the plant.[21] In this context, Suzano Papel and Cellulose recently installed an industrial scale plant for lignin extraction in Limeira, SP/Brazil (the first in Latin America). The unit has a capacity to produce 20 thousand tons per year of various types of lignin with technology fully developed by Suzano.

▶ The third generation biorefineries, according to EIA,[7] produce biofuels from aquatic raw materials such as algae. In this case, the

9
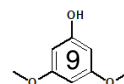
Table 1.1: Expansion of the Brazilian production of sugarcane and derivatives. [18]

		2005	2010	2030	2030
Sugarcane	Production (10^6 t)	431	518	849	1.140
	Occupied zone	5.6	6.7	10.6	13.9
Sugar (10^6 t)	Production	28.2	32.0	52.0	78.0
	Exportation	17.8	21-23	28-30	31.37
Ethanol (10^6 m^3)	Production	16.0	24.0	48.0	66.6
	Exportation	2.5	4.4	14.2	11.5
Biomass (10^6 t)	Bagasse	58	70	119	154
	Straw	60	73	119	160

production of biofuels generally depends on the lipid content of microalgae. [22]

1.3 Lignocellulosic biomass chemical composition

The lignocellulosic material is the most abundant natural renewable resource on Earth, with an estimated production of approximately 2 X 10^{11} tons per year, [23] that represents over 70% of the plant biomass. [24] Woody material, forestry residues, agricultural and industrial wastes, and grasses are examples of lignocellulosic biomass. Basically, these materials are built by structural compounds (cellulose, hemicellulose, and lignin, Fig. 1.3) and to a lesser extent by non-structural components such as ash and extractives that can alter its percentages depending on the botanical source, region, age and a set of environmental factors. [25]

Ash is the inorganic residue remaining after ignition of the biomass (between 525 - 850 °C) constituted by substances such as silicates, carbonates, sulfates, sodium, potassium, calcium or magnesium chlorides. On the other hand, the extractives are substances like fats,
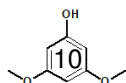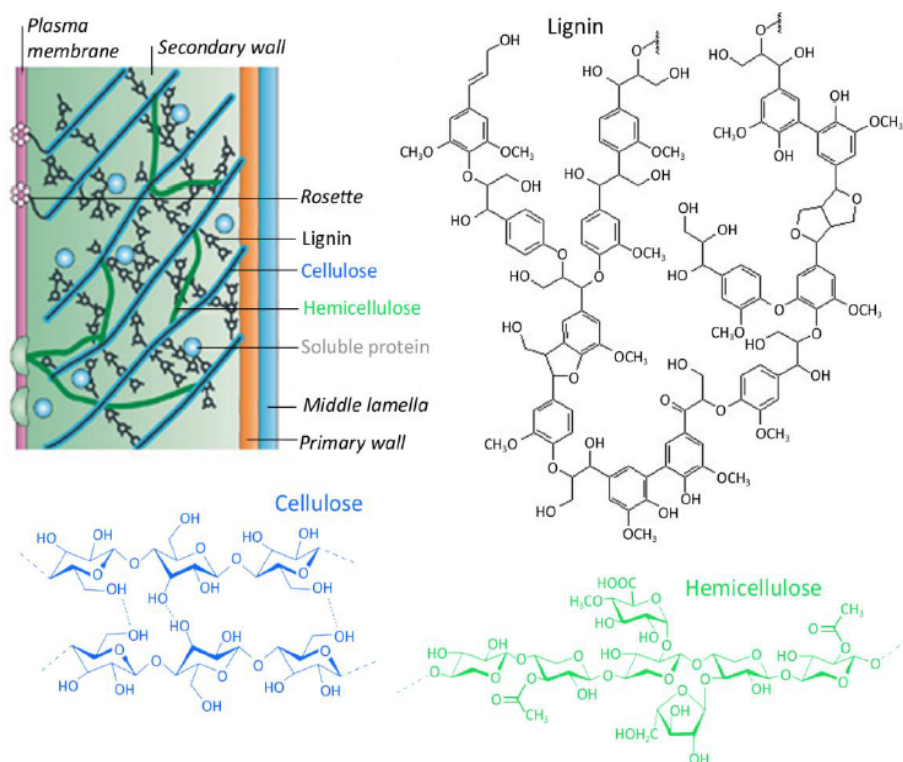
Fig. 1.3: Diagrammatic illustration of the framework of lignocellulose. - Structure and main constituents of lignocellulosic biomass (adapted from Menon[26]).

waxes, pectins, terpenes, aliphatic and aromatic acids, tannins and essential oils that can be easily removed from the biomass with water or solvents. These compounds do not contribute to the cell wall structure but are very important in the metabolism process, energy reserves and as a defense mechanism against the microbial attack of plants, besides influencing properties as color, odor, and resistance to decay.[27]

As mentioned, the chemical composition of the lignocellulosic material is highly variable in terms of the diversity and concentration of its compounds. Thus, when using this type of material, it is indispensable to know its chemical and physical composition, as this will interfere with the final properties of the product. The chemical composition of some lignocellulosic biomasses related in the literature

are summarized in Table 1.2. [18 28 29 30 31 32 33]

Table 1.2: Chemical composition of some lignocellulosic feedstocks.

Lignocellulosic material	Cellulose	Hemicellulose	Lignin
Eucalyptus	51 - 53	14 - 17	22 - 24
Hardwood	45 - 50	20 - 25	20 - 25
Pine	42 - 50	27 - 27	20
Softwood	35 - 40	25 - 30	27 - 30
Pecan shells	9 - 36	7 - 18	25 - 30
Sugar cane bagass	36 - 45	22 - 28	19 - 26

1.3.1   Cellulose

Cellulose is the majority constituent of cell-wall, comprising about 30 - 50% of the dry weight of the lignocellulosic biomass[34] as well as being present in other species such as marine animals, bacteria and fungi. This biopolymer is the most abundant available on the biosphere.[35 36] It consists of a long linear chain formed exclusively of cellobiose units, which are composed of two glucose molecules (*D*-glucose units) bound to each other by β-1,4-glycosidic bonds (Fig. 1.4). This network of highly developed hydrogen bonds results in a rigid structure of hard and stable regions that are partially crystalline.[37] This structure is incorporated into a matrix of hemicelluloses and lignin to form the cell-wall of the plant.

The worldwide production of the cellulose is estimated at more than 7.5 x 10^{10} tons per year, and since its discovery in 1838 by Anselme Payen, the cellulose has been extensively studied and applied industrially.[35] It is well known that cellulose is the basic building block for papermaking. Moreover, it is used to produce many textiles, biocomposites, and by-products such as cellophane, rayon, and cellulose acetate. The conversion of cellulose into useful commodity goods like cellulosic ethanol, lactic acid, ferulic acid and dif-
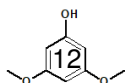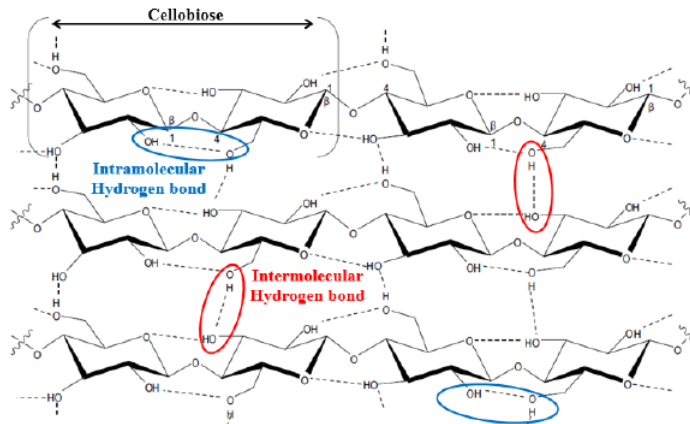
Fig. 1.4: Chemical structure of cellulose.

ferent types of cellulose derivative is another highly explored area and more recently, the use of nanocellulose has been extensively researched

1.3.2   Hemicellulose

On the other hand, hemicelluloses have a branched and amorphous structure built up of heterogeneous monosaccharides. The principal sugar components are pentose (*D*-xylose and *L*-arabinose), hexose (*D*-glucose, *D*-galactose, *D*-mannose and *L*-rhamnose) and uronic acid units such as *D*-galacturonic acid and *D*-glucuronic acid. Hemicelluloses are the second most abundant polysaccharides in nature and are found in the primary and secondary cell walls. They act as a kind of surface active intermediate between cellulose and lignin polymers to form a matrix in the cell wall of the plant.[38]

Hemicelluloses can be easier to break down with alkali chemicals and/or heat and are of lower molecular weight (degree of polymerization around 100-200) than cellulose polymers.[39] The amount of hemicellulose in the wood (% by dry weight) is usually between 23 and 32%,[40] however, its composition differs considerably depending

13

on the lignocellulosic source.
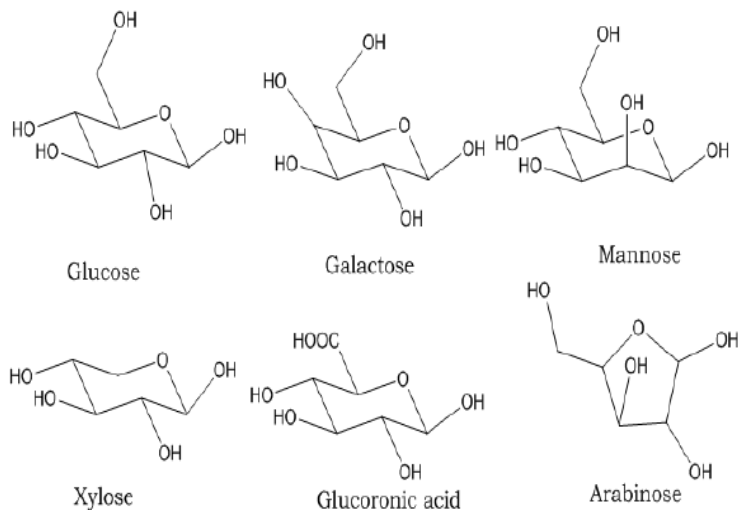
Fig. 1.5: The main monomeric sugars of hemicellulose.

1.3.3   Lignin

In 1938, Anselme Payen wrote the so-called "encrusting theory" beginning the story of what we now know as lignin. At the time, the French chemist reported that in treating the wood with nitric acid (HNO_3) and caustic soda (NaOH), he obtained two products, one he called cellulose and the other one of encrusted material, which soaked the cellulose in wood. Among the experts of the time, it is worth mentioning Peter Klason, who greatly contributed to the initial understanding of lignin chemistry with methods used up to now.[41]

Lignin is the most abundant aromatic polymer with phenolic compounds on Earth, comprising about 20-35% of dry lignocellulosic biomass and representing around 30% of all no-fossil organic carbon.[42] For this, the total lignin in the biosphere is estimated at more than 300 billion tons and an increase of around 20 billion tons per year.[43] The lignin macromolecule is polymerized by three phenyl-

propane units (monolignols) that differ in its degree of methoxylation: *p*-hydroxyphenyl (**H**), guaiacyl (**G**), and syringyl (**S**) which came from its respective alcohols: *p*-coumaryl, coniferyl, and sinapyl alcohols (Fig. 1.6). During the lignin biosynthesis, enzyme (laccases or peroxidases) mediated deamination, hydroxylation, reduction, and methylation reactions occur giving rise to a resonance stabilized phenoxy radical that, through a combinatorial process of radical coupling, allows the growth of the complex and three-dimensional lignin network.[41][44][45][46][47] This network is interconnected mostly by ether linkages (C-O-C), such as β-O-4, α-O-4, and condensed (C-C) bonds like β-β, β-5 and 5-5.[48][49]

Hardwood:	0 - 8	25 - 50	45 - 75
Softwood:	< 5	90 - 95	0 - 10
Grasses:	5 - 35	35 - 80	20 - 55

Fig. 1.6: The precursors in the building block of the lignin. a) Numbering system in generic phenylpropane, b) alcohol precursors, c) monolignols precursors and its percentage from some plants.
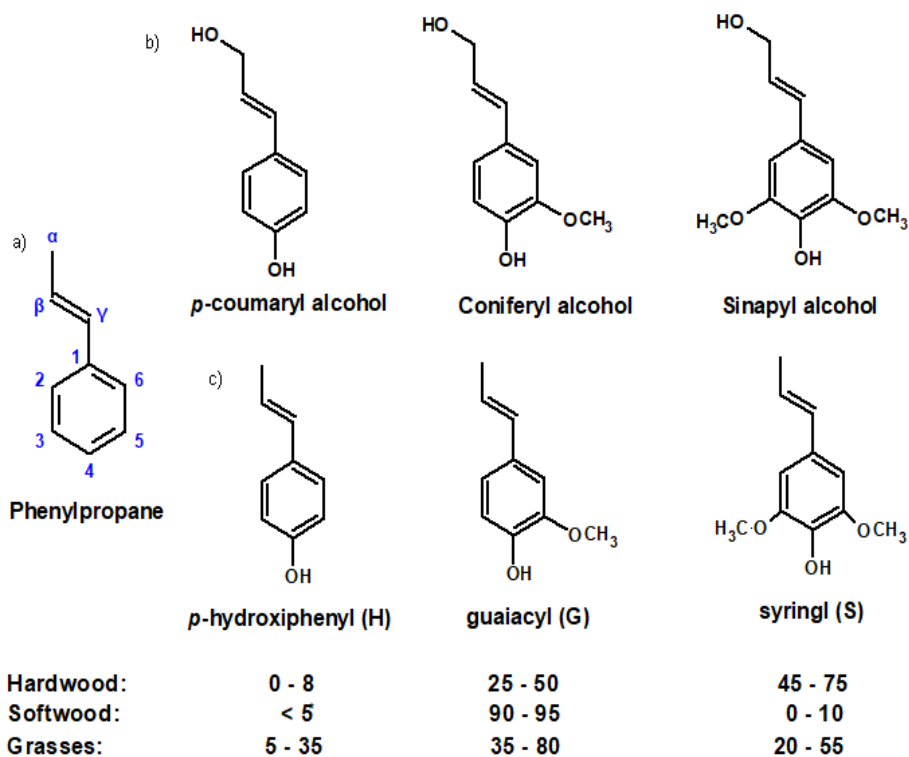
The structural configuration of lignin, as the ratio between monolignols (Fig. 1.6) and the frequency of different bonds as shown in
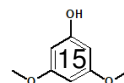
the Table 1.3,[41 50 51] is extremely dependent on its origin (Fig. 1.7 and 1.8).[45 52 53 54 55] However, the type of plant tissue, external environment and the process used for its isolation are other factors that interfere in its building block. The hardwood lignin mostly comprises **G** and **S** units with traces of **H** units. The latter can also be found in the compression wood of softwood lignin, which consist mainly of **G** units.[46 55] On the other hand, the lignin of non-woody species such as grasses are composed of the three monolignols, being that the percentage of **H** units is much higher than in the soft-hardwood lignins.

Lignin has a great potential to be used in many applications, such as carbon-derived or polymer-based materials, however, its complex structure and recalcitrant trend are some of the challenges that need to be overcome. Normally, lignin is subjected to modifications that may be by fragmentation (pyrolysis, hydrolysis, hydrogenation), sulfonation, amination or hydroxyalkylation as a way of inserting new active sites or by the functionalization of hydroxyl groups (etherification, esterification or phenolation).[56]

Table 1.3: Frequency of the main bonding in softwood and hardwood.

Linkage	Softwood (%)	Hardwood (%)
β–O–4	35 - 50	45 - 60
α–O–4	2 - 8	5 - 8
4–O–5	3 - 4	7 - 15
β–5	9 - 12	4 - 11
β–1	7 - 10	5 - 15
5–5	20 - 25	2 - 9
β–β	2 - 6	3 - 12
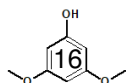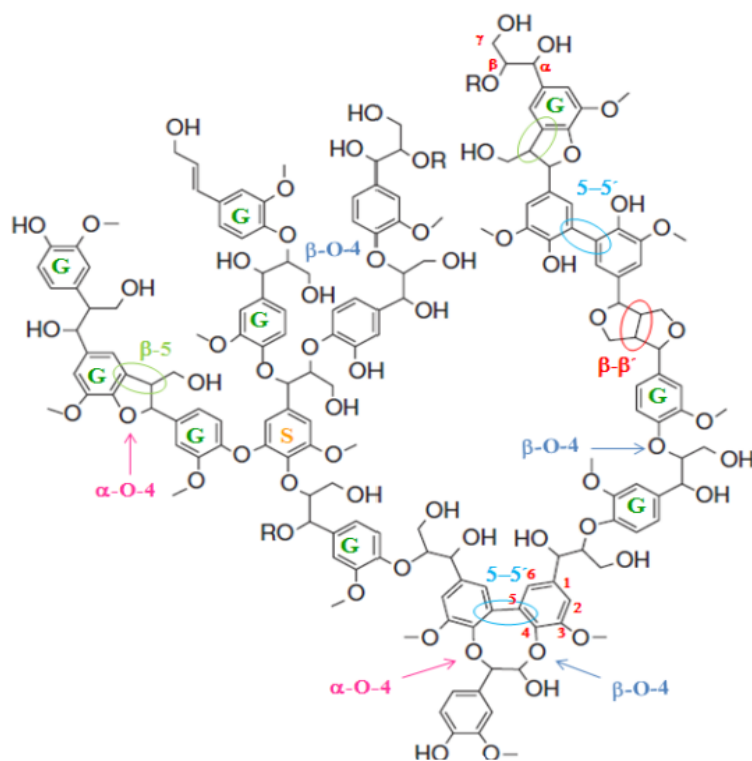
Fig. 1.7: Lignin structure of softwood adapted from Macfarlane[50].

1.3.3.1   Source of technical lignin

In addition to the natural variation in lignin structure due to its botanical origin, the method adopted to isolate it from biomass also affects its chemical composition, purity, molecular structure and consequently its properties for any further application.[43][56] Therefore, technical lignin is often classified as a function of the process applied to isolate it.

Currently, the main source of technical lignin comes from the pulp and paper industry, where lignin is a by-product of the production chain. Leading in the market, the Kraft process accounts for more than 95% of all chemical pulp produced. The versatility, the ease of recovery of chemicals (about 97%) and the excellent quality of the pulp produced are some of the factors that ensure the success
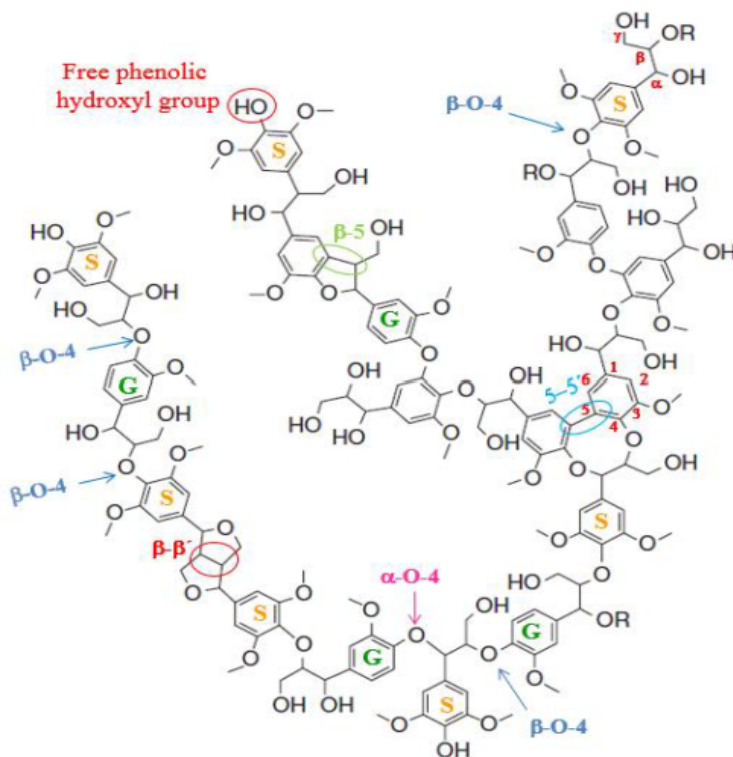
Fig. 1.8: Lignin structure of hardwood adapted from Macfarlane[50].

of the Kraft process.[21][43] In this process, wood chips are impregnated with a mixture of sodium hydroxide (NaOH) and hydrosulfides (HS$^-$) at 135 to 175 °C to ensure that the lignin is chemically divided into a fragment. During the process, the reactive groups, such as hydroxyl, are blocked and the hydrosulfide ion reduces the condensation reaction. Carbon-carbon bonds are more stable under alkaline conditions, so ether (oxygen-carbon) bonds are easily cleaved by the attack of the sulfide ion.[57] The presence of sulfur into lignin molecules (thiolignin) is one of the characteristics of Kraft lignin (Fig. 1.9).[58] Generally, part of the Kraft lignin dissolved in the black liquor is burned in a recovery boiler to produce energy and to recover the cooking chemicals. According to Berlin et al.,[58] around 6-7% of this liquor could be destined for lignin extraction without affecting the energy balance of the plant. Today, the Kraft lignin isolated and com-

mercially available is mainly obtained by the LignoBoost^{TM} process. Domtar (Plymouth plant in North America) was the first industry to install a full-scale LignoBoost^{TM} plant in 2013. With the capacity to produce 25.000 MT per year, it was possible de-bottleneck the recovery boiler, and increase the sale pulp. Stora Enso has also been using this process since 2013 at the Sulina Finlandia plant with a capacity of 50.000 MT annually. However, the purpose of this factory is to start a new line of business by selling high-quality pure lignin to external customers.[59] Kraft lignin is used as an additive for concrete, feed and food additives, dispersants, carbon fiber, thermoplastic, and thermoset polymers and composite applications.[58]
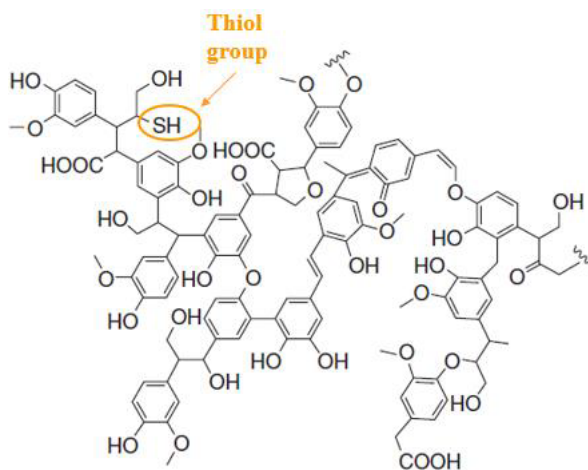
Fig. 1.9: Kraft Pine lignin adapted from Macfarlane.[50]

Sulfite technology is also used in the pulp industry, but in contrast to the Kraft process, the cooking conditions is less flexible and input raw materials are very selective, for this, occurs in a lesser extent. The sulphite process is carried out with aqueous solutions of a sulfite or bisulfite and a salt (sodium, ammonium, magnesium or calcium salt) at 140-170 °C. The cooking pH, as well as the nucleophilic attack target (by the sulfite ion) on the lignin molecule, is determined by the type of salt used in the digestion process.[60] The high amount of sulfur incorporated in the lignin, mainly in the form
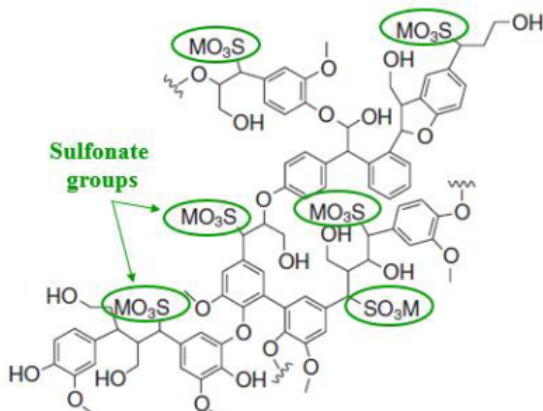
Fig. 1.10: Spruce Lignosulfonate adapted from Macfarlane.[50]

of sulfonate groups (SO_3, Fig. 1.10), causes it to have unique colloidal properties, favoring its use as stabilizers, dispersing agents, surfactants and adhesives.[43]

In addition, but to a lesser extent, technical lignins can be obtained by alkaline (soda) and organosolv process. The main characteristic and advantage of these lignins is that, in both situations, the obtained lignins are sulfur-free, in contrast to lignins of Kraft and sulfite technology. Soda delignification is mostly used in non-wood pulp mills and to a certain extent hardwood.[60] Lignocellulosic delignification by the organosolv process can be carried out, generally in aqueous solution, with an organic solvent such as methanol and ethanol or organic acids like formic and acetic acid.

1.4   Lignocellulosic biomass conversion

Currently, in a modern use of lignocellulosic biomass, the efficiency and effectiveness of its exploitation are the keywords. Therefore, in this investigation, industrial, agricultural and forestry wastes were used to obtain different value-added products, such as the production of bio-polymers of renewable origin, using them for the pro-

duction of polyurethanes and phenolic resins.
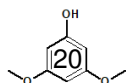
Cellulose, hemicellulose, and lignin are the three major compounds of lignocellulosic material, which are used in many applications because of its properties and functionalities, as mentioned along to section 1.3.

The two foremost pathways used to convert the lignocellulosic biomass into intermediate or end products are biochemical and thermochemical processes.[61][62] In the former case, the polysaccharides are converted, for example, into ethanol by fermentation based on microorganisms or into biogas (a mixture of methane and carbon dioxide) by digestion. Usually, it is a slow and very selective process.[63][64] In the other, a greater variety of raw materials is available to be wholly converted into products such as heat, fuels, energy, chemicals, and value-added materials, using different thermochemical techniques.[65] For example, pyrolysis occurs at high pressures and temperatures (300 - 550 °C) using dry biomass in the absence of oxygen to produce liquid fuel,[66] in contrast to combustion, which is characterized by the presence of oxygen and temperatures above 700 °C.[67] Gasification also uses much higher temperatures (above 700 °C) under the limited presence of a gasifying agent to generate firstly gas (syngas).[68]

Thermochemical techniques mainly comprise combustion, direct liquefaction (pyrolysis, solvolysis liquefaction and high-pressure liquefaction)[68][69] and indirect liquefaction as gasification (Fig. 1.11).[70][71] Parameters such as presence or absence of oxygen, with or without pressure and temperature range are the main differences characterizing each of these techniques.

Although the liquefaction process is ancient, in recent decades it has received special attention in the area of biomass, as it is a relatively easy procedure to convert biomass into bio-oil/bio-crude or polyol with interesting properties. Among these thermochemical
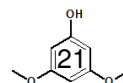
methods (Fig. 1.11), the solvolytic liquefaction or moderate acid-catalyzed liquefaction (MACL), has some very attractive reaction parameters, as it allows the conversion of lignocellulosic biomass in low/moderate temperature and atmospheric pressure in relation to the others.
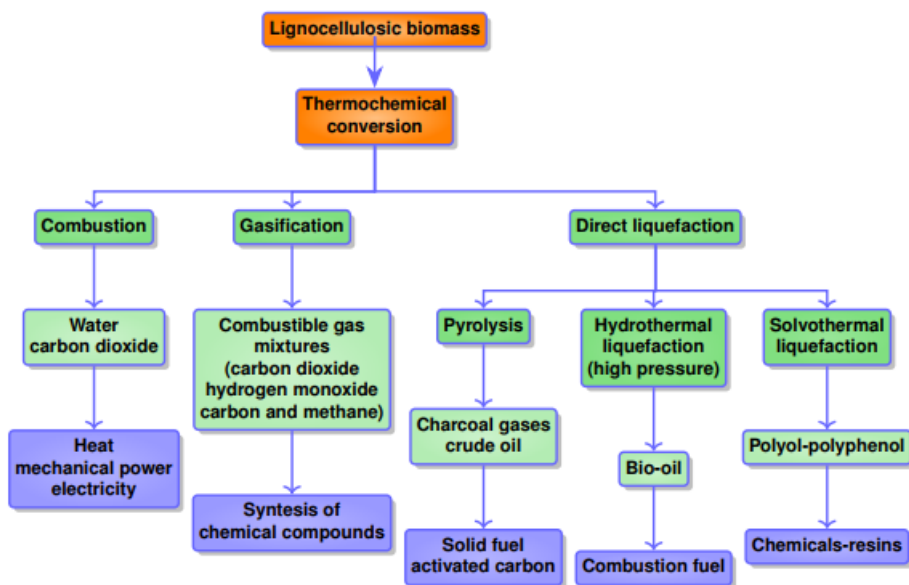
Fig. 1.11: Thermochemical conversion of lignocellulosic material.

1.4.1 Solvolytic liquefaction of biomass

The solvolytic liquefaction is mainly characterized by the use of phenol or polyhydric alcohols as solvents to convert the lignocellulosic biomass to polyphenol or polyol, respectively. In this situation, the solvent acts as nucleophilic molecule performing nucleophilic substitution or elimination reactions, thus the solvolytic and depolymerization reactions[72] occur simultaneously in the lignocellulosic structure generating smaller fragments. Then, such fragments can be rearranged with themselves or with the solvents to form molecular fragments or solvents-derived compounds rich in
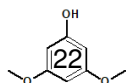
aromatic and/ or aliphatic hydroxyl groups.[64][73]

Solvothermal liquefaction often occurs in mild conditions, with temperatures between 110 °C and 180 °C at atmospheric pressure and by conventional heating. That is, by conductive and convective heat transfer, mainly by heating mantle source.[74] Under these conditions, the heating is relatively slow due to the low thermal conductivity in the reaction medium, so that the reaction time can range from 30 min to 4 h.

On the other hand, microwave heating has been used in organic chemistry since the mid-1980s[75] and, more recently, in the field of lignocellulosic liquefaction[76][77] to improve the heating mechanism and consequently the reaction time that is considerably less. This is because some materials can absorb microwave energy so when microwave radiation passing through these materials occur mainly the interaction of the electric field component and magnetic field component. The mechanism of dielectric heating occurs mostly due to effects of dipolar and interfacial polarization. For example, when microwave radiation passing through a polar molecule, such as water, this causes rotation and attempts to align in the permanent and induced dipolar by polarization dipoles. Increasing molecular rotation results in friction, resulting in loss of heat that is dissipated in the form of heat.[75]

1.4.1.1   Reaction time in solvolytic liquefaction

The reaction time is a very important variable that, together with other parameters, must be optimized not only because it affects the conversion rate, but also because it influences the final production cost of the polyol. It also presents environmental issues, as the higher reaction time, the higher energy time is consumed. The literature reports a reaction time ranging from 5 min to 240 min for various
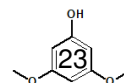
liquefied lignocellulosic biomass under conventional heating.[78][79][80] Nevertheless, under alternative microwave heating, due to its heating mechanism as mentioned above, the reaction time is much lower than conventional heating, ranging from 2 min to 40 min.[76][77][81] Typically in the literature, the temperature investigated in the lignocellulosic liquefaction process ranges from 110 to 220 °C for both heat sources.

1.4.1.2   Lignocellulosic biomass in solvolytic liquefaction

A wide variety of liquefied lignocellulosic material has been reported, including wood (softwood and hardwood),[78][81][82][83] soybean straw,[84] microalgae,[77][79] corn stover,[85] cork,[86] bagasse,[80][87] cotton stalks,[87] coffee grounds wastes,[88] enzymatic hydrolysis lignin,[89] and softwood Kraft lignin.[90][91] Usually, the percentage of these raw materials varies between 10% and 25% relative to the solvents used. Kraft lignin is obtained by acid precipitation mainly with concentrated sulfuric acid. This acid is widely used all over the world and has strong importance in almost the entire industrial segment[92] (Fig. 1.12) being used as a measure of the industrial development index of a country.[93] The great consumption of this acid causes the pollution of the environment and intensifies the occurrence of phenomena such as acid rain. It is noteworthy that, since 2012, strong inorganic acid (such as sulfuric acid) mists can be classified as carcinogenic to humans (Group 1).[94] In this research, beyond sulfuric acid, hardwood Kraft lignin was precipitated with organic acids such as acetic acid, citric acid and lactic acid as a cleaner precipitation alternative. These lignins were subjected to liquefaction and the influence of these acids (as precipitating agents) on the polyols was evaluated.
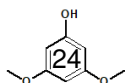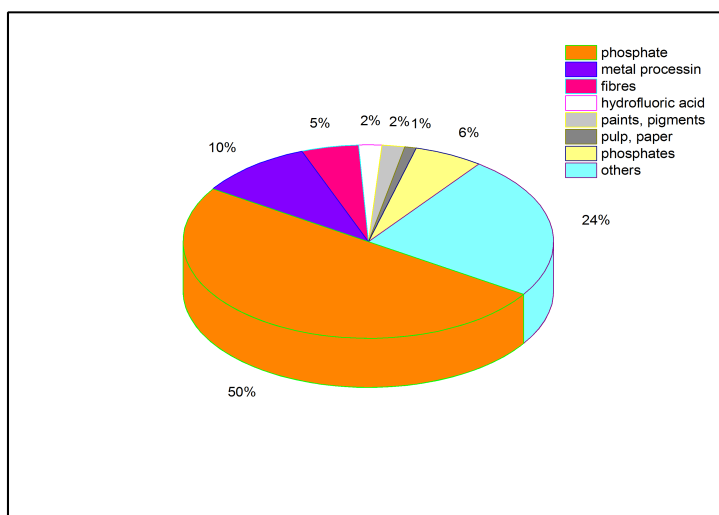
Fig. 1.12: Different applications of sulfuric acid.

1.4.1.3   Solvents in solvolytic liquefaction

Solvents play an important role in the liquefaction process because they influence the structure and properties of the polyols, as well as the yield efficiency, since the higher the solvent polarity, the higher the efficiency.[95] The most common polyhydric alcohols solvents used in the liquefaction process are the polyethylene glycol (PEG) mixed with glycerol (G) in various proportions.[78 82 87 96] Gycerol is often used as co-solvent to improve the liquefaction yield since it acts as a retardant of the re-condensation reactions,[83 97] and the viscosity when combined with a lower density solvent. Apart from, diethylene glycol (DEG)[98], ethylene glycol/ethylene carbonate,[85] propylene glycol, in the case of oxypropylation (a grafting process),[99 100 101] and 2-ethylhexanol/diethylene glycol[102] also are used. Solvent/mass ratio, type of mass, type of catalyst and solvent/catalyst ratio are parameters, which also play a very important role in the yield and properties of the obtained polyol.

1.4.1.4 Catalyst in solvolytic liquefaction

In the literature, sulfuric acid is the most used catalyst combined with polyhydric alcohols in the liquefaction of different raw materials like wood species, enzymatic hydrolytic lignin and recycled newspaper. [78][79][83][89][96][98][103][104] Zhuang et al.[77] investigated the effectiveness of sulfuric acid, hydrochloric acid, phosphoric acid, sodium hydroxide and sodium carbonate as catalyst for algae liquefaction using different solvents such as ethylene glycol, polyethylene glycol, *n*-octyl alcohol and phenol. The authors obtained the highest yields with sulfuric acid independent of solvent type. Jasiukaityte et al.[105] investigated *p*-toluene sulfonic acid monohydrate as a catalyst in the liquefaction of ground woody. Lu et al.[106] performed the liquefaction of woody biomass using an acidic ionic liquid as a green catalyst. The cork dust was studied by Yona et al.[86] under acid and base catalysts using sulfuric acid and sodium hydroxide respectively. The authors reported that under alkaline conditions the yield of liquefaction was higher than in acidic conditions. In the oxypropylation process, the basic catalyst such as potassium hydroxide and sodium hydroxide are most used. [99][100][101] Ross et al.[107] studied KOH, Na_2CO_3 and some organic acids (acetic and formic acids) as catalysts for different microalgae using hydrothermal liquefaction technique. In this work, the authors concluded that yields were higher using organic acids than alkaline catalysts. In the literature, the catalyst load generally ranges from 1% to 9% based on the amount of solvents used.

To our knowledge, organic acids have not been used as catalysts in the liquefaction of lignocellulosic materials based on polyhydric alcohols as solvents. Thus, the three different organic acids (acetic acid, citric acid, and lactic acid) were used as catalyst in the liquefaction of Kraft lignin and their effects on the polyols were evaluated.
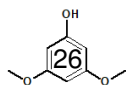
1.5   Liquefied lignocellulosic residues as a source of value-added products

By definition, a polyol is an organic compound containing more than two hydroxyl groups in its structure. This reactive group (OH) coupled with a variety of backbone make polyols a class of compounds extremely versatile and useful in many areas such as food industry, cosmetic and beauty industry, automotive, pharmaceutical and biomedical area, adhesives, foams and others. Some commercially available polyols are shown in Fig. 1.13.

Fig. 1.13: Some commercial polyols.

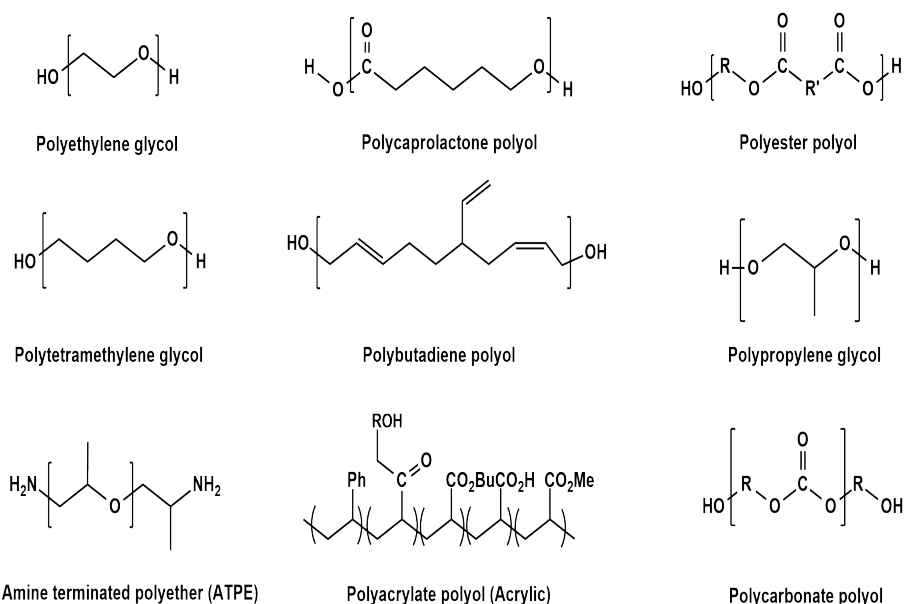The final properties and applicability of a polymer are strongly influenced by the properties of the polyol. Among them, a low acidity level is desirable because the acids can react with the catalyst by acid-based neutralization reaction, affecting the catalytic activity of the system. The number of hydroxyl groups plays an important role, since these groups mean the reactive sites of a polyol.

When a polyol results from the solvothermal liquefaction of lignocellulosic material, its aromatic or aliphatic character is directly influenced by the liquefaction solvent used. In the former, phenol is usually used as solvent and the obtained polyphenol is largely applied in the field of PF resins, while the other, the most common is a mixture of polyhydric alcohols as solvent. Due to the predominance of the aliphatic compounds in its structure, the polyol is mainly used in PU application. [108][109][110][111][112]

Gama et al.[88] synthesized PU foams for thermal insulation, using liquefied coffee grounds residue with polyhydric alcohols (PEG/G) and pMDI as isocyanate. In another study paper waste (newspaper and box paper) was liquefied with PEG/G and used to prepare rigid PU foams.[113] The authors concluded that PU foams have good mechanical properties, thermal stability and are potentially biodegradable. In addition, they found that there were no mutagenic or carcinogenic agents in the aqueous extracts of the foams. Kurimoto et al.[114] polymerized pMDI and liquefied wood to prepare PU films. The authors studied several NCO/OH ratios as well as different formulations of liquefied wood (with several wood percentages) under constant NCO/OH ratios and concluded that the crosslink density and Tg can be controlled as a function of the percentage of wood in the polyol. In this study, polyols obtained from different lignocellulosic sources were used in the synthesis of PU rigid foam.

However, in this investigation, the lignocellulosic residues were liquefied using a mixture of PEG/G as solvent and evaluated as a potential alternative to partially replace phenol in resol formulations.

1.5.1 Phenolic resins

The initial experiments between phenol and formaldehyde date from 1872, performed by Adolf von Bayer, a German chemist. In
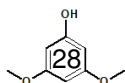
1907, it began to be marketed with a brand of Bakelite.[115] Phenol-formaldehyde resin or simply phenolic resin, when synthesized with an acid catalyst and an excess of phenol, is called NOVOLAC resin. On the other hand, Resol phenolic resin is obtained with higher formaldehyde content and using a basic catalyst, since, under alkaline conditions, the *ortho* and *para* positions of the phenol become more susceptible to the reaction with formaldehyde. This reaction was first observed (1894) by L. Lederer and O. Manasse and therefore is known as Reaction of Lederer-Manasse.[116] Resol resin synthesis occurs mainly in two stage.[117] In the first, addition reactions happen. For this, initially the alkaline catalyst quickly attacks the phenol to form the phenolate ion by displacing negative charges at the *ortho* and *para* positions (Fig. 1.14).
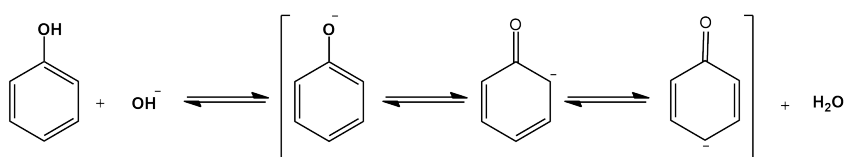
Fig. 1.14: Formation of phenolate ion.

Now, with these more reactive positions, the addition reactions begin to occur between phenol and formaldehyde to form hydroxymethyl phenol (HMP) compounds (Fig.1.15).

As in the resol resin, the molar ratio of formaldehyde is higher than the phenol, during this addition step, mono, di-, and tri-hydroxy methyl phenol (Fig. 1.16) can be formed as intermediate compounds

Finally, the prepolymer begins to be formed by condensation reactions, which can occur between two HMPs or a HMP and a phenol, by bonds of dimethyl ether or methylene releasing only water or water and formaldehyde, respectively (Fig.1.17).[117]

Phenolic resin has excellent properties such as mechanical stability, electrical and thermal insulation capacity and high levels of resistance, making them extremely interesting for use in many in-

Fig. 1.15: Initial addition reactions.

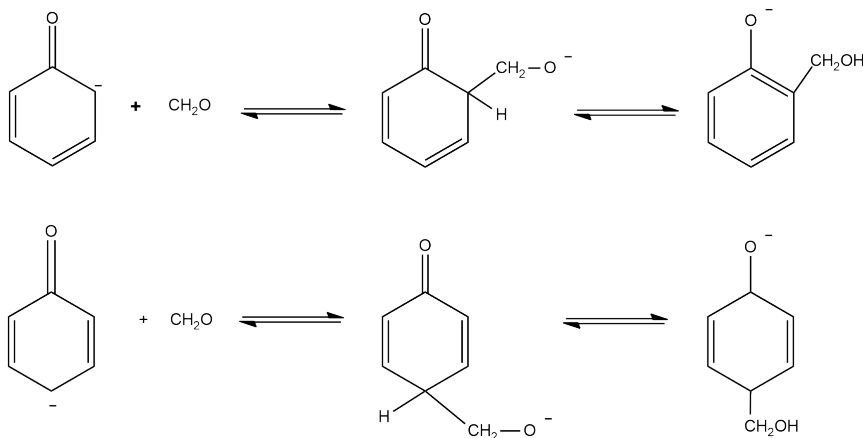dustrial segments such as aeronautical, automotive, and electronic components.[118] Phenolic resol resin is widely used as a wood adhesive in many wood processing.

However, factors related mainly to the steady increase in the consumption of petroleum derivatives and to the political and economic interest aggravate the instability of the oil price. These aspects and issues concerning health and the environment are the main reason for the growing increase in the last decades of research on more economical and eco-friendly alternatives to solve these questions.

In this scenery, lignocellulosic biomass, especially lignin, can be considered as a strong candidate to replace phenol due to its similar structure, it is a renewable resource and widely available. However, lignin is less reactive than phenol and, for this; the researchers generally carry out modifications in lignin, mainly, by the method of phenolation, when its application is for phenolic resins.

Han et al.[119] liquefied spent liquor from wheat straw and phenol to produce phenolic adhesives. The resins were formulated with a molar ratio of formaldehyde/phenol of 2.0, NaOH/phenol molar ration ranging from 0.25 to 0.8 and the substitution of phenol by the spent liquor phenolated ranged from 0 to 35%. The authors con-
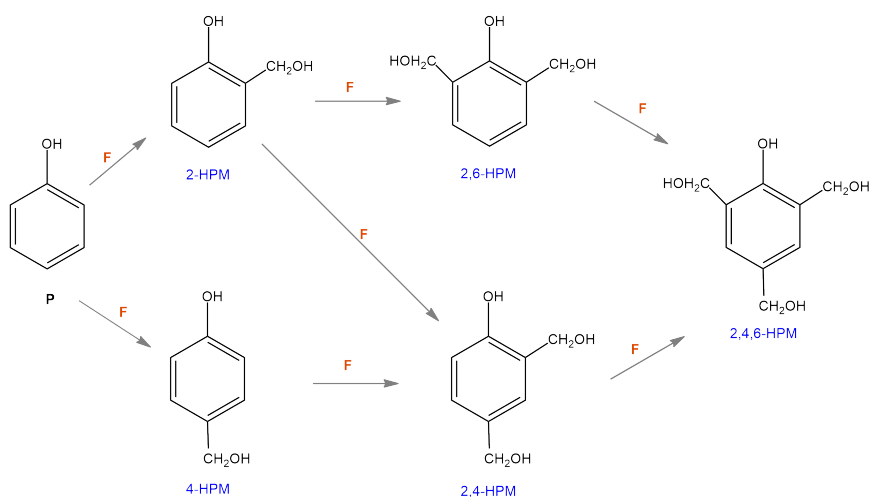
Fig. 1.16: Intermediate compounds formed during addition reactions.

cluded that, with a catalytic molar ratio of 0.5 and a substitution of 20% phenol, the resin presented better values of FFC, gel time and adhesion strength than the synthesized control resin.

Khan et al.[93] investigated the partial substitution of phenol by phenolated lignin extracted from eucalyptus bark. Under optimized conditions (formaldehyde/phenol molar ratio of 2.0, NaOH 10 wt% for phenol and a 50% replacement of phenolated lignin), adhesive and shear strength were reported to be higher than formulated control resin, while thermal stability and curing temperature was lower. Lee et al.[120] investigated the liquefaction of the bark powder of two species with sulfuric acid and chlorhydric acid as catalyst and phenol as the solvent. The authors concluded that the viscosity of the resins was affected by both bark species and catalyst type. The lignin-phenol-formaldehyde adhesive was prepared using the optimum conditions: lignocellulosic ethanol residue to replace 50% phenol, F/Ph molar ratio 3.0 and 20% concentrated NaOH. The results showed an adhesive with good properties and potential as external-grade use according to the standard requirements.[121]

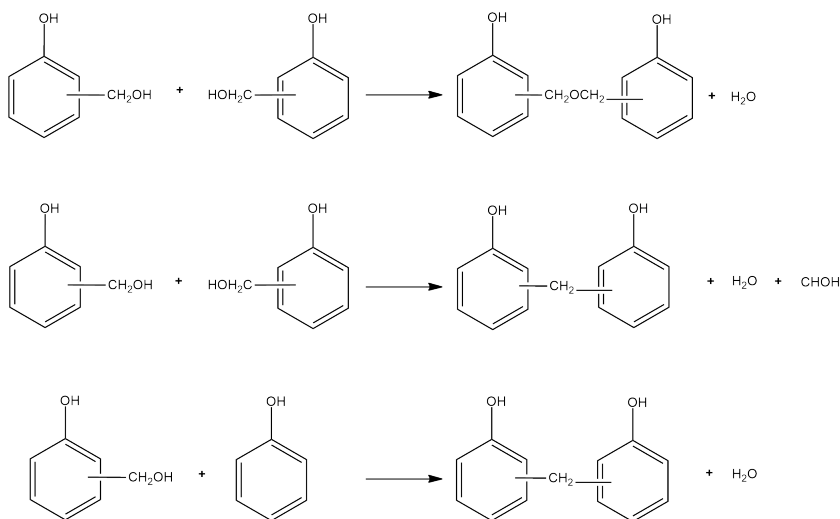Yang et al.[122] prepared lignin-PF adhesive using four types of

31
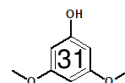
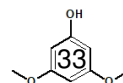Fig. 1.17: Condensation reaction to form the phenolic prepolymer.

lignin from biorefinery process (corn cob, two poplar wood and wheat straw). In the first step, the authors modified the lignins with phenol and NaOH, followed by the addition (in two parts) of formaldehyde and NaOH. Finally, additional NaOH was added with urea. The resins showed structure and tendency of curing comparable with commercial PF adhesive and low emissions of formaldehyde in the plywoods. Hussin et al.[123] produced organosolv lignin-based wood adhesive (from palm oil fronds) as a partial substitute for phenol, and glyoxal as the source of aldehyde. The authors found that the resin formulated with 50% organosolv lignin showed adhesive strength values higher than the commercial PF adhesive.

Wang et al.[124] studied the use of lignin from corn stalk to produce phenolic adhesive, but first, corn stalk was subjected to pretreatment with steam-explosion to improve the elimination of carbohydrates. The solid residue, after drying for 48 h, was cooked with NaOH solution for lignin extraction. Then the concentrated alkaline lignin solution was methylated using formaldehyde. In a second step, the pure phenolic resin was produced with phenol, formaldehyde and 20% NaOH solution in the molar ratio of 1:1.6:0.15, re-

spectively. The modified phenolic adhesive was obtained by mixing different percentage of methylolated lignin liquor with pure PF resin at room temperature, stirring at 200 rpm for 2 min. As a result, the authors reported that the addition of 50% methylolated lignin is the maximum to obtain good adhesion strength and lower content of free formaldehyde and phenol.

These studies show that the maximum phenol substitution is about 50%, generally using lignin pre-modified with phenol and eventually with formaldehyde to improve its reactivity. This means that the same toxic and expensive chemicals used in resin synthesis are used to modify the lignin.

In this investigation, the liquefied residues using polyhydric alcohols as a solvent were used to partially replace the phenol in the resol resin. The objective was to evaluate the possibility of replacing the aromatic OH with mainly aliphatic OH (from renewable source) and in what proportion, to produce wood adhesive with similar standard properties.
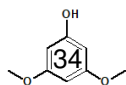
Chapter 2

Experimental design of liquefied Kraft lignin

2.1   Introduction

The Kraft process (or sulfate process) refers to the delignification of wood chips in an alkaline medium using NaOH and Na_2S as chemical agents. In contrast to the sulfite process, which is performed under acidic conditions with bisulfite ions. The latter was invented by Benjamin Tilghman (Great Britain)

Fig. 2.1: Kraft lignin powder.

in 1866, and a few years later, in 1879, Carl F. Dahl (Germany) invented the Kraft process. However, at that time, Kraft pulp was only used on unbleached and semi-bleached paper products.[125] The sulfite process then dominated cellulose production until around Second World War,[126] when some factors allowed the Kraft pulp to become competitive and totally dominant to this day. Among them, the possibility of recycling almost all pulping chemicals due to the invention of the recovery boiler, by G.H. Tomlinson and the incorporation of chlorine dioxide as a chemical, allowed to bleach efficiently the dark brown Kraft pulp.

In this process, 45 - 50% of cellulosic pulp is obtained in relation to input wood, remaining mainly lignin and some carbohydrates dissolved in the alkaline solution called "black liquor".

2.2   Objectives

The main objective of this chapter was to optimize the reaction conditions of liquefied Kraft lignin using polyhydric alcohols under two different heating sources.

37
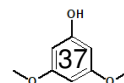
These goals were achieved through the following specific objectives:

- Characterization of the Kraft lignin;

- Development of an experimental design to liquefy Kraft lignin under reflux;

- Characterization of obtained biopolyols;

- The optimization of the reaction conditions of the biopolyol;

- Development of an experimental design to liquefy Kraft lignin under microwave heating;

- obtained under microwave-heating;

- The optimization of reaction conditions of the biopolyol obtained under microwave heating;

2.3 Experimental procedure

2.3.1 Raw materials

Kraft lignin was used as raw material to produce biopolyols. Polyhydric alcohols (polyethylene glycol and glycerol), sulfur acid, citric acid, acetic acid or lactic, NaOH, toluene, ethanol, acetic acid glacial, 1,4-Dioxane, KOH, phthalic anhydride, pyridine, acetone, solution of dimethylformamide and lithium bromide, dimethyl sulfoxide and methanol were the reagents used in the synthesis and characterization procedures performed in this chapter. Technical information on these chemicals are listed in Appendix C.

Kraft lignin (KL) was precipitated by acidification of black liquor provided by CMPC-Cellulose Riograndense in Guaíba/RS, Brazil.
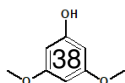
The precipitation with sulfuric acid was performed by adding a desirable amount of concentrated acid to the black liquor under manual stirring with glass stick until reached pH 4 and was allowed to stand for 24 h at room temperature. After, the precipitated lignin was filtered and washed using acidified water (in the case of sulfuric acid), followed by distilled water until neutral the pH. The precipitated lignin was oven dried for 24 h at 60 °C, then ground by mortar and pestle into powder, to be used without further modification. To carry out the precipitation with organic acids, 500 mL, 100 mL or 50 g of acetic acid, lactic acid or citric acid respectively were added to 2200 mL of black liquor following the same procedure used with sulfuric acid.

2.3.1.1 Characterization methods

The purity of precipitated Kraft lignin was characterized as Klason lignin (AIL), acid soluble lignin (ASL) and carbohydrate content, as well as ash and moisture. The molecular weight distribution was performed by gel permeation chromatography (GPC) and sulfur content was determined by elemental analysis. The structural composition was evaluated by infrared spectroscopy (FTIR) and pyrolysis/gas chromatography-mass spectroscopy (Py/GC-MS) and thermogravimetric analysis (TGA) was performed to evaluated the thermal stability of lignins. These techniques and procedures are described in the Appendix section; in addition, a summary is shown in Fig. 2.2.

2.3.2 Liquefaction procedure

In a typical run, liquefying solvents without or with the desired amount of catalyst were added into a 500 mL neck glass flask reactor with magnetic stirrer, temperature control and condenser. When the set temperature was reached, the Kraft lignin was added into
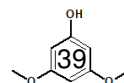
the flask and the reaction time was started. After, the reactor was immersed in a cooled water bath to quench the reaction. Liquefied mixture was washed with acetone under vacuum and solid residue was dried in an oven to determine the yield (Equation A.10). Acetone was removed by rotary evaporator under reduced pressure at 49 °C.

2.3.3 Experimental design

In order to investigate the effects of reaction conditions (time, mass, catalyst) on the properties of the polyols, a factorial design was used. Reaction time, mass, and catalyst were the independent variables (predictors), while the yield and basic properties of polyols (acid and hydroxyl number and viscosity) were dependent variables (responses). The independent variables were coded according to the following equation A.11:

The experimental design was performed using polyethylene glycol (PEG) and glycerol (G) in a weight ratio of 80/20 (wt%) as the mixing solvents and sulfuric acid (SA) as catalyst at 160 °C. The thermochemical conversion for Kraft lignin was investigated using two different sources of heat, the thermal conduction (with heating mantle and reflux) and microwave heating both at 160 °C. In these designs, the values of the variables catalyst (0, 3 and 6%) and mass (15, 20 and 25%) were the same. However, the liquefaction by reflux was performed during 60, 80 and 100 min and at 300W during 5, 17:30 and 30 min under microwave heating. Each factorial design generated 27 runs, as it can be seen in Appendix A.0.2, Tables A.1 and A.6 respectively.
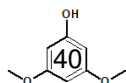
2.3.3.1 Liquefied lignin - characterization methods

The yield of obtained polyols from the experimental design were determined and the yield was determined according to equation **??**. The acid numbers (*An*) and hydroxyl number (*OHn*) were verified following the standard procedures ASTM D974 (Appendix A.0.2.3) and ASTM D4274 (Appendix A.0.2.4), respectively. The viscosity was measured at 25 °C (Appendix B.5.3) and molecular distribution was determined as reported in Appendix B.2.1. These procedures and techniques are described in Appendix section and summarized in Fig. 2.2.
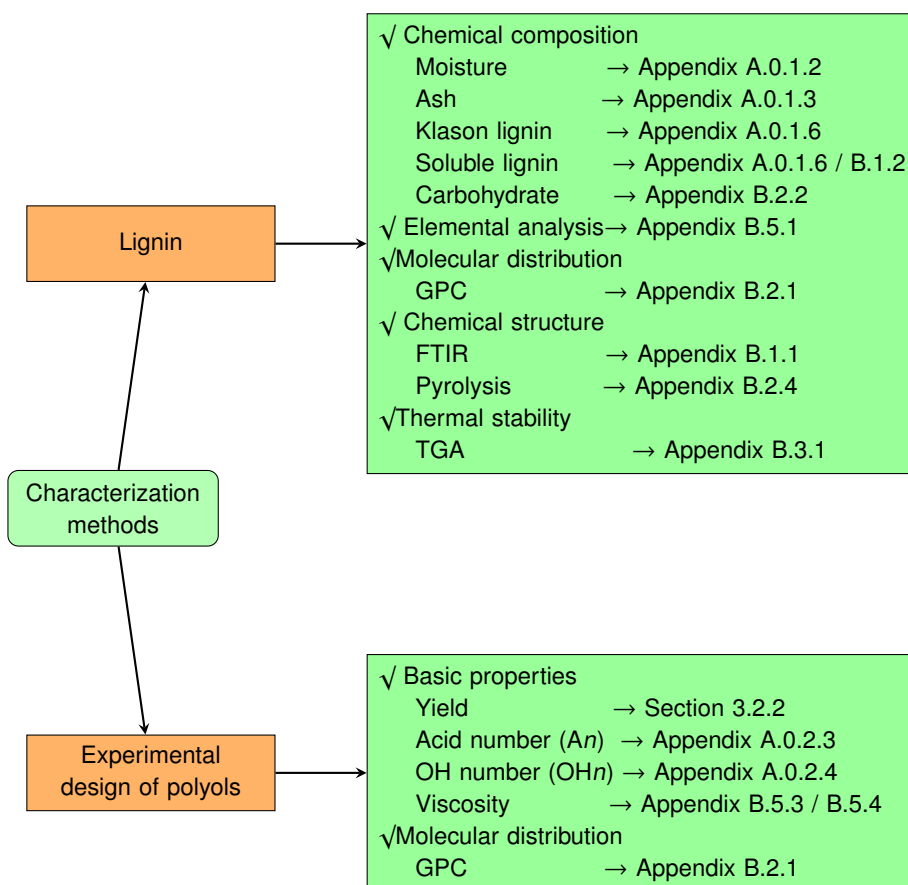

Fig. 2.2: Characterization scheme of Kraft lignin and liquefied Kraft lignin.

41
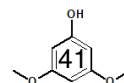
2.3.4 Statistical analysis

Data was analyzed by the analysis of variance (ANOVA) to determine the variables that are significant in the properties of the polyols, with confidence level of $p < 0.05$, as well as the optimization of multiple responses using the software STATGRAPHICS Centurion XV. The overall contribution of each variable was analyzed using the Pareto chart. Moreover, response surface method (RSM) was used to investigate the interaction effect between the variables and build a mathematical model to describe the overall process.
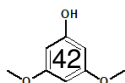
2.4 Results and discussion

2.4.1 Chemical composition of Kraft lignin

Purity of Kraft lignin samples precipitated from hardwood black liquor, which was based on Klason lignin and acid-soluble lignin content is presented in Table 2.1. The use of organic acids such as acetic, citric and lactic acids (KLA, KLC, KLL) as acidifying agents produce lignins with higher purity (93-94%) than using sulfuric acid (SA) for the precipitation step (81.8%). Several papers published high purity values (90-94%) for softwood Kraft lignins,[127][128][129] while reporting that the purity related for hardwood Kraft lignin is generally lower.[130][131] Therefore, besides having enhanced the purity of wood Kraft lignins with the use of organic acids, the level of purity achieved is totally comparable to the purity of the lignin obtained by the Lignoboost^{TM} process. Conversely, the sulfur content was observed higher in KLA, KLL, and KLC than in KL precipitated with sulfuric acid and higher than that obtained by other authors who used organic acids as precipitating agent.[132] No clear reasons were found to explain these results. However, previous works about the chemical reactions during the Kraft pulping process together with the usual elemental analyses of the black liquors and the chemistry of the dissolved Kraft lignin[133][134] were taken into account to understand and explain these unexpected results. During the Kraft pulping, several chemical reactions take place which partially degrade the lignin structure and allow its dissolution in the black liquor.[135] Because of the alkaline conditions of the medium the OH groups of lignin become ionized.[136] Therefore, when some acid is added to the black liquor, the precipitation occurs since the proton concentration [H$^+$] increases and hence th protonation of the ionized phenolic groups on the lignin happen. The authors have considered that SO$_4{}^-$ ions from the sulfuric acid could have react with the remained chemicals, which
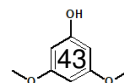
are also in ionic state in the black liquor (Na$^+$, HS$^-$, OH$^-$, CO$_3$$^{2-}$), forming Na$_2SO_4$, Na$_2S, H_2$S or Na$_2CO_3$. However, in the case of organic acids as precipitating agent, their lower dissociation capacity in the black liquor, could lead to lower concentration of protons, being not enough to protonate all ionized OH groups present in the Kraft lignin.[132] Although the amount of sulfur was found higher, the ash content was lower in Kraft lignins precipitated with organic acids, because these acids did not form as many salts as those formed during precipitation with sulfuric acid. Hence, the use of organic acids for the precipitation of lignin may be a greener progress in relation to environmental issues and future potential commercial applications of these industrially available lignins.

Regarding carbohydrate contamination, it is well know that during the Kraft cooking process, dissolved lignin fragments contain covalently bound carbohydrate and as result, they can precipitate with the lignin, being so difficult to eliminate them during the washing step.[137] The results of acid hydrolysis of Kraft lignins revealed that KLA aside, Kraft lignin precipitated with lactic and citric aids had lower carbohydrate contamination than KL, which was recovered by the use of sulfuric acid. Moreover, common CHO composition was observed for analyzed Kraft lignins without notable differences between them.

2.4.1.1 Molecular distribution

Due to the strong kraft pulping conditions, which fragment the lignin by attacking the ether bonds in order to be removed from the wood, kraft lignins usually present low molecular weight properties.[138] Moreover, previous studies reported lower average molecular weight for hardwood kraft lignin than for softwood kraft lignin, because of the higher content of beta-aryl ether linkages in hardwood lignin, the smaller amount of C-C bonds between the syringyl units and the lack of reactive positions (C5 positions) in the aromatic
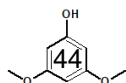
Table 2.1: Chemical composition of the lignins.

	KL	KLA	KLC	KLL
Klason lignin (%)	75.4^a	89.9^b	89.6^b	88.7^b
Soluble lignin (%)	6.4^a	4.2^b	3.9^b	5.6^c
Carbohydrate (%)	0.60^a	0.35^b	0.13^c	0.33^b
Ash content (%)*	4.68	0.07	1.99	1.02
C (%)	56.23	57.24	56.81	55.41
H (%)	5.93	6.35	6.12	5.56
N (%)	nd	nd	nd	nd
S (%)	5.49	6.53	6.98	6.39
O (%)**	32.1	36.41	37.07	39.03
H/C molar ratio	0.11	0.11	0.11	0.10
O/C molar ratio	0.57	0.64	0.65	0.70

* Determined by TGA. nd: Results out of reach <1.6%). ** By difference. The values followed by the same superscript letter in the same line are not statistically different at 95% significance, p<0.05).

ring for condensation reactions.[139]

The weight-average molecular weight ($\overline{M}w$), the number-average molecular weight ($\overline{M}n$), and the polydispersity index (PDI=$\overline{M}w/\overline{M}n$) of Kraft lignin obtained from the precipitation with SA and different organic acids are listed in Table 2.2. The lignins presented different molecular distribution regarding to the precipitating acid. The KLA which was precipitated with acetic acid has the lowest $\overline{M}w$ and PDI, while the lignin precipitated with citric acid (KLC) has the highest $\overline{M}w$ and PDI. Sulfuric acid and lactic acid had a similar effect on lignin precipitation with $\overline{M}w$ and PDI around 2000 g.mol^{-1} and 4.0, respectively, however, KL presented molecular distribution values higher than KLL.

As can be observed, the used of acetic acid and lactic acid precipitated very similar lignins in terms of molecular weight distribution. However, kraft lignin precipitated with citric acid had the highest molecular weight distribution as well as the highest polydispersity index. Other author also observed that the use of citric acid for
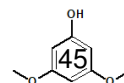
Table 2.2: Molecular distribution of the lignins precipitated with different acids.

	KL	KLA	KLC	KLL
$\overline{M}$w	2416	1824	4187	2005
$\overline{M}$n	510	458	806	458
PDI	4.7	3.9	5.1	4.3

the kraft lignin precipitation, made the lignin high molecular weight and broad molecular weight distribution.[140] Additionally, a clear trend was observed between the molecular weight and the polydispersity of kraft lignins with the strength of the used organic acids. The molecular weight was increased with increased ionic strength (AA > LA > CA) of the organic acid. Fig. 2.3 shows the molecular distribution of precipitated Kraft lignin samples.
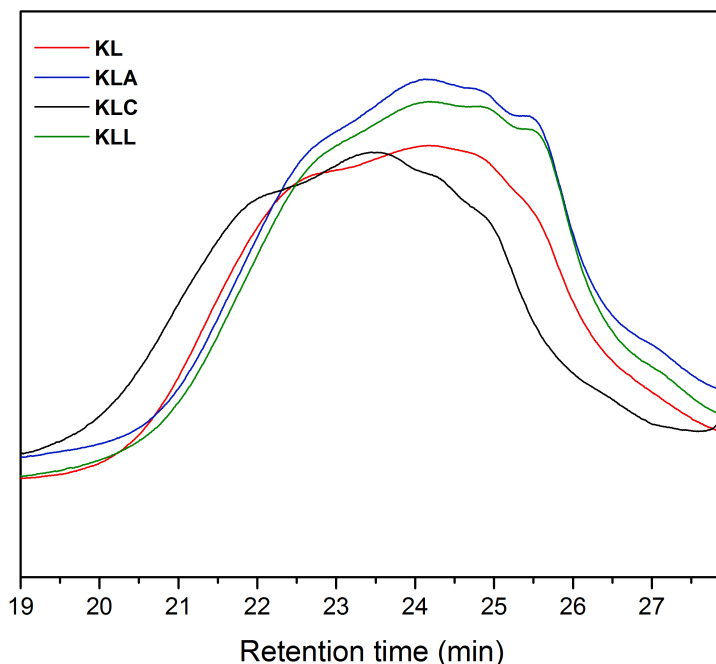

Fig. 2.3: Molecular distribution of precipitated Kraft lignin samples.

2.4.1.2   Chemical structure

The functional groups present in the lignin structure precipitated with SA and some organic acids were analyzed by spectroscopy as shown in Fig. 2.4. The FTIR spectra of the lignins showed similar peaks between them; however, some differences in the intensity of the lignin spectrum precipitated with SA compared with those precipitated with organic acids were observed. The broad band between 3700 and 3000 cm^{-1} can be attributed to aliphatic and aromatic OH groups stretching vibration. In this region, the most intense absorbance was observed in KL can be related to its higher moisture content (Table 2.1). Lignin precipitated with organic acids presented a sharp and weak peak around 2971 and 2943 cm^{-1} due to the asymmetric and symmetric stretching, respectively, of C-H in methylene and methyl groups, whereas for lignin precipitated with SA these two peaks were more intense. In addition, the peak at 2841 cm^{-1} which correspond to the C-H stretching of the methoxyl group[141] appears in the lignins precipitated with organic acids. The spectra of these lignins show that the stretching vibration of the carbonyl groups (C=O) appears at 1738 cm^{-1} which corresponding to the ester, aldehyde, and unconjugated ketones. And at 1700 cm^{-1}, attributed to non-conjugated carboxylic acids carboxylic acids.[142] On the other hand, in the KL spectrum, C=O was shown as a shoulder but the signal of carboxylic acids was more intense.[143][73][144] These indicating that Kraft lignins precipitated with organic acids manifested higher oxidized substructures in their chemical structure than KL. Peaks around 1600 and 1515 cm^{-1} were due to the C=C related to aromatic skeletal vibration and the peaks at 1462 and 1425 cm^{-1} were assigned to C-H deformation in -CH$_3$ and -CH$_2$-, respectively. The signal at 1365 cm^{-1}, which corresponds to the aliphatic C-H stretch in -CH$_3$ of syringyl unit, was only observed in the case of Kraft lignins precipitated with organic acids. Moreover, the peak at
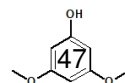
1330 cm^{-1} demonstrated the presence of syringyl units (aromatic ring breathing). Some characteristic bands associated with elemental units in lignin molecule were detected at 1220, 1110 and 1025 cm^{-1}, corresponding to C-C, C-O, and C=O stretching, aromatic C-H in-plane deformation (syringyl) and aromatic C-H in-plane deformation (guaiacyl).
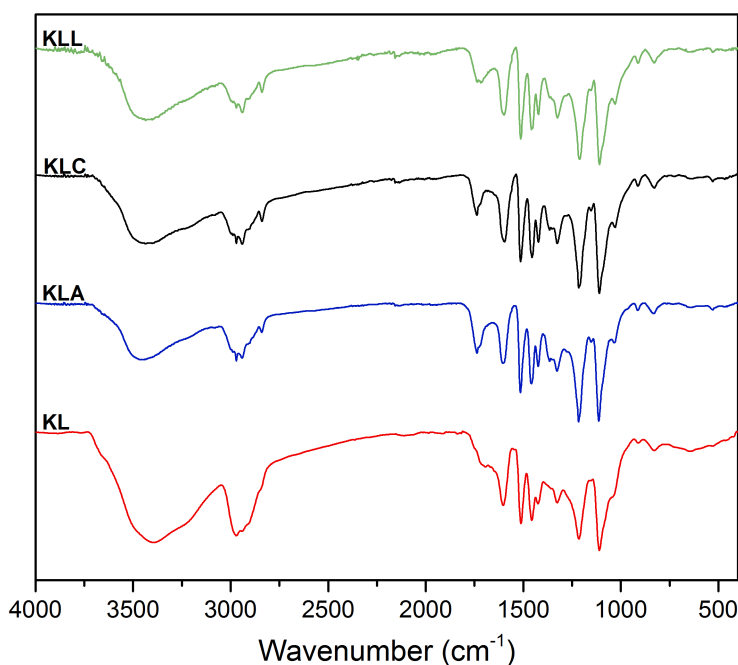

Fig. 2.4: FTIR spectra of precipitated Kraft lignin with sulfuric acid and some organic acids.

The volatile compounds of different Kraft lignin samples were analyzed by pyrolysis gas chromatography mass spectrometry (Py/GC-MS) at 600 °C and the syringyl/guaiacyl ratio (**S/G**) was figured out. Released products during pyrolysis are usually related to phenols, acids, esters, and aldehydes. Table 2.3 catalogs the identification of 29 phenolic compounds, which represents 93-96% of the lignin samples. The identified pyrolysis products were classified into four
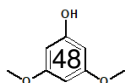
categories according to their aromatic structure: phenol-type compounds (**H**), guaiacyl-type compounds (**G**), syringol-type compounds (**S**), and catechol-type compounds (CA). Although in all Kraft lignin samples the majority of compounds released during the pyrolysis derived from syringyl units, as expected for coming from hardwood, as regards to the monomeric composition, significant differences were observed between them. Despite the origin being the main responsible of the monomeric compositions of lignin molecule, this study evidenced that the precipitation step also have a significant contribution on the final chemical structure.

Lignins precipitated with organic acids presented higher **S**/**G** ratio than Kraft lignin precipitated with SA, especially in the case of lignins precipitated with citric and lactic acids; where found around 76% of syringyl units and 14-16% of guaiacyl units were found. Therefore, the use of organic acids for the precipitation of lignin, apparently, promote the generation of lignin with less condensed structures because of their higher content on **S**-unit. This content (**S**-unit) is widely related to the degree of condensation in lignins, since the presence of methoxyl groups (-OCH$_3$) in C$_3$ and C$_5$ positions of the aromatic ring avoid the formation of the condensed bonds like β-5' and, especially 5-5', which is formed during the pulping stage.[145]

Besides, high amount of fatty acids derivatives (esters) were detected in the case of Kraft lignin precipitated with SA. The presence of fatty acids are commonly associated to the origin and their resistance to thermochemical extraction process.[146][147] However, in the case of lignins precipitated with organic acids, substantially lower amount of fatty acid derivatives was observed ($<$ 2%), confirming once again, that the use of organic acids for the recovery of Kraft lignin from the industrial black liquor make the resultant lignin less contaminated of impurities.

In order to get a better understanding about the structure differ-
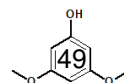
Table 2.3: Identification of the pyrolysis products from Kraft lignin precipitated with different acids.

Compound	Area percentage (%)				Mass fragments
	KL	KLA	KLC	KLL	
Phenol	0.30	0.31	0.19	0.25	94/66/65
p-cresol	0.44	0.42	0.22	0.31	107/108/77
o-cresol	0.47	0.26	nd	0.19	107/108/46
4-Ethylphenol	0.58	nd	0.17	nd	107/122/77
mp-xylenol	nd	nd	nd	0.18	122/107/121
Total	*1.79*	*0.99*	*0.58*	*0.94*	
Catechol	1.71	nd	1.02	0.76	110/64/63
3-Methoxycatechol	11.19	11.67	7.75	9.42	140/125/97
4-Methylcatechol	0.60	0.88	0.38	0.56	124/123/78
Pyrocatechol	0.81	nd	nd	nd	110/82
Total	*14.32*	*12.55*	*9.15*	*10.74*	
Guaiacol	5.01	3.69	8.35	5.63	109/124/81
3-Methylguaiacol	1.12	nd	0.58	nd	123/138/77
4-Methylguaiacol	6.04	6.57	1.47	2.99	138/123/95
4-Vinylguaiacol	2.62	1.94	2.32	2.04	150/135/107
4-Ethylguaiacol	4.04	2.17	0.91	1.78	137/152/122
Isoeugenol	1.04	0.59	0.33	0.43	164/77/149
Vanillin	0.72	1.24	1.15	0.92	151/152/81
Guaiacyl acetone	0.32	0.64	0.47	0.47	137/180/122
Acetoguaiacone	0.42	0.62	0.42	0.61	151/123/166
4-Propylguaiacol	0.38	0.55	nd	nd	137/166/122
Total	*21.70*	*18.01*	*15.99*	*14.87*	
Syringol	17.78	17.78	44.65	30.47	154/139/111
4-Methylsyringol	13.12	15.08	6.86	13.74	168/153/125
4-Ethylsyringol	5.56	5.89	3.12	5.31	167/182/168
4-Vynilsyringol	5.03	5.59	5.43	5.23	180/165/137
4-Allylsyringol	4.91	8.47	5.35	6.62	194/91/179
3,4-dimethoxyphenol	nd	0.60	nd	1.83	154/139/151
Acetosyringone	nd	0.67	0.77	0.72	181/196/153
Syringaldehyde	nd	1.72	0.97	1.10	182/181/111
4-Propylsyringol	0.97	1.13	0.39	0.89	167/196/168
Total	*47.67*	*56.92*	*67.54*	*65.91*	
Sulfur derivatives	2.44	1.87	1.44	1.58	
Furan derivatives	0.30	0.06	nd	0.10	
Fatty acids	4.78	1.99	0.64	0.86	
S/G	**2.86**	**3.86**	**4.80**	**5.10**	

ences between precipitated Kraft lignins, lignin-originated pyrolysis products were grouped according to their structural characteristics, as was reported in a previous work[148] (Table 2.4). This analysis is a useful tool to show clearly structural differences between isolated Kraft lignins.

The results demonstrated that Kraft lignins from the precipitation using organic acids had higher content of methoxylated phenolic substructures than KL, and these substructures were more abundant as increased the ionic strength of the organic acids used as precipitating agent.

On the other hand, it was observed that guaiacyl and syringyl derived compounds with non-substituted saturated chains were less abundant in the case of the Kraft lignins isolated with organic acids than in KL.

In general, KLA, KLC and KLL showed higher content of units with unsaturated side chains and oxygen-containing groups in the side chains than KL. The highest amount for these two functional groups was found for KLA, and it was noticed a clear reduction as the ionic strength of the organic acid increased. Although double C=C bonds can be formed during the pyrolysis process,[148] oxidized substructures come from the original chemical structure when lignin is pyrolyzed.[149] Therefore, the use of organic acids generated lignins with largest amount of aromatic substructures containing aldehydes and ketones, which indicated the presence of greater content of carbonyl groups in the chemical structure. This result is in accordance with the FTIR, which showed that characteristic absorption of C=O stretching vibration was stronger in the case of KLA, KLC, and KLL.
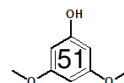
Table 2.4: Relative content (%) of groups of lignin-derived compound with phenolic hydroxyl groups and other specific functional groups.

| Pyrolysis products	KL	KLA	KLC	KLL
Methoxylated phenolic groups (%)[a]	80.56	86.60	91.28	90.19
Non-substituted saturated chains (%)[b]	33.62	32.95	14.11	25.95
Unsaturated side chains (C=C) (%)	13.59	16.59	13.43	14.33
Oxygenated groups in the side chains (C=O) (%)	1.46	4.88	3.78	3.82
$(ArC_1+ArC_2)/ArC_3$[c]	5.6	4.0	4.1	4.5

[a] Guaiacyl and syringyl derived compounds; [b] Short and propanoid side chains; [c] Ratio between phenols with 1 and 2 carbons and 3 carbons in the side chains

2.4.1.3 Thermal stability

The change in mass that a polymer undergoes as a function of temperature and/or time is measured by thermogravimetric analysis. Such information is very useful for predicting the thermal stability of the polymeric material, which in some cases may restrict its processing temperature by losing its applicability in some fields.[150]

In this context, precipitated lignin was analyzed by thermogravimetric analysis and the influence of the type of precipitating acid on its thermal degradation was evaluated. The thermogravimetric (TGA) and first derivative (DTG) curves of lignin samples under nitrogen atmosphere are presented in Fig. 2.5 and the main characteristic temperatures together with the char residue are summarized in the Table 2.5.

It was verified that the use of stronger organic acid as a Kraft lignin precipitating agent leads to less thermally stable lignin (KLC). However, KLA presented slightly higher thermal decomposition temperatures than KL. It was previously reported that lignins with high ether bonds content and low condensation degrees in their chemical structure usually have lower thermal stability.[129][151] It is widely associated to the S unit content in the monomeric composition of lignin since the high methoxyl content or high S/G ratio limit the formation of C-C linkages.

52
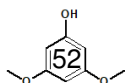
From DTG curves it was observed several weight loss stage in the lignin samples. The first weight loss stage (3.-7%) below 100 °C was related to the gradual evaporation of moisture. Besides that, around 150 °C a small loss of mass was observed, probably due to the presence of fatty acids as detected in the Py/GC-MS.

In relation to the decomposition of lignin, two main stages of degradation were observed. The first stage of mass loss, centered between 230-243 °C was related to dehydration of the hydroxyl group located in the benzyl group, as well as the fragmentation of the bond between β-aryl and α-aryl ether units.[152] The maximum degradation rate (T_{max2}) was identified between 327-368 °C. During this degradation step, aliphatic side chains start splitting off from the aromatic ring (around 300 °C). After, methyl-aryl ether bond and C-C cleavage (300-400 °C) between structural units take place.[144][153]

Table 2.5: Thermogravimetric parameters of different Kraft lignin samples.

Samples	T_{max1} (°C)	wt%	T_{max2} (°C)	wt%	Char yield at 800 °C (%)
KL	240.2	9.29	365.2	30.6	39.3
KLA	243.6	8.10	368.0	28.6	39.8
KLC	230.7	10.34	327.2	27.2	40.9
KLL	236.9	9.93	345.6	29.5	39.2

2.4.2   Experimental design of liquefied Kraft lignin under reflux

2.4.2.1   Effect of reaction conditions on the liquefied lignins

The results of yield, A*n*, OH*n*, and viscosity of the obtained polyols under reflux as a function of reaction conditions are shown in the Tables 2.6-2.8. As it can be observed in Table 2.6, the conversion of Kraft lignin varied from 61.97% (7C, Table A.1) to 98.88% (4C, Ta-
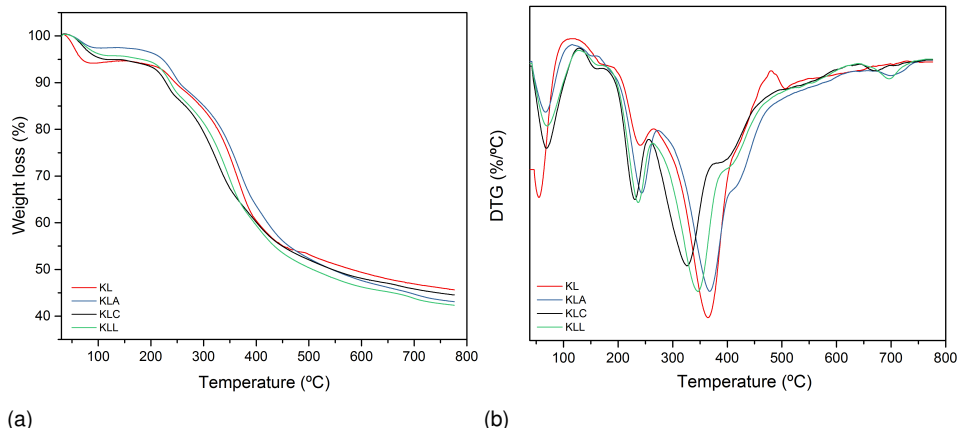
(a)   (b)
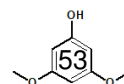
Fig. 2.5: TG (a) and DTG (b) curves of lignin samples precipitated with different acids.

ble A.1). These extreme yield values were found at 60 min with 6% SA, 15% mass (7C) and 3% SA, 20% mass (4C), respectively. In these samples, the increase from 15 to 20% of lignin together with the decrease of 6 to 3% catalyst increased its conversion to 59%. Regarding to the catalyst, most of the high yield values occurred in the presence of 3% SA. This suggests that, in the absence of SA the conversion of lignin is more difficult, while in high concentrations, the repolymerization reaction were dominant.

Table 2.6: Yield of liquefied Kraft lignin under reflux.

| | | Yield (%) | | |
| | | Weight of lignin (%) | | |
Catalyst (%)	Time (min)	15	20	25
	60	68.32	68.41	96.70
0	80	81.58	78.62	94.13
	100	81.68	67.78	70.30
	60	95.70	98.88	95.40
3	80	97.90	97.26	93.19
	100	98.17	96.80	92.10
	60	61.97	95.88	79.79
6	80	82.67	81.54	94.98
	100	72.24	72.43	84.63

54

ANOVA analysis of the yield of polyols showed that only the catalytic variable was significant ($p < 0.05$, Table A.2) and that the adjusted mathematical model could explain 46.28% of the yield behavior following equation **??**. The contribution of each variable on the yield is shown in a standardized Pareto chart and the response surface method exhibited the interaction of the variables (Fig. 2.6).
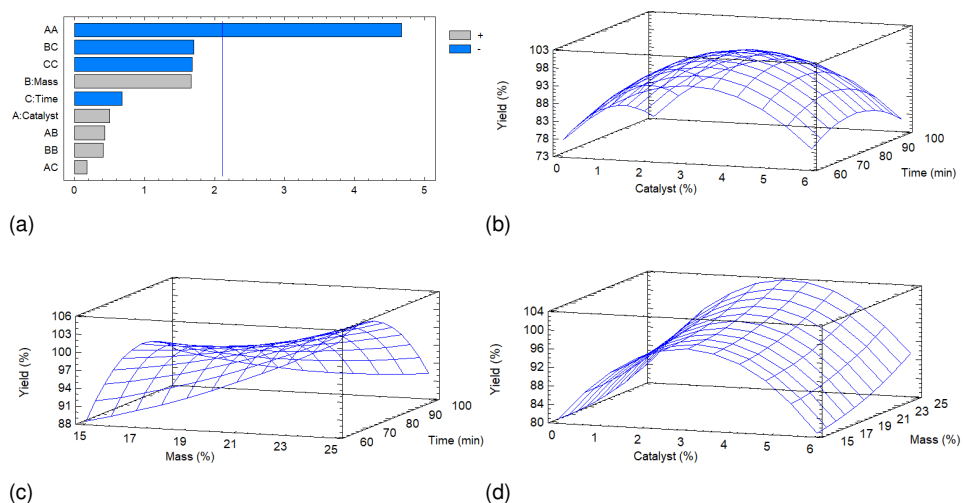

Fig. 2.6: Pareto chart and response surface plot showing the influence of the variables on the yield of the polyols. The vertical line in Pareto chart (a) represents the p-value ($p < 0.05$).

Table 2.7 shows the acidic substances and hydroxyl groups of the obtained polyols. The minimum content of the acid compounds (6.04 mg KOH.g^{-1}) was formed over 100 min (10C, Table A.1) while the maximum (16.63 mg KOH.g^{-1}) was during 80 min (6C, Table A.1). Based on the catalyst parameter, the lowest and highest formation of acidic substances occurred in the polyols performed in the absence of SA. In relation to the percentage of mass, a high A*n* value was obtained with 25% of lignin and at 15% was observed low acid content.

The different reaction conditions promoted a wide variation in the values of the hydroxyl groups in the polyols (Table 2.7). The result-
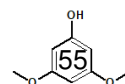
Table 2.7: Acidic substances and hydroxyl groups of liquefied Kraft lignin under reflux.

Catalyst (%)	Time (min)	mg KOH.g^{-1} Weight of lignin (%) 15 An	OHn	20 An	OHn	25 An	OHn
	60	8.28	402.43	10.84	983.09	10.06	1687.97
0	80	16.63	1827.66	14.77	2314.11	50.49	1363.59
	100	6.04	2556.47	7.57	904.61	11.96	1773.06
	60	17.29	2092.55	23.17	924.97	12.48	1582.62
3	80	24.25	2399.51	13.95	2351.04	12.64	2354.60
	100	12.42	544.83	14.22	1731.10	14.23	1672.99
	60	13.54	733.45	33.35	2173.90	28.30	1280.53
6	80	26.31	1372.81	37.03	1716.15	34.00	1550.40
	100	44.44	1275.65	6.39	902.34	15.85	558.74

ing OH groups in the liquefied products are generally associated with the conversion of the mass and amount acidic compounds formed during the liquefaction process. At 15% of the lignin and without catalyst, the OH ratio was increased from 402 mg KOH.g^{-1} to 2556.47 mg KOH.g^{-1} by increasing the reaction time from 60 min (8C, Table A.1) to 100 min (10C, Table A.1). Under this condition, the liquefaction yield was similar to 80 and 100 min (81%, Table 2.7). However, the An formed over 80 min (16.63 mg KOH.g^{-1}) is much higher than at 100 min (6.04 mg KOH.g^{-1}). This indicates that hydroxyl groups were more consume by the acidic substances at 80 min (1827.66 mg KOH.g^{-1}) than at 100 min (2556.47 mg KOH.g^{-1}).

ANOVA analysis showed that the independent variables did not statistically influence the acidic substances of the polyols by reflux (p>0.05, Table A.3) and the adjusted model presented a low coefficient of determination (R^2_{aj}=8.31%). Whereas, ANOVA showed that to the hydroxyl groups of polyols by reflux showed that only the reaction time variable was significantly different (p<0.05, Table A.4) and the adjusted model presented a low coefficient of determination (R^2_{aj}=13.24%). The contribution of each variable on acid number and

OH number is shown in a standardized Pareto chart (Fig. 2.7)
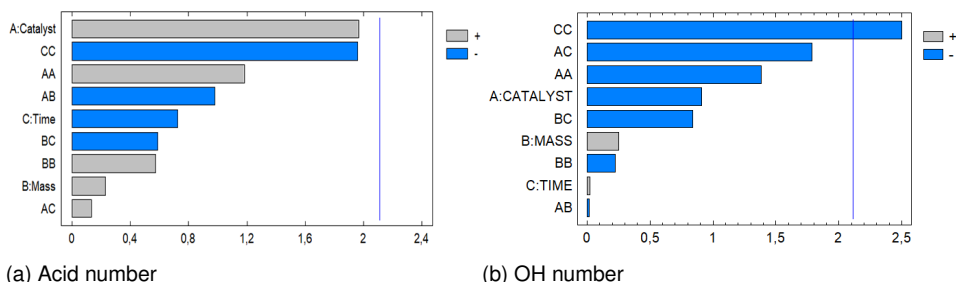

(a) Acid number   (b) OH number

Fig. 2.7: The effect of independent variables on the acid number and hydroxyl groups of liquefied Kraft lignin under reflux shown by a standarized Pareto chart; the vertical line represents the p-value ($p<0.05$).

The highest viscosity was found in sample 26C (1.846 Pa.s, Table 2.8) and the lowest of 0.136 Pa.s in sample 2C (Table A.1). The high ratio of SA (6%) and lignin (25%) used in this liquefaction, indicating that the repolymerization and condensation reactions were dominant. This high viscosity is confirmed by GPC analysis, which showed high molecular weight and polydispersity (3428 g.mol^{-1} and 5.75, respectively). On the other hand, the lowest viscosity value was determined in the short reaction time (60 min) with 20% lignin and without SA.

Table 2.8: Viscosity of liquefied Kraft lignin under reflux.

		Viscosity (Pa.s)		
		Weight of lignin (%)		
Catalyst (%)	Time (min)	15	20	25
	60	0.183	0.136	0.267
0	80	0.190	0.261	0.291
	100	0.196	0.238	0.282
	60	0.556	0.203	0.512
3	80	0.445	0.619	0.386
	100	0.426	0.328	0.605
	60	0.272	0.791	0.644
6	80	1.336	0.869	1.846
	100	0.440	0.688	0.700

Based on the statistical analysis (ANOVA) of the viscosity of liquefied lignin under reflux, time and catalytic variables have significant influence on viscosity ($p < 0.05$, Table A.5). The adjusted mathematical model ($R^2_{aj} = 46.75\%$) can explains 46.75% of viscosity behavior by Equation A.17. The significance of the regression coefficients in the second-order model is shown in a standardized Pareto chart (Fig. 2.8)
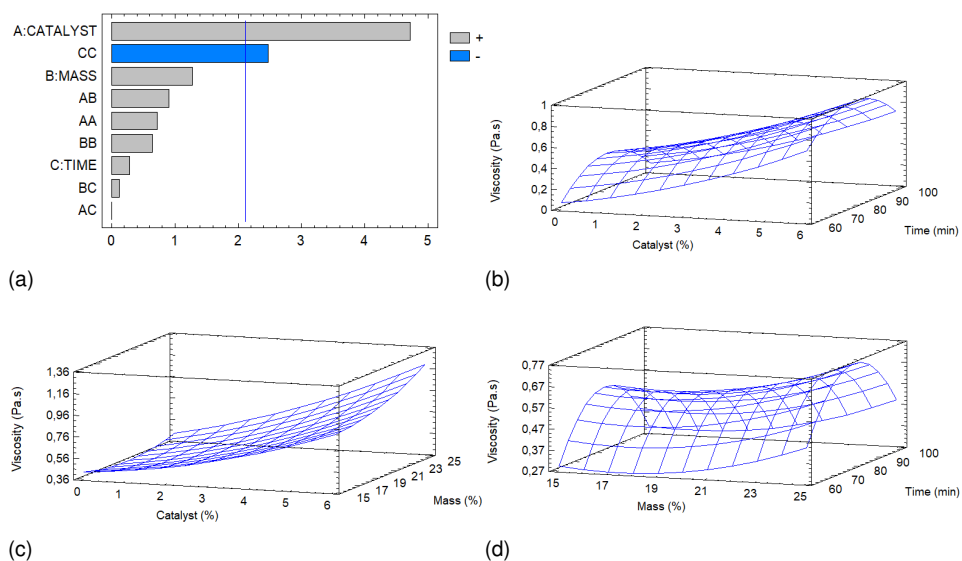

(a)

(b)

(c)

(d)

Fig. 2.8: The effect of independent variables on the viscosity of liquefied Kraft lignin shown by a standarized Pareto chart and RSM; the vertical line in Pareto chart represents the p-value ($p < 0.05$).

The molecular distribution of the polyols obtained by reflux ranged from 1125 g.mol^{-1} to 4855 g.mol^{-1} as summarized in the Table 2.9 and shown in Fig. 2.9. The highest molecular weight was determined in sample 6C which was performed with high concentration of lignin (25%), without catalyst for 80 min. While the lower Mw values were found with 25% lignin, 3% SA at 80 min (1138 g.mol^{-1}) and in the absence of SA, 20% lignin at 60 min (1125 g.mol^{-1}). In addition, a slight upward trend of the Mw values was observed with increasing catalyst concentration, except for sample 6C which was carried out
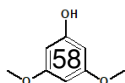
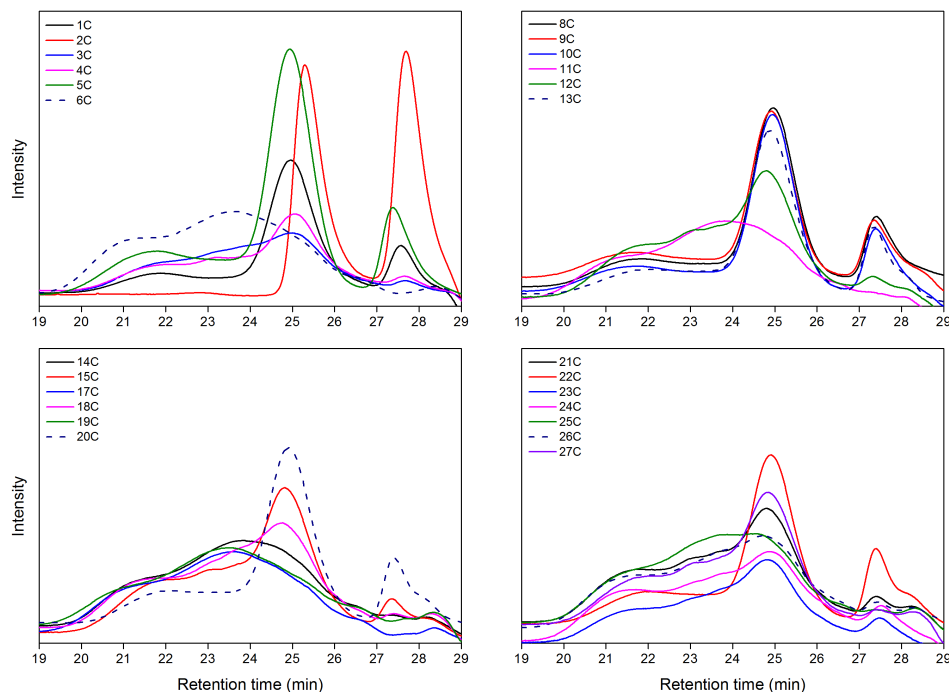without catalyst and shows the larger value of Mw.

Fig. 2.9: Molecular distribution of liquefied Kraft lignins under reflux.

Table 2.9: Molecular distribution of liquefied Kraft lignin under reflux.

Catalyst	Time	Weight of lignin (%)								
		15			20			25		
(%)	(min)	$\overline{M}n$	$\overline{M}w$	PDI	$\overline{M}n$	$\overline{M}w$	PDI	$\overline{M}n$	$\overline{M}w$	PDI
	60	398	1748	4.38	397	1125	2.75	413	1518	3.67
0	80	467	2643	3.69	428	2242	5.24	863	4855	5.62
	100	427	2049	4.79	389	1456	3.74	388	1529	3.94
	60	507	1856	3.65	614	2334	3.79	525	2466	4.69
3	80	551	3009	5.46	537	2831	5.27	404	1138	2.81
	100	522	2200	4.21	556	2458	4.42	541	2359	4.36
	60	nd	nd	nd	514	2247	4.36	589	2351	3.99
6	80	750	4213	5.61	624	3240	5.19	595	3428	5.75
	100	562	3808	6.77	610	3606	5.91	600	3034	5.05

nd = No determined.

The optimization of the experimental design of liquefied lignin under reflux, considering reaction time, catalyst and mass as independent variables, was determined by the analysis of multiple responses (yield, acid number, OH number and viscosity) using the

59

STATGRAPHICS Centurion XV software. The results showed that optimized reaction conditions are 15% of lignin without catalyst for 60 min.

2.4.3 Experimental design of liquefied Kraft lignin under microwave-heating

2.4.3.1 Effect of reaction conditions on the liquefied lignins

The experimental design of lignin under microwave heating had as independent variables the reaction time (5:00 min, 17 min 30 s and 30:00 min), mass (15, 20 and 25%) and catalyst (0, 3 and 6%). The yield, acid number, hydroxyl number, and viscosity were the dependent variables adopted. Tables A.6 shows the experimental conditions and the results of dependents variables (Appendix A.0.2)

The yield of liquefied lignin obtained under microwave heating as a function of different reaction conditions is presented in Table 2.10. The highest conversion of lignin (97.69%) was obtained in a very fast reaction time (5 min, 12M). The microwave liquefaction process takes place in very fast time due to its inherent heating mechanism that allows energy-efficient volumetric heating in the presence of microwave absorber material.[154][155] In the case of lignin, which has very low microwave absorber capacity, this process happens through PEG/G as mixing solvents that present high dipole moment allowing the depolymerization of the lignin in a short time.[156] Similar results of microwave liquefied lignin were found in the literature.[76] In contrast, the lowest yield (63.79) was obtained in 30 min (1M), indicating that the repolymerization and condensation reactions were dominant in a prolonged reaction time. Moreover, the low percentage of lignin (1M) compared to the 12M sample and the absence of catalyst contributed to this lower conversion of lignin. In addition,
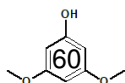
it was observed that most of the high yield values were determined with 3% catalyst, whereas in the absence of catalyst most of the low yield values were observed.
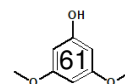
Table 2.10: Yield of liquefied Kraft lignin under microwave-heating.

		Yield (%)		
		Weight of lignin (%)		
Catalyst (%)	Time (min)	15	20	25
	5:00	75.75	84.16	74.19
0	17:30	68.06	64.94	68.80
	30:00	69.97	63.79	66.61
	5:00	93.27	95.27	97.69
3	17:30	94.82	88.37	92.11
	30:00	93.40	95.74	94.22
	5:00	82.08	83.99	91.90
6	17:30	90.65	86.03	71.49
	30:00	73.72	81.67	80.86

Statistical analysis (ANOVA) of the yield of polyols under microwave showed that the reaction time and catalyst variables were significantly different as shown in Fig. 2.10 ($p<0.05$, Table A.7). The behavior of yield can be explained in terms of the adjusted model (R^2_{aj}=75.75%) by equation A.18.

Table 2.11 shows both the acids and hydroxyl groups present in the polyols obtained under different parameters and using microwaves as a heat source. It was observed that the formation of An increases with increasing catalyst loading. SA is a strong acid and in high concentration the lignin fragments can be more easily oxidized, favoring the formation of acid groups.[157] This may occur in samples 5M and 15M which were performed with 15% lignin over 30 min. However, in the first (5M), was used 6% SA and the highest An of 59.58 mg KOH.g^{-1} was found while the lowest (4.72 mg KOH.g^{-1}) was verified without catalyst (15M).

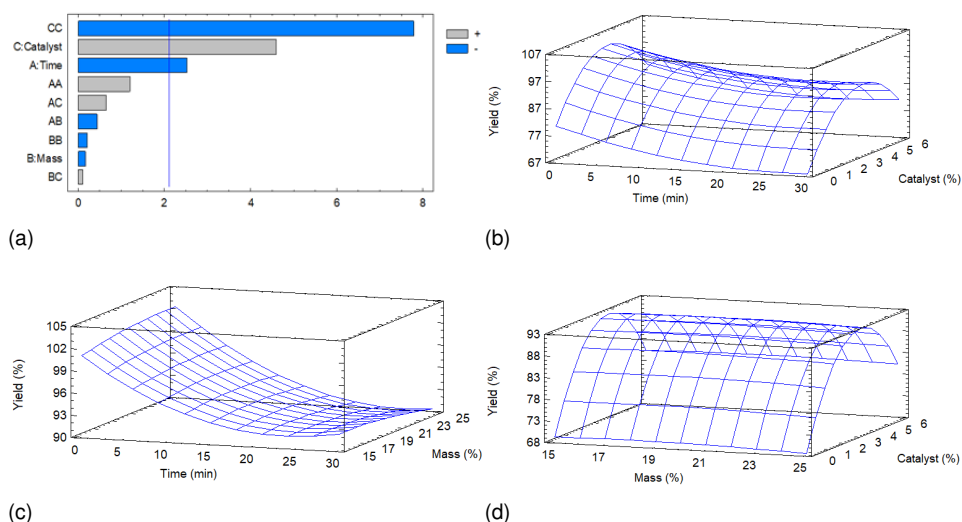Regarding the OH groups, the extreme values were found at 30

61

(a)

(b)

(c)

(d)

Fig. 2.10: The effect of independent variables on the yield of liquefied Kraft lignin under microwave is shown by a standarized Pareto chart and RSM; the vertical line on Pareto chart represents the p-value (p<0.05)

min with different percentages of mass and catalyst (Table 2.11). In the absence of SA and 20% of lignin, the lowest OHn of 188 mg KOH.g^{-1} (1M) was verified. This suggests that apart from the low conversion (63.79%), dehydration and oxidation reactions between solvents and small lignin/polyol fragments were dominant. On the other hand, the highest concentration of OHn (1651 mg KOH.g^{-1},22M) was obtained in the polyol with 3% SA and 25%.

ANOVA analysis of the acid groups of polyols under microwave showed that the catalyst and the interaction of catalyst with mass variables were significantly different (p<0.05, Table A.8). The behavior of acid substances in the polyols may be explain following equation A.19 obtained from adjusted mathematical model (R^2_{aj}=66.07%). Whereas, the effect of independent variables on the hydroxyl groups of polyols under microwave heating was not significant (p>0.05, Table A.9).

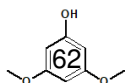Under different reaction conditions and microwave heating, the

62

Table 2.11: Acidic substances and hydroxyl groups of liquefied Kraft lignin under microwave-heating.

		mg KOH.g^{-1}					
		Weight of lignin (%)					
Catalyst	Time	15		20		25	
(%)	(min)	An	OHn	An	OHn	An	OHn
	5:00	10.17	1243.33	9.39	1152.04	15.85	1504.29
0	17:30	7.70	1401.66	21.70	424.52	7.20	1314.84
	30:00	4.72	333.05	18.64	188.96	11.05	671.53
	5:00	33.43	220.15	17.83	537.95	27.09	1147.78
3	17:30	34.49	1579.20	24.41	1150.76	15.80	1175.69
	30:00	27.64	1032.71	20.37	973.31	21.59	1651.24
	5:00	50.79	1189.87	42.52	1425.13	16.93	265.60
6	17:30	37.31	1196.10	44.44	1000.42	37.28	623.58
	30:00	59.58	467.13	36.33	609.11	45.11	1390.89

(a)

(b)

(c)

(d)
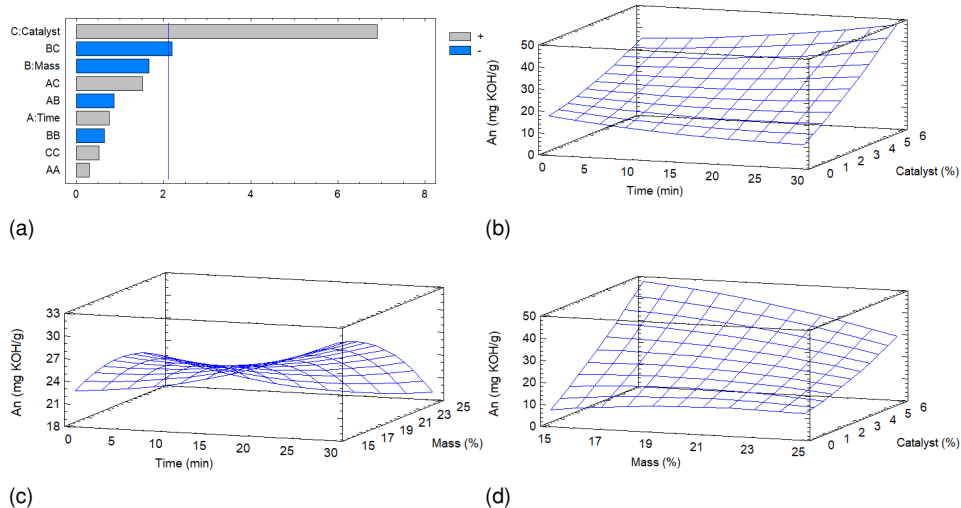
Fig. 2.11: Response surface method plot and Pareto chart showing the effect of independent variables on the acid number of liquefied Kraft lignin under microwave. The vertical line (a) represents the p-value ($p<0.05$).

viscosity of the polyols ranged from 0.055 Pa.s (9M) to 0.612 Pa.s (21M) as shown in Table 2.12 In fact, viscosity values majority were below 0.280 Pa.s. The lowest viscosity was obtained at 5 min without catalyst and 20% of lignin (9M) and the highest value was observed in high catalyst load and mass (6% and 25%, respectively) over 17
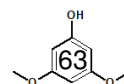
min 30 s. It was noted that the viscosities of the polyols increased with increasing mass and catalyst loading.
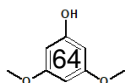
Table 2.12: Viscosity of liquefied Kraft lignin under microwave-heating.

		Viscosity (Pa.s)		
		Weight of lignin (%)		
Catalyst (%)	Time (min)	15	20	25
	5:00	0.099	0.055	0.087
0	17:30	0.116	0.062	0.168
	30:00	0.070	0.091	0.088
	5:00	0.073	0.524	0.282
3	17:30	0.139	0.126	0.241
	30:00	0.220	0.116	0.284
	5:00	0.178	0.546	0.530
6	17:30	0.149	0.418	0.612
	30:00	0.093	0.189	0.081

The viscosity of the polyols under microwave heating was statistically influenced ($p < 0.05$, Table A.10) by the reaction time, catalyst, mass and the interaction between time and catalyst variables, and the adjusted model (R^2_{aj}=54.77%) may explain 54.77% of the viscosity behavior by Equation A.20.

The molecular distribution of the assisted microwave biopolyol is shown in Fig. 2.13 and summarized in Table 2.13. The minimum molecular weight values of 881 g.mol^{-1} and 831 g.mol^{-1} were observed in samples 8M and 25M, respectively. Both polyols were obtained at 30 min, however, the first was run without catalyst and 25% lignin, while the other with 15% lignin and 3% catalyst. Also at 30 min the highest molecular weight of 5240 g.mol^{-1} and PDI of 7.78 (20M sample) was found. However, this sample was processed with high catalyst load and mass (6% and 25%, respectively). In general, the Mw of liquefied lignin under microwave irradiation was similar to or greater than those reported by Xiao and collaborators.[158]

Based on the results of the experimental design, optimized con-
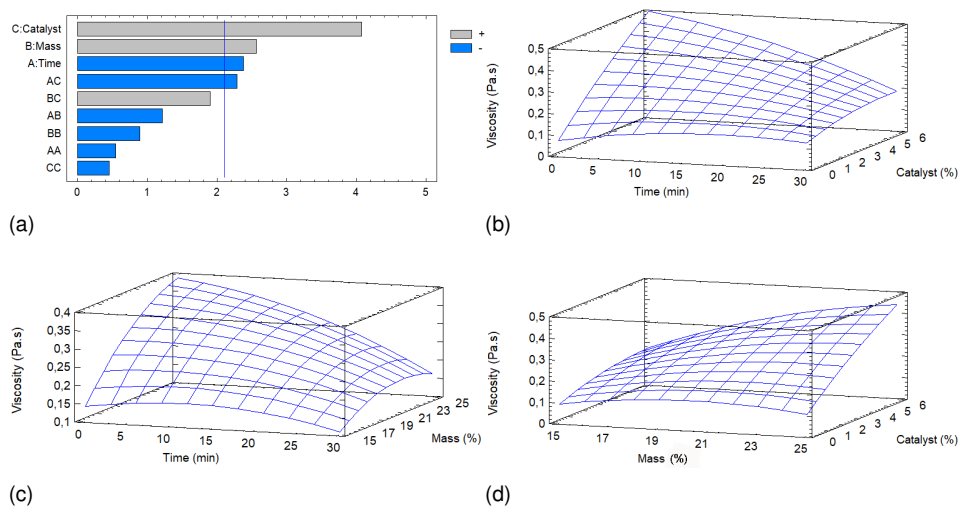
(a)

(b)

(c)

(d)

Fig. 2.12: Response surface method plot and Pareto chart showing the effect of independent variables on the viscosity of liquefied Kraft lignin under microwave. The vertical line (a) represents the p-value (p<0.05).

Table 2.13:   Molecular distribution of liquefied Kraft lignin under microwave-heating.

Catalyst	Time	Weight of lignin (%)								
		15			20			25		
(%)	(min)	$\overline{M}n$	$\overline{M}w$	PDI	$\overline{M}n$	$\overline{M}w$	PDI	$\overline{M}n$	$\overline{M}w$	PDI
	5:00	440	1087	2.47	470	1508	3.20	496	1816	3.65
0	17:30	445	1187	2.66	442	1019	2.30	496	1688	3.40
	30:00	440	1116	5.25	434	1241	2.85	447	881	1.96
	5:00	603	2080	3.44	505	1775	3.51	nd	nd	nd
3	17:30	578	2063	3.56	645	2691	4.17	669	2822	4.21
	30:00	526	837	1.59	666	2723	4.09	562	2234	3.97
	5:00	649	3476	5.35	nd	nd	nd	601	2505	4.16
6	17:30	648	2784	4.29	649	3433	5.28	nd	nd	nd
	30:00	633	3170	5.00	660	3202	4.84	673	5240	7.78

nd No determined.

ditions for liquefied Kraft lignin under microwave heating were determined by the analysis of multiple responses as 20% lignin, 3% SA during 5 min.
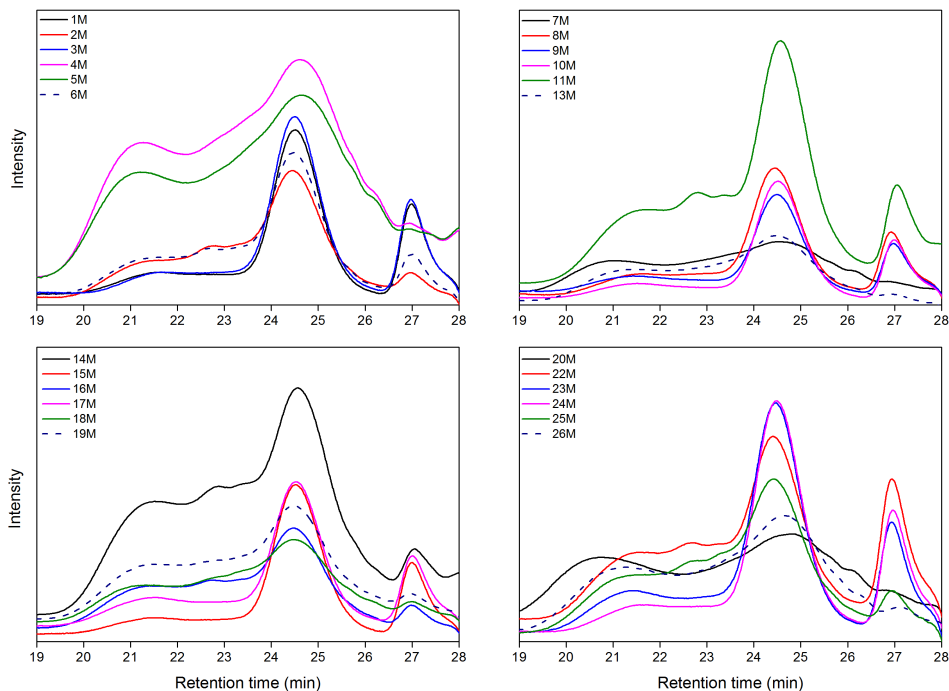
65
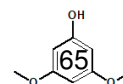
Fig. 2.13: Molecular distribution of liquefied Kraft lignin under microwave heating.

2.4.4 Comparison between liquefied Kraft lignin under reflux and under microwave heating

Liquefied Kraft lignin was performed under reflux and microwave heating and a comparison of obtained yields in terms of reaction conditions is shown in Fig. 2.14. In our experiments under reflux, the highest yield value was observed at 60 min, whereas, under microwave heating the highest conversion occurred at 5 min. This can be explained by the intrinsic volumetric heating of the microwave system, in which radiation penetration and simultaneous heating promote the rapid conversion of lignin.[159] Nevertheless, great percentage of lignin can be converted in a short period of time according to each technique. In the literature, a comparison of these techniques with corn straw, ethylene glycol as solvent and SA at 160 ºC was found.[158] The authors reported high conversion (95.15%) in
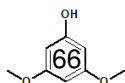
5 min by microwave-assisted heating and 73.98% by reflux in 120 min. It was reported in the bibliography, that at more extent time, the condensation and re-polymerization reactions were dominant causing diminishing of conversion in both techniques.[160] Here, low yield values were observed at 17 min 30 s and 30 min under microwave heating, however, under reflux it this occurred at 60 and 120 min.

Regarding the mass concentration (Fig. 2.14), under microwave heating, most of the low conversion was observed with 15 and 25% of lignin. This indicates that 15% of lignin is insufficient to be liquefied under microwave heating, while at high mass concentration, microwave irradiation promotes a greater depolymerization of the lignin. Therefore, the repolymerization reactions prevail among the small fragments, resulting in low yield. Under reflux, this trend was observed with 15 and 20% lignin.
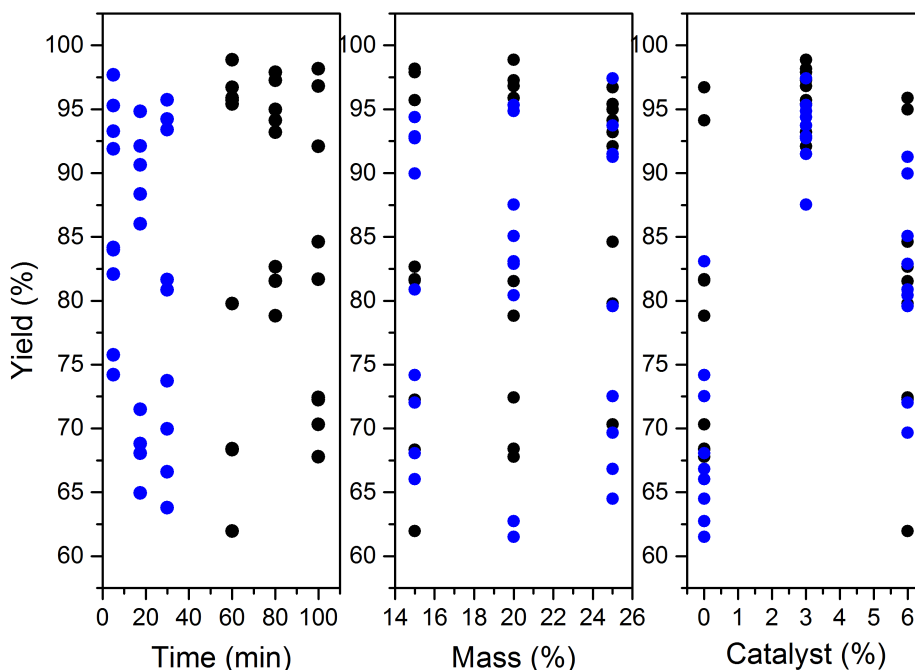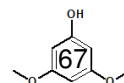

Fig. 2.14: A comparison of the yield of liquefied lignin obtained under reflux (black filled circle) and microwave (blue filled circle).

The catalyst variable had a strong impact on both liquefaction

techniques, as shown in Fig. 2.15. All liquefied lignins made with 3% SA had high conversion values regardless to type of heat source. Pan *et al.*[161] study the liquefaction of wood by both heating techniques using 3% SA. The authors reported lower yields under conventional liquefaction than those by microwave heating. However, in the absence of catalyst, many of the low yield values were checked under microwave conditions. The liquefying residue may be reduced under an appropriate amount of catalyst.[83] Therefore, as observed, the intense heating mechanism promoted by microwaves in the absence of catalyst increases the repolymerization of lignin fragments more than by conventional liquefaction.

A comparison of the number of acids present in the liquefied lignins under reflux and microwaves in shown in Fig. 2.15. The formation of acid substances in the polyols obtained over a long time (100 min) by the conventional technique was generally smaller than those under microwave performed at the long reaction time (30 min). Furthermore, regardless of mass concentration, the acid groups were mostly slightly higher under alternative liquefaction than the conventional ones. This behavior may be related to the oxidation reactions of both the alcoholic solvents and the lignin fragments,[74] which were more predominant under microwave irradiation than through reflux. In the catalyst variable, the number of acids was also higher under microwave than by reflux. In addition, a tendency of increase of the *An* in relation to the increase of the concentration of catalyst for both techniques was observed. This can be explained because SA is a strong acid with high oxidation capacity. Thus, oxidation reactions increased with increasing catalyst concentration, resulting in more acidic substances.

Fig. 2.16 shows the hydroxyl groups obtained by refluxing and microwave liquefaction. The conventional liquefaction presented values of OH groups higher than those of the microwaves, indepen-
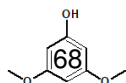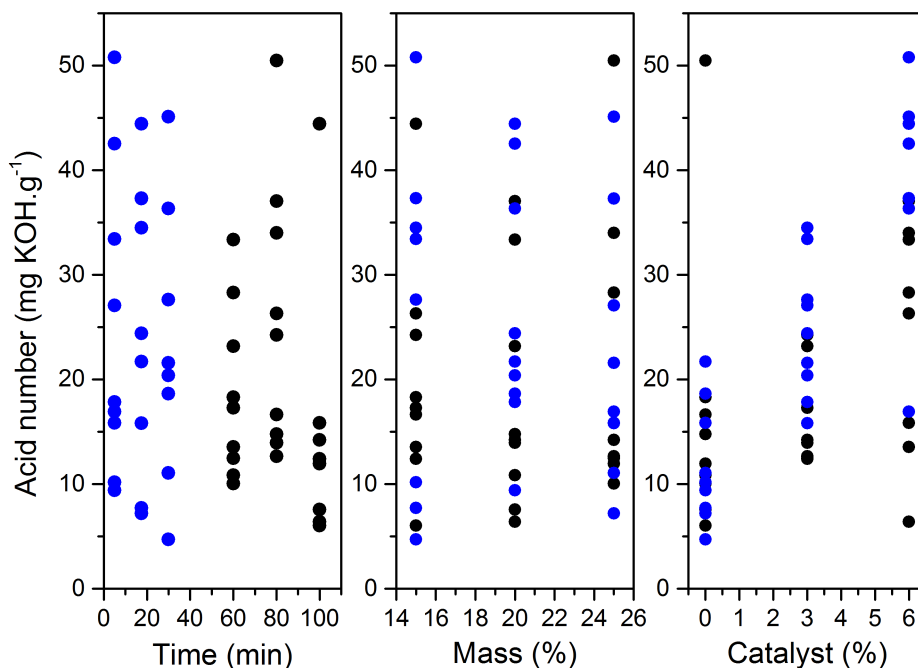
Fig. 2.15: A comparison of the yield of liquefied lignin obtained under reflux (black filled circle) and microwave (blue filled circle).

dently of the reaction time. This suggests that, under microwave irradiation, the dehydration and thermal oxidation of solvents and fragmented lignin prevailed.[162]

In terms of mass concentration, the highest values of OHn were observed in conventional liquefaction, mainly with 15 and 20% of lignin. As mentioned earlier, the liquefied lignin under microwave heating is more susceptible to dehydration, oxidation, re-condensation and repolymerization reactions than by reflux, thus consuming more OH groups.[74 87 90]

Taking into account the concentration of the catalyst, polyols obtained under microwave heating had lower *OHn* values than conventional liquefaction. In addition, a trend of decrease of OH groups in relation to the increase of SA load was observed in liquefaction by reflux.
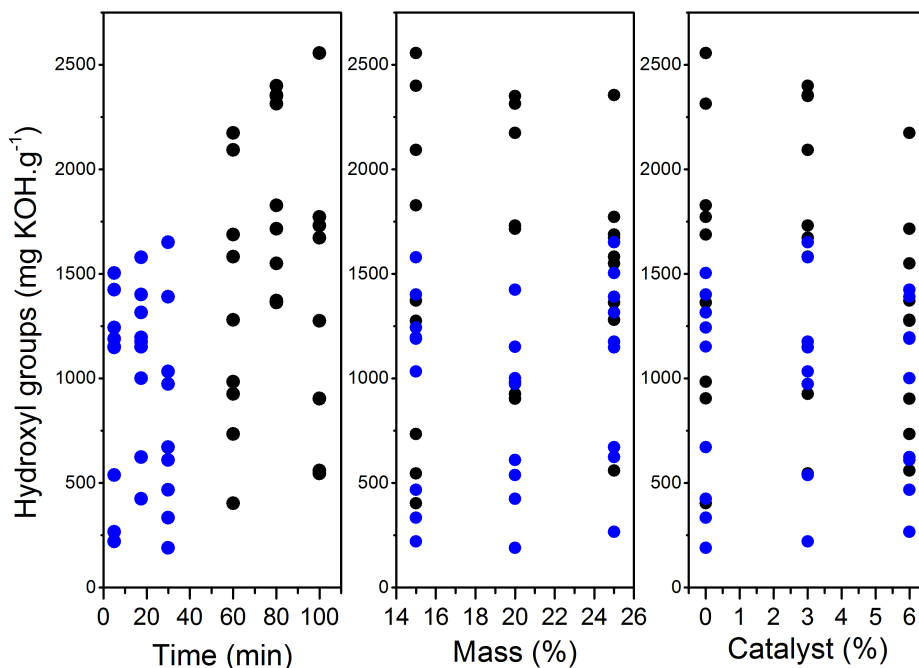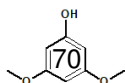
69

Fig. 2.16: A comparison of the hydroxyl groups of liquefied lignin obtained under reflux (black filled circle) and microwave (blue filled circle).

From Fig. 2.17 the viscosity of liquefied lignin under reflux or microwave heating is shown. In terms of reaction time, liquefied lignin using an alternative technique had lower viscosity values than conventional liquefaction.

The viscosity as a function of the mass concentration also presented lower values under microwave heating compared to those by reflux. In addition, in the first technique a viscosity increase behavior is observed with the increase of th mass loading.

Regarding the concentration of catalyst, the viscosity of polyols showed the same tendency in both heating techniques. That is, the viscosity increased when increasing catalyst concentration.
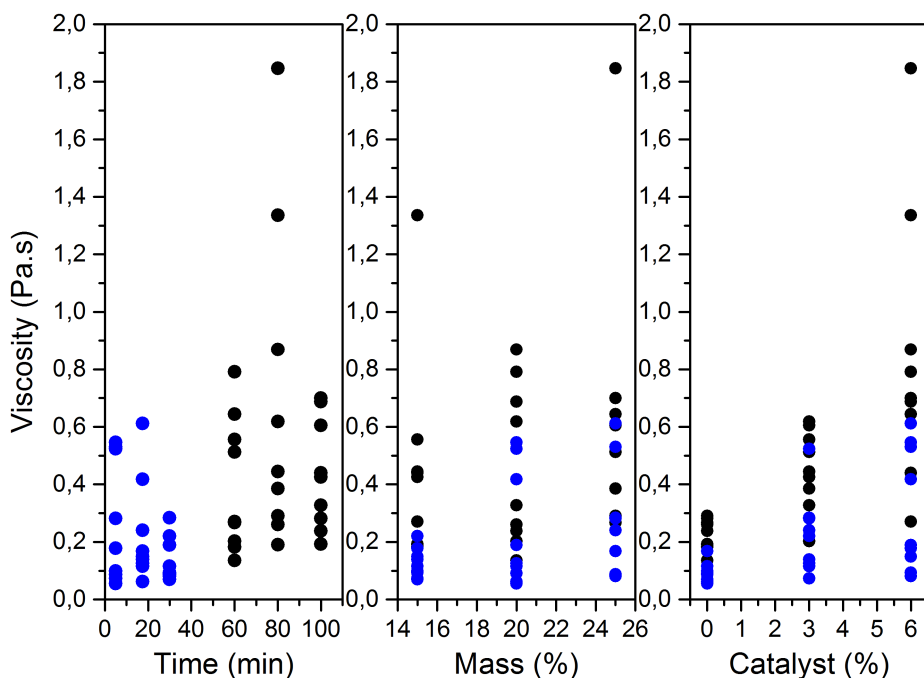
Fig. 2.17: Viscosity of liquefied lignin obtained under reflux (black filled circle) and microwave (blue filled circle).

2.5   Conclusion

The Kraft lignin was characterized and the results are shown below.

Lignins precipitated with organic acids showed higher purity than with traditional sulfuric acid. Moreover, a clear relationship was observed between the ionic strength of organic acids and the molecular characteristics (functional groups, monomer composition and molecular weight) of Kraft lignins. The pyrolysis analysis showed that organic acid precipitated Kraft lignins had a higher content of methoxylated phenolic substructures than KL, as well as a greater number of functional groups, such as carbonyl groups and carbon-carbon double bonds. In addition, thermal analyzes revealed that the use of stronger organic acids leads to less thermally stable lignin, but in all cases, decomposition temperatures were verified above 200 °C.
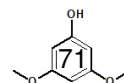
Moreover, the experimental design under reflux showed that the yield of the polyol was influenced by the catalyst variable, while the reaction time affected the OH groups. Viscosity was influenced by reaction time and catalyst variables.

Under microwave heating, the experimental design revealed that the reaction time and the catalyst influenced the yield and, the number of acids was affected by the catalyst and mass variables. On the other hand, the viscosity was influenced by all variables.

The optimized conditions under reflux were determined as 15% lignin, without catalyst at 60 min, while under microwave heating it was 20% lignin, 5 min and 3% catalyst.

The comparison between the techniques of liquefaction showed higher values of yield in 3% SA in both situations. At long reaction time, the formation of acid substances was higher by reflux (100 min) than under microwave (30 min). In addition, a tendency of increase acid number with increasing catalyst loading was observed in both techniques. In general, OH values were higher in conventional liquefaction than the alternative ones, in terms of reaction time and catalyst. The viscosity as a function of reaction time was higher by reflux than under microwave. Moreover, a trend for viscosity growth with increased catalyst loading was verified for both techniques.
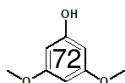
Chapter **3**

Synthesis of optimized polyols

In this chapter, in addition to Kraft lignin, different residues of lignocellulosic materials were used to produce polyols under optimized conditions. But, first, a brief introduction on each agroforestry residue is shown. Moreover, there is a section for the characterization of these wastes.

3.0.1 Agricultural residues

The almond (*Prunus dulcis* Miller [D.A. Webb] syn. *P. amygdalus*) is a species of tree that belongs to the family Rosaceae, native to Mediterranean climate regions of the Middle East and Southern Asia, from Syria and Turkey to Pakistan. Over the centuries, it has been introduced elsewhere and today it is commercially an important agricultural crop. The fruit consists of an edible seed or kernel, shell, and outer hull. It has wide application in the field of food and cosmetic industry, and due to its health benefits and high nutritional value has been used in many formulations of diets. Among nut types, almond is the most consumed in the world in high-income economies.[163]

Fig. 3.1: Almond shells.

The largest producer of almonds, the United States of America, accounts for about 81% of worldwide production, followed by Australia (7%) and Spain with a production of around 4%.[164] which corresponding to approximately 60.400 t of almond, an increase of 12.64% compared to 2017.
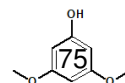
Fig. 3.2: Pecan shells.

Pecan *Carya illinoinensis* (Wangenh.) K. Koch (Juglandaceae) is an edible nut from Central and Eastern North America and the valleys of the rivers of Mexico. It is a large tree, which can exceed 40 meters in height, and can produce for a long time, sometimes during more than 100 years. The pecan is only tree nut native to North America and its name "pecan", derived from the Native American (Algonquin) word "pacane", which described "nuts requiring a stone to crack".[165] It is considered a healthy food because of the high monounsaturated fatty acid content[166] and phytochemical compounds with strong antioxidant properties.[167] Like almond, it is used in a variety of food products and can be consumed raw, roasted and salted.

According to INC Statistical,[163] the global production of pecans was 124,000 metric tons (kernel basis) in the 2017/2018 harvest, with the US and Mexico being the largest producers, accounting for 51% and 41% of world production, respectively.

The first pecans were introduced in Brazil around 1870 by American immigrants.[168] and only began to be economically exploited in the 1970s.[169] Currently, the production of pecans in Brazil accounts for less than 1% of world pecan production.[163]
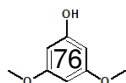
Fig. 3.3: Sugarcane bagasse.

The literature relates to the existence of sugarcane, originally in New Guinea around 8000 BC and slowly spread through Southeast Asia. Notwithstanding, it was only in the middle of the first millennium BC, in India, that sugarcane began to be exploited for the organized production of sugar. However, it was in the 5th century AD, after an Indian chemist discovered how to crystallize extracted sucrose that sugar became a very expensive commercial item from India. Thus, sugarcane plantations began to spread initially in Asia and the Middle East, then in the Mediterranean, Europe, and finally in the New World (the Americas).[170]

Sugarcane is a species of tall perennial grasses of the genus *Saccharum*, tribe Andropogoneae belongs to the family Poaceae. It is an important family of seed plants that includes corn, wheat, rice, and sorghum, in addition to many forage crops. Today, sugarcane is the largest crop of the world,largest crop and Brazil leads the list of sugarcane producers, with an estimated production of 625,96 millions tons for 2018/2019 harvest.[171] Brazil has a well-established and self-sustaining sugarcane plantation, and in recent decades, besides sugar, the production of ethanol from residual molasses is another important product obtained from sugarcane. In both cases, sugar and ethanol production generates huge amounts of bagasse and cane straw (about 35% of the total weight of sugar cane).[172] Bagasse is the main source of energy required in sugar facilities and ethanol distilleries, furthermore, to generate electricity to be sold to the public grids. Although practically everything from the cane can be used, since its by-products and residues can be used in food and feed, or in the co-generation of energy as mentioned above,[173] large
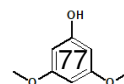
amounts of bagasse remain as a waste, causing problems related to its handling and the environmental impact of its poor disposal. Syrup, molasses, sugarcane juice, rapadura and cachaça (the most popular distilled alcoholic beverage in Brazil) are some foods and popular drinks derived directly from sugarcane.

3.0.2 Forest residues

Pinus radiata D. Don is a softwood tree belonging to the Pinaceae family native to North America, more precisely on a narrow stretch of coast in Southern California.[174] It is also called Pinus insignis, Monterey pine and Radiata pine.[175]

Trees about 30 m tall can be grown in a variety of environments and in some cases

Fig. 3.4: *Milled Pinus radiata sawdust.*

provide higher yields of timber in a shorter time than many native species. Pinus radiata is one of the widely cultivated timber species in the world. Countries such as New Zealand, Chile, Australia, and Spain have large areas for planting. This softwood is easy to work in the manufacture of furniture, presenting very small defects in brushing and molding. It is also used in the pulp and paper industry and to produce packaging, agglomerates, plywood and fiber boards.

Sometimes the term softwood tree is mistaken for low-density wood. Therefore, it is worth mentioning that the first refers to wood that has no pores in its anatomical structure and the other is the amount of mass per cubic metric of wood. For example, radiata pine is a softwood with a density of around 390 kg.m^{-3}, so it is harder (denser) than some hardwoods such as balsa with an average density of 140 kg.m^{-3}
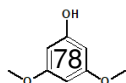
Fig. 3.5: Milled Oak saw-dust.

Oak is a generic term used to refer to more than 600 species of trees and shrubs of the genus *Quercus* belonging to the Fagaceae family and some species of the genus *Lithocarpus*.[176] The genus *Quercus* is native to the Northern Hemisphere and is one of the most important species of wood angiosperm in relation to species diversity, ecological dominance and economic value.[177] This genus is also found in the Americas, Asia, Europe, and North Africa, being dominant in a wide variety of environments.

Oak-wood has a high density (about 0.75 g.cm^{-1}) with high strength and hardness and is very resistant to insect and fungus attack due to its high tannin content. This noble woody is considered as traditional carved wood and has been used since ancient times. For example, in the Viking Age, oak wood was mainly used for the construction of its ships.[178] Today oak wood is mainly used for furniture and floor fabrication wooden structure constructions and barrels production, which is the wood especially preferred for storing and aging wine.[179]

3.1   Objectives

The main objective of this chapter was the production of optimized polyols from different types of lignocellulosic residues, for this, the following specific objectives were carried out:

- Characterization of the lignocellulosic materials;

- The synthesis of the optimized polyols of different lignocellulosic biomass;

- Characterization of the obtained polyols.
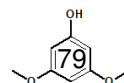
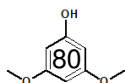## 3.2   Experimental procedure

3.2.1   Raw materials

In this chapter, three agricultural wastes (almond shells, sugarcane bagasse and pecan shells) and two forest residues (pine and oak sawdust) were used. Polyhydric alcohols (polyethylene glycol and glycerol), sulfur, NaOH, toluene, ethanol, acetic acid glacial, 1,4-Dioxane, KOH, phthalic anhydride, pyridine, acetone, solution of dimethylformamide and lithium bromide, and dimethyl sulfoxide were the reagents used in the synthesis and characterization procedures performed in this chapter. Technical informations about these chemicals are listed in Appendix C.

Almond shells were provided by the company "Eloy Castillo Fernandez" in Arnedo/La Rioja, Spain, which produces the varieties Largueta and Marcona of almond. Divinut Industry LTDA located Cachoeira do Sul/RS, Brazil, specializing in shelling of pecans and packaged root seedlings, kindly provided the pecan shells of the Barton, Shawnee, Choctaw and Stuart varieties. The sugarcane bagasse was supplied by Fermentec in Piracicaba/São Paulo-Brazil.

Both forest residues the *Pinus radiata* and American oak, as representative of softwood and hardwood, respectively, were kindly supplied by Serraria Pikabea, Spain. Agricultural and forest raw materials were milled to obtain particles between 0.25-0.40 mm and dried at room temperature before its utilization.

3.2.1.1   Characterization methods

In order to better understand the influence that the different raw materials may have on thermochemical conversion, the lignocellulosic wastes were characterized using different techniques and pro-

cedures described in Appendix A. Fig. 3.6 shows a summary of the characterizations carried out.

3.2.2   Liquefaction procedure

In a typical run, liquefying solvents without or with the desired amount of acid were added into a 500 mL neck glass flask reactor with magnetic stirrer, temperature control and condenser. When the set temperature was reached, the lignocellulosic material was added into the flask and the reaction time was started. After, the reactor was immersed in a cooled water bath to quench the reaction. Liquefied mixture was washed with acetone under vacuum and solid residue was dried in an oven to determine the yield (Equation A.10). Acetone was removed by rotary evaporator under reduced pressure at 49 °C.

3.2.2.1   Liquefied lignin - characterization methods

The yield of polyols obtained from the experimental design were determined as previously mentioned. The acid numbers (*An*) and hydroxyl number (*OHn*) were verified following the standard procedures ASTM D974 (Appendix A.0.2.3) and ASTM D4274 (Appendix A.0.2.4), respectively. The viscosity was measured at 25 °C (Appendix B.5.3) and molecular distribution was determined as reported in Appendix B.2.1. In addition, chemical structure were verified. These procedures and techniques are described in Appendix section and summarized in Fig. 3.6.
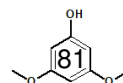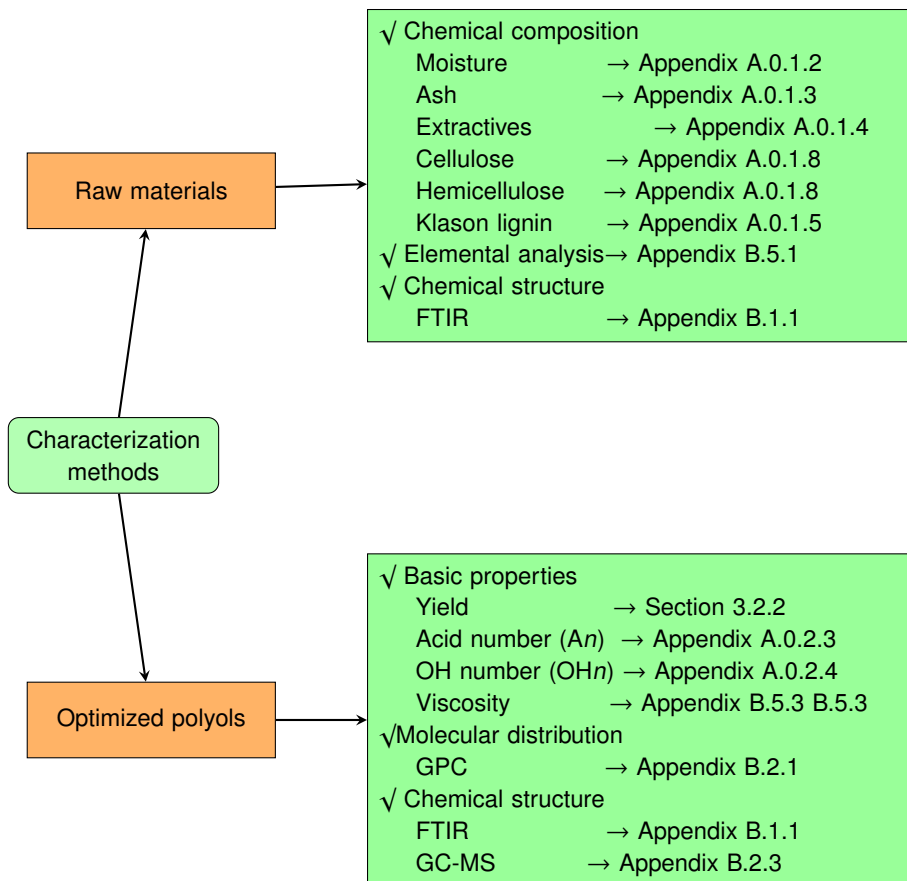
Fig. 3.6: Scheme of the characterization of optimized polyols .

3.3   Results and discussion

3.3.1   Raw materials

3.3.1.1   Chemical composition of raw materials

Chemical composition of agroforestry residues are shown in Table 3.1. Agricultural wastes have similar and lower extractive contents than forest residues. Among the woods, as expected, oak sawdust presented higher extractive content than pine sawdust. It is know that oak barrels are much appreciated to the production of wine because of its extractive content. Behavior similar to the ex-

82
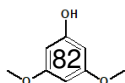
tractives was verified for cellulose and hemicellulose content in relation to the two groups. Otherwise, forest residues presented lower ash content than agricultural residues. Regarding the lignin, the values were significantly different ($p < 0.05$) between the samples, being the highest value for the almond shells and the lowest value for the bagasse.

Table 3.1: Chemical composition of the agricultural and forest residues.

(%)	Almond shells	Bagasse	Pecan shells	Pine sawdust	Oak sawdust
Extractives	2.28^a	2.57^a	2.79^a	4.82^b	6.22^c
Cellulose	35.63^a	35.84^a	35.53^a	38.62^b	40.01^b
Hemicellulose	20.48^a	21.26^a	21.90^a	28.75^b	27.83^b
Klason lignin	38.33^a	22.14^b	37.42^c	27.07^d	24.87^e
Moisture	9.77^a	7.91^b	15.57^c	8.47^b	6.10^d
Ash	3.59^a	2.83^b	1.88^c	$0.41^{\ d}$	0.61^e

The values followed by the same superscript letter in the same line are not statistically different at 95% significance, $p < 0.05$).

3.3.1.2 Chemical structure

FTIR spectra of agricultural and forest wastes are shown in Fig. 3.7. All samples showed a broad band observed between 3700 and 3000 cm^{-1}, attributed to the O-H vibrations, mainly derived from cellulose, hemicellulose and lignin.[180] The peaks around 2900 and 2880 cm^{-1} are assigned to the C-H stretch of the methylene and methyl groups and were found in all samples with different intensities. The C=O vibrations in the carbonyl groups were observed mostly around 1730 cm^{-1}, indicating the presence of ester, aldehyde, Ketone, and carboxylic acid groups. This peak was more intense in the Oak sawdust and almond shells. The spectra showed peaks around 1600 and 1500 cm^{-1} are reported as aromatic ring skeleton.[83 181 182] In PS spectrum these peaks are more evident at 1606 and 1524 cm^{-1}. In addition, at 1458 cm^{-1} the C-H deformation was assigned to the methoxy group in lignin and the symmet-

rical scissoring in pyran ring.[183]. The peak around 1430 cm^{-1} is assigned to the methylene group.[83] Between 1300 and 1000 cm^{-1}, the peaks are ascribed to the C-O stretching and O-H deformation vibrations, indicating the presence of alcohols, phenols, ethers, and esters.[181][184] Moreover, at 1044 cm^{-1} and around 1030 cm^{-1} corresponding to C-O-C stretching glycosidic linkages and C-O stretching of methylol groups were observed.[182][185]
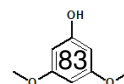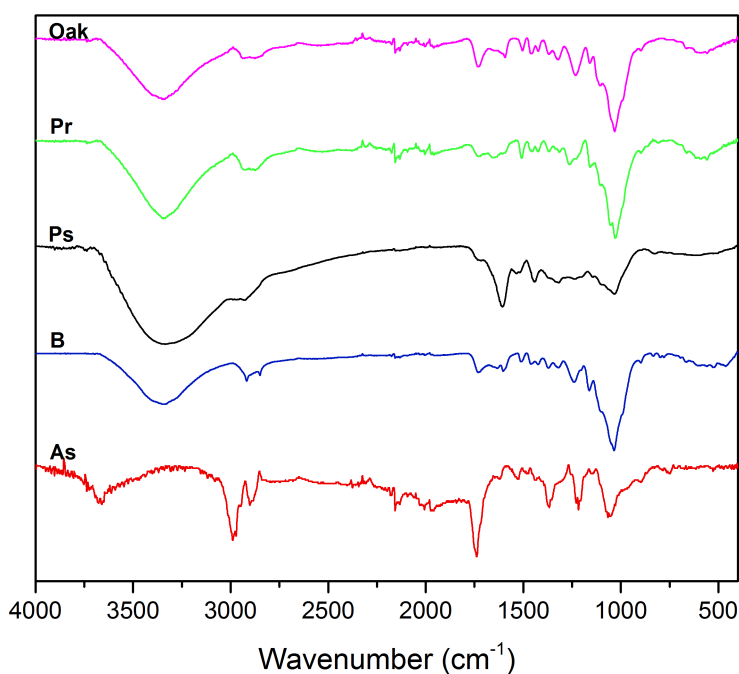

Fig. 3.7: FTIR spectra of agricultural and forest residues.

84

3.3.2   Optimized liquefied lignin

A large amount of Kraft lignin, precipitated with SA was liquefied under optimized reaction conditions (15% of lignin, without SA, at 60 min) how determined in Section 2.4.2. In addition, polyols were produced from lignin precipitated with different organic acids (acetic acid, citric acid and lactic acid) to evaluate the influence of these organic acids, as precipitated agents, on the obtained polyols.

3.3.2.1   Liquefied lignin of different precipitated agents

Fig. 3.8 shows the yield of liquefied lignins obtained from different acids as precipitating agent. The polyol synthesized from lignin precipitated with SA presented higher yield values than those with organic acids. Among the lignins precipitated with organic acids the minimum conversion values were found in LKLA (95.57%) and LKLC (95.65%) polyols, precipitated with acetic acid and citric acid, respectively. In terms of lignin conversion, it can be said that organic acids are an interesting alternative to replace sulfuric acid as a lignin precipitating agent.

Acid number, hydroxyl groups, viscosity and molecular weight of liquefied lignins using different acids as the precipitating agent are shown in Table 3.2. The maximum formation of acidic substances was found in the polyol produced with acetic acid as the precipitating agent (LKLA). Meanwhile, the polyol LHKL and LKLL presented similar values (around 80.0 mg KOH.g^{-1}). Among the lignins obtained with organic acids, it was expected that the LKLC polyol had higher concentration of acid groups than the others due to its ionic strength, but such behavior does not occur. On the other hand, the large amount of acidic compounds observed in LKLA polyol suggesting that the acetic acid used to precipitate the lignin during the liquefaction process contributed to the formation of acid groups, since
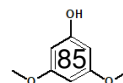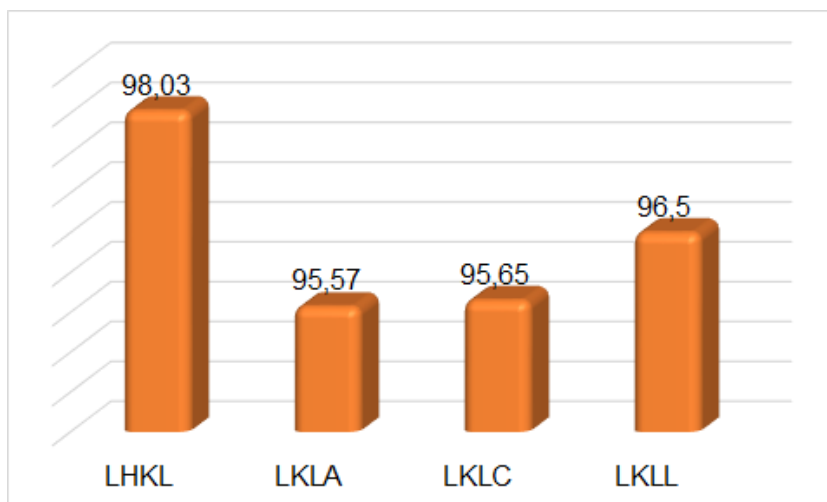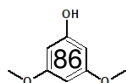
Fig. 3.8: Yield of liquefied Kraft lignin precipitated with sulfuric acid (LHKL) and different organic acids such as acetic acid (LKLA), citric acid (LKLC) and lactic acid (LKLL) with PEG/G = 80/20 (wt%), 15% of lignin, without catalyst, at 160 °C for 60 min.

both LKLA and LKLC polyol have the even yield and similar hydroxyl groups.

The LHKL polyol (precipitated with SA) exhibited the largest hydroxyl groups while the minimum *OHn* value were obtained for LKLC polyol. The results of the OH groups are in agreement with the yield of the polyols, since the *OHn* can be thought in terms of lignin conversion.

The precipitated lignins with different acids were significant in the obtained viscosity ($p<0.05$). Polyols made from lignin extracted with organic acids presented lower viscosity than the LHKL polyol. Moreover, a tendency of decrease of viscosity with increase of the ionic strength of the acid of the precipitation was observed.

Regard to molecular weight, lignins precipitated with SA and lactic acid resulting in polyols with similar molecular weight and polydispersity, as did polyols made using lignins extracted with acetic acid and citric acid. Moreover, lignin precipitated with citric acid provides

86

a polyol with higher molecular weight and polydispersity as shown in Fig. 3.9.

Table 3.2: Results of the basic properties and molecular distribution of the liquefied kraft lignin precipitated with different acids.

	LHKL	LKLA	LKLC	LKLL
An (mg KOH.g^{-1})	0.89 (0.61) [a]	2.21 (0.01) [b]	0.21 (0.01) [a]	0.80 (0.01) [a]
OHn (mg KOH.g^{-1})	871.04 (41.44) [b]	267.32 (17.38) [a]	215.18 (34.76) [a]	353.58(26.26) [c]
Viscosity (mPa.s)	134.40 (1.06) [d]	85.90 (0.07) [c]	53.90 (0.21) [a]	63.30 (0.07) [b]
$\overline{M}$w	1416	2130	2401	1723
$\overline{M}$n	445	491	537	465
PDI	3.1	4.3	4.4	3.7

Values in parentheses are standard deviation. The values followed by the same superscript letter in the same line are not statistically different at 95% significance, p<0.05.
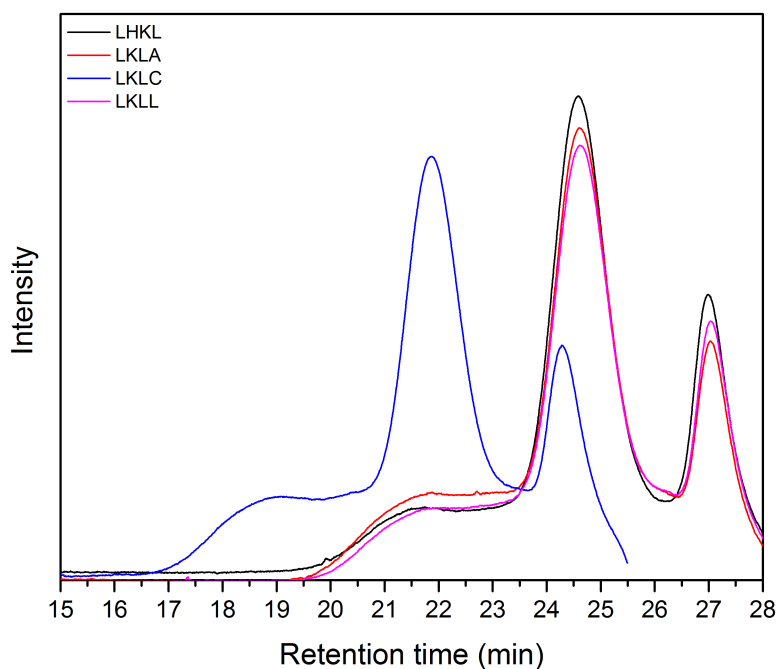
Fig. 3.9: Molecular distribution of the polyol using lignin precipitated with different acids.

The structural changes of the biopolyols were verified by ATR-IR spectra (Fig. 3.10). The broad peak at 3400 cm-1 corresponds to O-H stretching vibration of hydroxyl groups. The peak at 2870 cm-
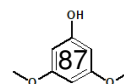
1 was attributed to vibrations of aliphatic C-H bonds of methylene mainly due to the solvents and methyl groups[89]. The absorption at 1709 cm-1 was assigned to C=O stretching of carbonyl and carboxyl groups[98][186]. The signal at 1455 cm-1 is related to C-H asymmetric deformations in methyl, methylene and methoxyl groups whereas at 1350 cm-1 is assigned to O-H in-plane deformation[98]. The region from 1300 to 1000 cm-1 may be assigned to C-O stretching and O-H deformation vibrations, which indicates the presence of alcohols, phenols, ethers and esters groups[187]. The peak at 1222 cm-1 is assigned to C-O stretch derived from methoxyl group due to the presence of syringyl rings[143]. The sharp band observed around 1093 cm-1 could be due to the C-O linkage of alcohols or ether groups[188]. The intensity of this band that could correspond to PEG and the absence of the peak at 1740 cm-1 which is characteristic of ester group, indicated that the liquefied lignin with organic acids are polyether polyols. The peak at 885 cm-1 is ascribed to aromatic C-H out-of-plane deformation[189].

3.3.2.2 Influence of different acids as a liquefying catalyst

The influence of acetic acid, citric acid and lactic acid as catalyst agent in the solvolytic liquefaction process was investigated (Fig. 3.11). For this, SA-precipitated Kraft lignin was liquefied using organic acids at three different concentrations (3, 6 and 9%).

The results show that the different organic acids and its different concentrations did not have influence on the yield of polyols ranging from 88.07% with 6% lactic acid to 85.68% in presence of 3% citric acid. No information was found in the literature on liquefied lignin with organic acids as catalyst in moderate reaction medium using polyhydric alcohols as solvents. Conversion of liquefied Kraft lignin using complex catalyst formulations (acid and metal oxide catalysts) was reported to be around 85.9 - 95.6% under severe reaction con-
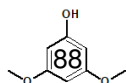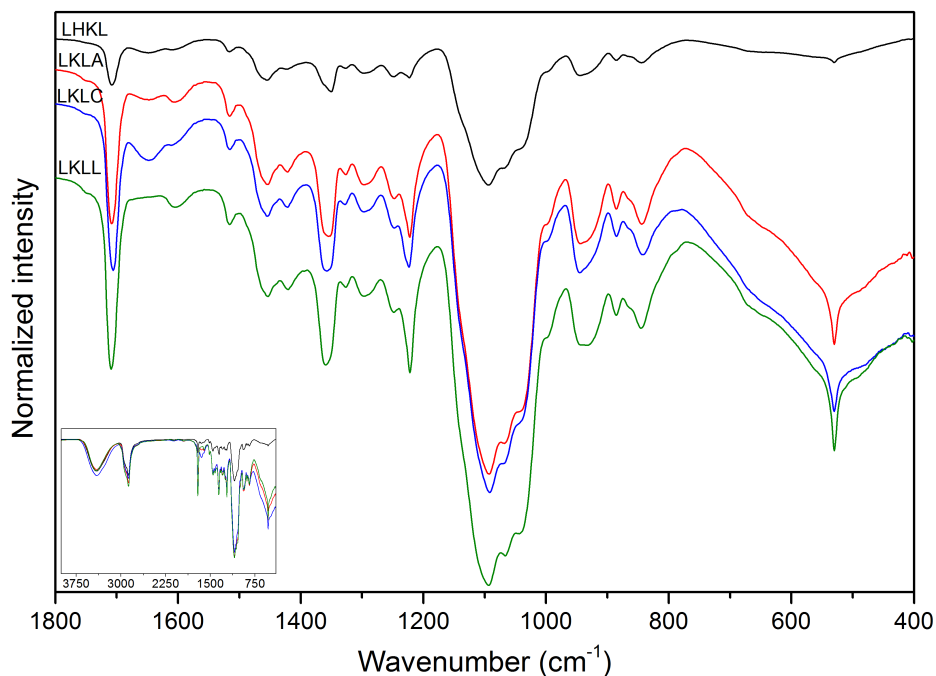
Fig. 3.10: FTIR spectra of the polyols from lignin precipitated with different acids.

ditions such as high temperature and pressure.[190][191] Therefore, renewable organic acids can be considered as a green alternative to the catalysts commonly used in the liquefaction process with polyhydric alcohols.

Fig. 3.12 shows the influence of the organic acids and their concentrations on the acid number and the OH groups of the polyols. The liquefied lignin using acetic acid had the lowest amount of acid groups (0.80 mg KOH.g^{-10}, Fig. 3.12a), while the highest was found with citric acid (10.70 mg KOH.g^{-10}). Acid compounds showed a tendency of increase as ionic strength of catalyst. This indicates that the three carbonyl groups in citric acid could contribute to higher acid values. In fact, with 3% citric acid, the values of *An* were six times higher than those obtained with acetic acid and three times more than the one obtained with lactic acid at the same concentration. Moreover, the concentration also influences the formation of
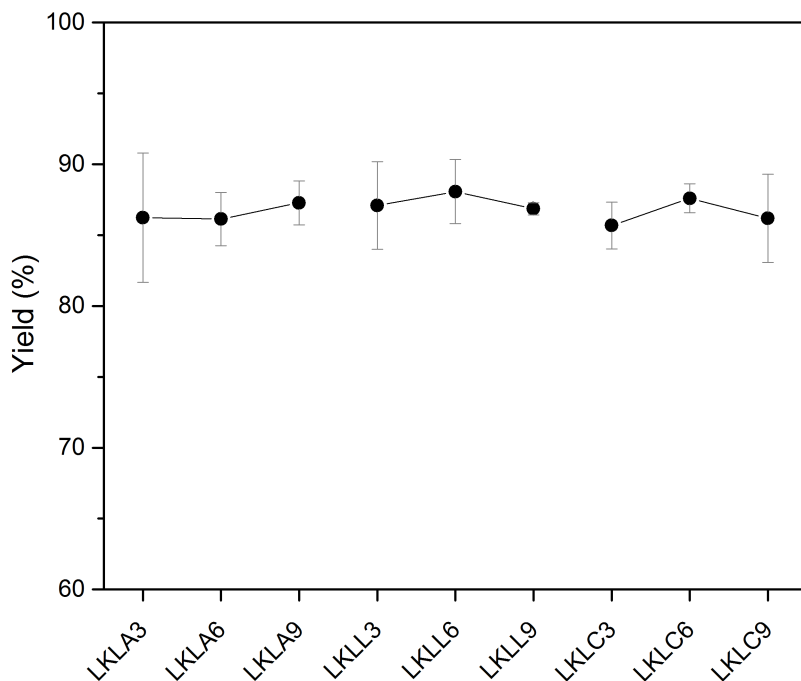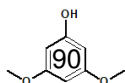
Fig. 3.11: Yield of liquefied Kraft lignin using acetic acid (LKLA), citrit acid (LKLC), and lactic acid (LKLL) as catalyst with 3%, 6% and 9% each one, with PEG/G = 80/20 (wt%), 15% of lignin at 160 °C for 60 min.

An. In general, the acid substances increased with catalyst concentration. All acid values are in agreement with those reported in the literature. [78] [192] [193] [194]

Regard to the hydroxyl groups (3.12b), the lowest *OHn* in all polyols was obtained with 6% of catalyst. As mentioned before, the decrease of the OH groups can be thought in terms of low conversion rate and/or large amount of acidic compounds. At 6% catalyst, the number of acids increases while the hydroxyl groups are consumed, resulting in their decrease. This may be due to the dominant reactions such as the oxidation of lignin[87] and esterification reactions that occur during the liquefaction process. The latter corresponds to the dehydration reactions between acidic substances and polyhydric alcohols, producing ester and consuming the hydroxyl groups.[87] However, at a higher concentration (9%) these reactions were less

outstanding and the OH groups increased for all catalyst. Among the catalysts, the lactic acid provides the highest value at 3% of concentration (660.08 mg KOH.g^{-10}). The obtained *OHn* values are in accordance with those reported in another studies.[76][96][195]
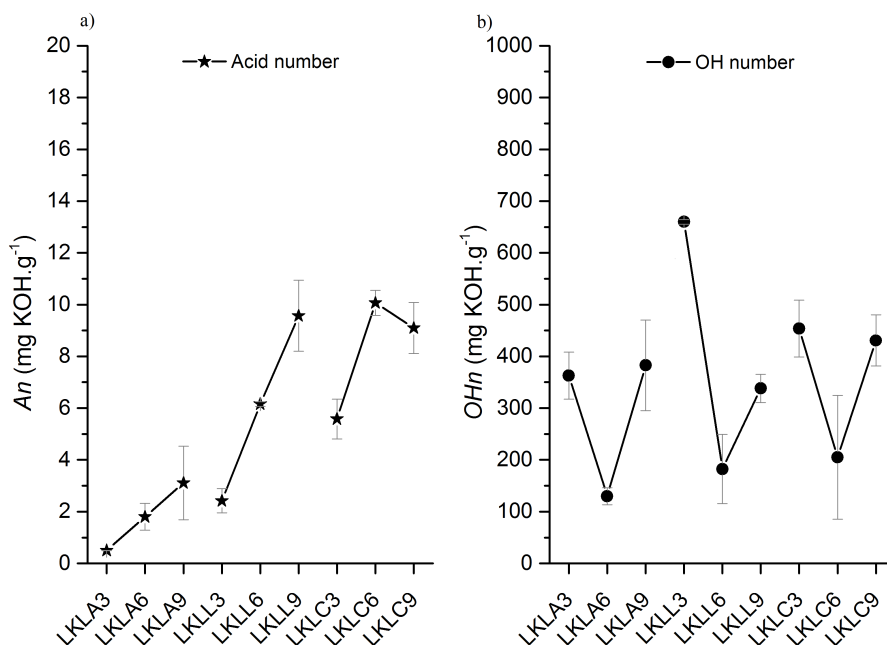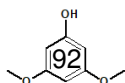

Fig. 3.12: Effect of the catalysts on the acid number (a) and hydroxyl number (b) of liquefied Kraft lignin using acetic acid (LKLA), citrit acid (LKLC), and lactic acid (LKLL) as catalyst with 3%, 6% and 9% each one, with PEG/G = 80/20 (wt%), 15% of lignin at 160 °C for 60 min.

The viscosity and molecular distribution are displayed in Table 3.3. The polyols with organic acids presented the highest and the lowest viscosity using citric acid at 9% (LKLC9) and at 3% (LKLC3), respectively. The lactic acid as liquefaction catalyst provided polyols with a more homogeneous viscosity, ranging from 148.8 mPa.s (LKLL9) to 179.1 mPa.s (LKLL6) and also with acetic acid, whose viscosity varied between 118.0 (LKLA3) and 156.8 mPa.s (LKLA6). Similar results were found in the literature.[192][196] Under organic acid as catalyst, the polyols showed a molecular weight ranging from 1459 g.mol^{-1} (LKLL9) to 1990 g.mol^{-1} (LKLC9) with polydispersity

around 3-4. These values are higher than those reported by Esteves and collaborators.[197]

Table 3.3: Results of the viscosity and molecular weight of liquefied lignin with organic acids.

Samples	Viscosity (mPa.s)	$\overline{M}w$ (g.mol^{-1})	$\overline{M}n$ (g.mol^{-1})	PDI
LKLA3	118.0	1570	410	3.83
LKLA6	156.8	1692	417	4.05
LKLA9	140.0	1592	424	3.75
LKLL3	160.3	1575	410	4.82
LKLL6	179.1	1705	398	3.05
LKLL9	148.8	1459	433	3.36
LKLC3	114.5	1561	441	3.40
LKLC6	201.6	1837	477	3.94
LKLC9	345.8	1990	509	3.92

The structural changes of the Kraft lignin and polyols were verified by FTIR spectra (Fig. 3.13). All liquefied lignin spectra showed a similar profile. The broad band between 3600 and 3100 cm^{-1} corresponds to O-H stretching vibrations of hydroxyl groups and between 2936 and 2870 cm^{-1} was attributed to vibrations of aliphatic C-H bonds of methylene mainly due to the solvents and methyl groups.[89] The absorption at 1709 cm^{-1} was assigned to C=O stretching of carbonyl and carboxyl groups.[98][186] The signals at 1600 and 1515 cm^{-1} were due to the C=C of the aromatic skeletal vibration and the peaks at 1460 and 1425 cm^{-1} were attributed to the C-H deformation in -CH$_3$ and -CH$_2$, respectively. The low intensity of these signals indicates the participation of lignin in the formation of the polyols. The peak at 1220 cm^{-1} assigned to C-O in hydroxyl phenol groups. indicating that the aromatic OH of phenylpropane units participated in the liquefaction reaction.[89] The broad band observed at 1093 cm^{-1} is ascribed to C-O-C ether groups.[188] Their intensity indicate that the obtained liquefied lignins with organic acids are polyether poyols.[90]

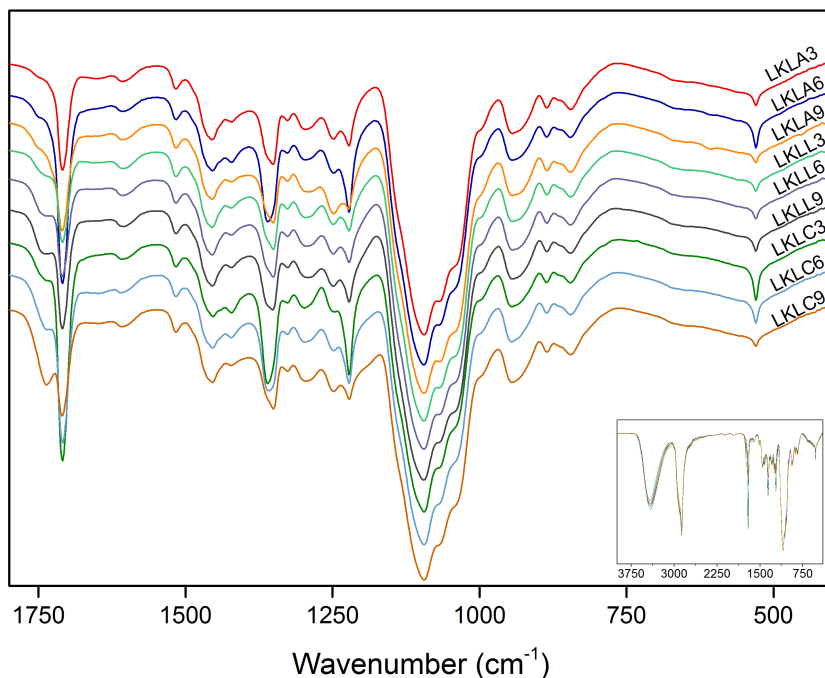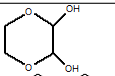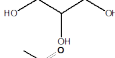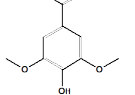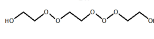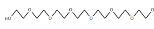Fig. 3.13: FTIR spectra of liquefied Kraft lignin using acetic acid (LKLA), citrit acid (LKLC), and lactic acid (LKLL) as catalyst with 3%, 6% and 9% each one, with PEG/G = 80/20 (wt%), 15% of lignin at 160 °C for 60 min.

Volatile compounds of the liquefied lignin were characterized by GC-MS. The identified compounds are shown in Table 3.4 and the percentage area of each one is depicted in Fig. 3.14 As expected, the identified compounds were obtained mainly from solvents (PEG and G), while others corresponds to lignin derived compounds such as alcohols, ethers, aldehydes, ketones, and phenolics groups (Table 3.4 and 3.5). The presence of some polyhydric alcohols and their derivatives such as glycerol, hexagol, 2-[2-[2-[2-[2- [2-[2-(2-hydroxyethany)ethoxy] ethoxy] ethoxy] ethoxy] ethoxy] ethoxy]ethanol, and 2-[2-[2-[2-[2-[2-[2-[2-(2 hydroxyethany)ethoxy] ethoxy] ethoxy] ethoxy] ethoxy]ethoxy] ethoxy]ethanol may indicate that these solvents not only acts as a solvent but also can enhance the liquefaction process with its intermediate products.[106] Some detected compounds qualitatively from lignin derivatives showed peaks with very

small area below 0.5%, therefore, they were not shown in Fig. 3.14

In addition, the polyols were analyzed quantitatively (calculated by the area normalization method, ppm units) using GC-MS technique and the standards in the mass spectra database. Table 3.5 shows that some of compounds are derived from guaiacyl and syringyl units such as acetosyringone, acetovanillone, syringol and syringaldehyde. The obtained low quantitative content of lignin derivatives indicates that most lignin were depolymerized and reacted with the solvents.

Table 3.4: Volatile compounds of polyols obtained with different organic acids as catalyst.

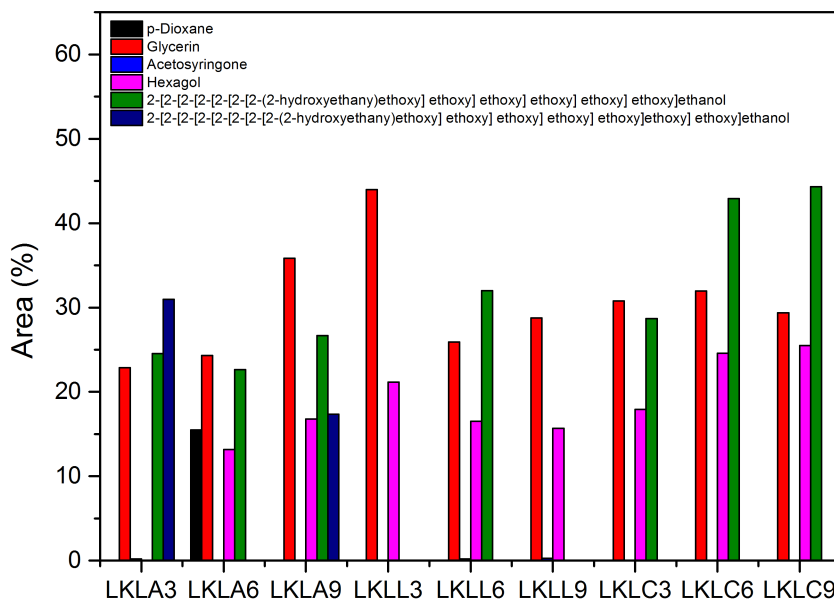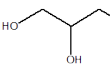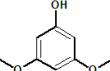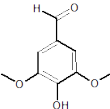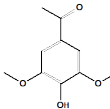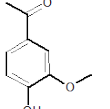| Retention time (min)	Name of compound	Structure
3947	*p*-Dioxane-2,3-diol	
6244	Glycerol	
20487	Acetosyringone	
24052	Hexagol	
26562	2-[2-[2-[2-[2-[2-[2-(2- hydroxyethany)ethoxy] ethoxy]ethoxy] ethoxy] ethoxy] ethoxy] ethanol	
28850	2-[2-[2-[2-[2-[2-[2-[2-(2- hydroxyethany) ethoxy]ethoxy]ethoxy]ethoxy] ethoxy]ethoxy]ethoxy]ethanol	

94

Fig. 3.14: Area of volatile compounds (%) of liquefied Kraft lignin using acetic acid (LKLA), citrit acid (LKLC), and lactic acid (LKLL) as catalyst with 3%, 6% and 9% each one, with PEG/G = 80/20 (wt%), 15% of lignin at 160 °C for 60 min.

Table 3.5: Volatile compounds of polyols obtained with different organic acids as catalyst.

| Samples	Glycerol	Syringol	Syringaldehyde	Acetosyringone	Acetovanillone
LKLA3	184.40	0.71	0.20	0.15	1.01
LKLA6	139.38	0.35	0.15		0.85
LKLA9		0.74	0.10		1.05
LKLL3		0.58	0.22		1.11
LKLL6	139.94	0.62	0.15		0.76
LKLL9	131.27	0.64	0.15		0.92
LKLC3	148.63	0.54			0.82
LKLC6	114.19	0.53			0.76
LKLC9	93.87	0.52			0.68

3.3.3   Optimized liquefied agroforestry residues

Based on the optimized conditions determined in section 2.4.2, further experiments were carried out with the aim of adjusting the reaction conditions for agricultural and forest residues. Thus, the

variables were set as time = 60 min, mass = 15%, and 4.5% of sulfuric acid at 135 °C for LB, LPr, and LO. In the case of LAS and LPS, were liquefied at 120 °C and 100 °C, respectively, to avoid boiling during the reaction. The yield of these liquefied residues is shown in Fig. 3.15. The minimum conversions were obtained in the liquefaction of the pecan shells (69.16%) followed by the almond shells (80.39%). These yields can be attributed to the low reaction temperature (100 °C and 120 °C respectively) used among the liquefied waste (135 °C). The highest yield of 95.17% verified in the liquefied oak sawdust may be related to its inherent structural composition, since hardwood species, such as Oak wood, present higher S/G ratio than softwood or grass, like pine and sugarcane bagasse. As shown in Fig. 1.6, the syringil (S) units have less reactivity than the guaiacyl (G) and *p*-hydroxyphenyl (H) units because the former have both C_3 and C_5 positions occupied, thus, re-condensation reactions are more difficult to occur. On the other hand, the liquefied pine sawdust and bagasse yielded around 93%. This value was higher than that found by Lee *et al.*,[78] which studied the liquefaction of pine wood using crude glycerol and PEG (1/9) as solvent, 3% SA, and 10% wood powder at 170 °C for 60 min, and obtained 73.2% as the maximum yield. However, in another study, the authors obtained 93% yield on bagasse liquefaction using PEG/G (80/20) and 3% SA at 150 °C for 90 min. Briones *et al.*[196] studied the liquefaction of some agricultural residues and found yields varying from 61.5% to 94.6%.

3.3.3.1 Basic properties and molecular distribution of polyols

From Table 3.6 is shown the results of acid number, hydroxyl number, and viscosity as well as the molecular distribution of liquefied lignocellulosic residues. Acid substances are naturally present in cellulose, hemicellulose and lignin composition. However, dur-
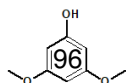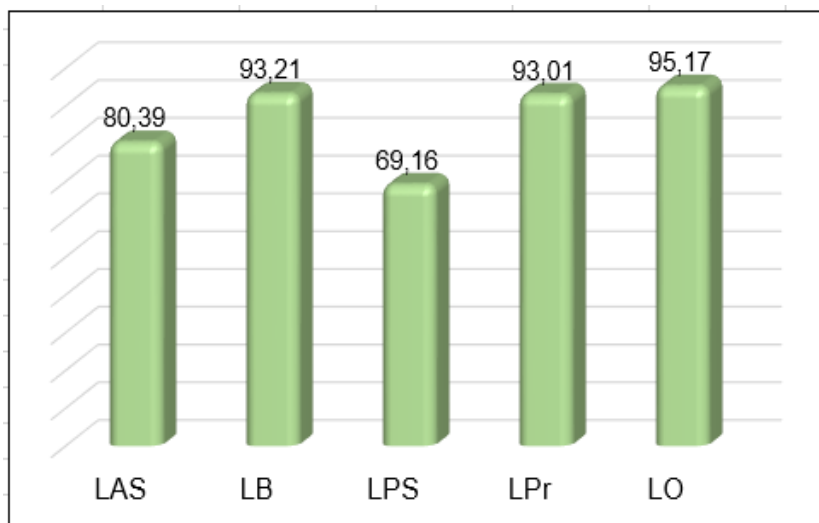
Fig. 3.15: Yield of optimized liquefied agricultural and forest residues. Conditions: PEG/G = 80/20 (wt%), 4.5% SA, at 60 min.

ing liquefaction process using polyhydric alcohols as solvents and a strong catalyst such as sulfuric acid, the acid groups can increase. In this study, the polyols presented acid values ranging from 36.72 mg KOH.g^{-1} in liquefied pecan shells to 44.05 mg KOH.g^{-1} in liquefied Oak sawdust. These values are higher than those found in the literature.[78][87][96]

Regard to OH content, the liquefied Oak sawdust exhibited the highest value with 257.70 mg KOH.g^{-1}, which is explained in terms of the yield this polyol. The same behavior was observed for LB, LPS, and LPr polyols. On the other hand, the LAS polyol showed similar OH and acid values compared to the LO polyol. However, the LAS polyol has lower conversion than the LO polyol. This indicates that oxidation reactions were dominant in the liquefied almond shells, resulting in high acid groups. The *OHn* of the agricultural residues were lower than those reported in the literature.[196]

Liquefied Oak sawdust showed the highest viscosity with 120.20 mPa.s. Although the condensation and repolymerization reactions appear to have not been dominant due to its high yield, this polyol

is formed by a high molecular weight and polydispersity, which may explain the high viscosity. On the other hand, the high viscosity observed in the liquefied pecan shells may be associated with the low yield obtained in this polyols, where condensation and repolymerization reactions prevailed. In the case of liquefied almond shells, which also have small yield, the low viscosity can be attributed to their molecular distribution. Although the high average molecular weight and PDI, this polyol is formed largely (about 85%) by small molecules. The LB and LPr polyols had similar viscosity, however, the LB polyol had a viscosity slightly higher than LPr, as well as the molecular weight and PDI. The molecular distribution of the polyols is shown in Fig. 3.14.

Table 3.6: Results of basic properties and molecular distribution of the polyols from different raw materials.

	LAS	LB	LPS	LPr	LO
An (mg KOH.g^{-1})	42.06 [b]	41.11 [b]	36.72 [a]	41.58 [b]	44.05 [c]
OHn (mg KOH.g^{-1})	245.49 [b]	204.27 [ab]	178.52 [a]	210.91 [ab]	248.77[b]
Viscosity (mPa.s)	81.9 [b]	78.15 [a]	116.35 [c]	77.75 [a]	120.20 [d]
Mw	3511	2534	2357	1823	4999
Mn	502	496	468	488	687
PDI	7.0	5.1	5.3	3.7	7.3

The values followed by the same superscript letter in the same line are not statistically different at 95% significance, $p<0.05$).

3.3.3.2 Chemical structure

Structural changes in the liquefied agricultural and forest residues were investigated by infrared spectroscopy and the FTIR spectra are shown in Fig. 3.17. The broad adsorption band centered at 3408 cm^{-1} is attributed to O-H stretching vibrations and was found for all polyols with different intensities. As well as, the characteristic peaks of C-H stretching in methyl and methylene groups at 2905 and 2870
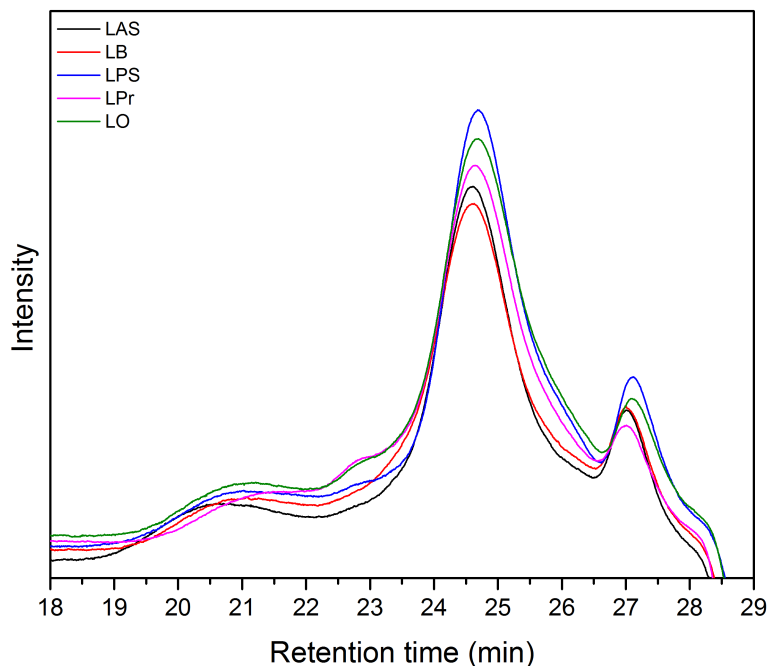
98
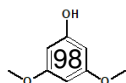
Fig. 3.16: Molecular distribution of optimized liquefied agricultural and forest residues. Conditions: PEG/G = 80/20 (wt%), 4.5% SA, at 60 min.

cm^{-1}. The polyol spectra showed a peak at 1711 cm^{-1} which is attributed to the stretching of C=O in saturated open chain ketones.[73] The peaks assigned to skeletal vibration were observed between 1600 and 1400cm^{-1}.[189] The intense peak at 1092 cm^{-1} indicates the presence of C-O vibrations mainly from solvents. Peaks at 942, 882, and 839 cm^{-1} correspond to the aromatic ring in the lignin.[189][185][196]
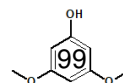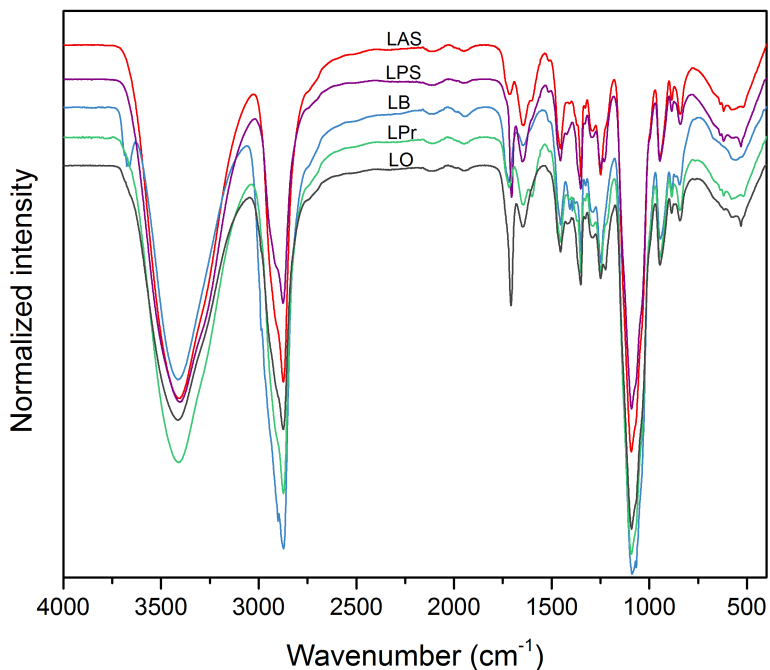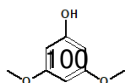
Fig. 3.17: FTIR spectra of liquefied lignocellulosic biomass residue.

3.4   Conclusion

The different lignocellulosic residues were successfully converted to polyols under optimized conditions and using polyhydric alcohols as solvents.

The lignin precipitated with SA provided polyol with higher yield, OH number and viscosity values than those precipitated with organic acids. While the precipitation with acetic acid resulted in a polyol with the highest acid number. LHKL and LKLL polyols (precipitated with SA and lactic acid, respectively), showed similar molecular weight and polydispersity, as did LKLA and LKLC polyol (precipitated with acetic acid and citric acid, respectively). The lignin precipitated with organic acid presented great potential to produce polyol with properties similar to those that use lignin precipitated with SA.

On the other hand, liquefied lignins using organic acids in differ-

ent concentrations as catalysts showed yield around 86%. Liquefied lignin using citric acid as catalyst showed the highest acid number. In addition, a tendency of increasing the acid number with increase of the ionic strength (acetic<lactic<citric acids) and the concentration of catalyst was observed. The minimum OH values were found at 6% of the catalyst, regardless of the type of organic acid used. Maximum viscosity values were found in the presence of 6 and 9% citric acid. The molecular weight of the products was in the range of 1459-1990 $g.mol^{-1}$1 with polydispersity around 3-4. The chemical structure and volatile compounds showed traces of lignin derivatives and a few intermediate products from solvents. The studied organic acids in the present work showed their potential value to be used as catalysts in the liquefaction process, being renewable and environmentally friendly reagents.

Among the agricultural and forest residues, the liquefied Oak sawdust (LO) presented the maximum yield, as well as a high molecular weight viscosity. While the minimal yield, acid substances and hydroxyl groups were found in liquefied pecan shells (LPS). The chemical structure showed that the polyols are rich in hydroxyl groups, apart from characteristic peaks of lignin.
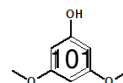
102
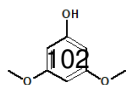
Chapter 4

Biopolyol-based bioresin

4.1   Introduction

Resol resin is widely used as wood adhesive for the manufacture of panels such as medium density fiberboard (MDF), oriented strand board (OSB), laminated veneer lumber (LVL), blockboard, and multi-layer veneers plywood for its high bond strength and water resistance.

The liquid resol is a fusible resin that is cured under heating to become a thermosetting polymer. This occurs when the prepolymer (a) is subjected to heating, which causes its linear chains to begin to grow and branch simultaneously (b). At some point, the resin reaches the gelification state (c), that is, the viscous liquid and the elastic solid coexist in equilibrium in the resin. Thereafter, there is rapid growth in molecular weight due to condensation reactions until the complete polymerization of the resin (d).
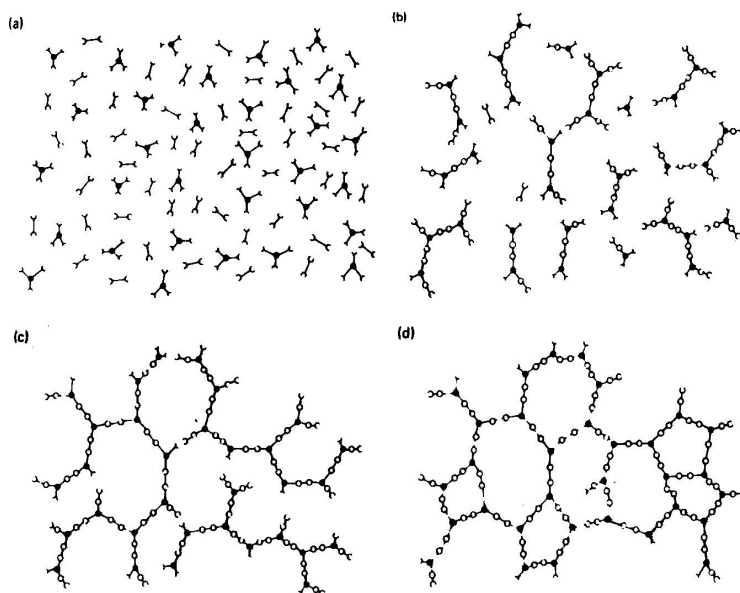

Fig. 4.1: Illustration of the different curing phases of resol resin.

However, a good performance between the wood and the adhesive is necessary. The adhesion process, in this case the interac-

tion between the wood (substrate) and the adhesive, usually occurs by a combination of some theories known as chemical or covalent bonding theory, adsorption or wetting theory, mechanical interlocking theory, diffusion theory, acid-base theory and the theory of weak boundary layers (Fig. 4.2). The theory of covalent bonding occurs at the atomic level and is thought to form an adhesive bond due to the chemical forces of the surface.[198] The acid/base theory is a fairly recent finding that also occurs at atomic level. The adhesion obtained is based on the polar attraction of Lewis acids and bases. The diffusion theory proposes the nanoscale interdiffusion of adhesive molecules within cell wall pores. In mechanical interlocking, the adhesive penetrates in millimeters or micron-length in pores or other irregularities of the surface of the wood. Adsorption or wet theory suggests that adhesion happens from the molecular interaction of the adhesive and the surface of the wood and the resulting surface forces between them. The weak limit theory relates the bond failure that is caused by a cohesive break or a weak boundary layer that may be due to the adhesive the adherent, the environment, or a combination of any them.[199]

In this sense, some adhesive properties are very important such as pH, which, at low values, can cause poor cross-linking, resulting in a weak adhesion strength with the wood. At high pH the resin is very hygroscopic and tends to age rapidly. Also, during resin synthesis, the pH is generally related to the conversion of formaldehyde. As well, the acid-base theory could be affected by resin pH causing a weak boundary layer.

During the curing step, the organic solvents present in the resin are volatilized, so that the solids content is the part of the resin that will be retained in the pores of the wood, as described in the theory of mechanical interlocking.

Viscosity plays an important role during the gluing process. When
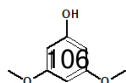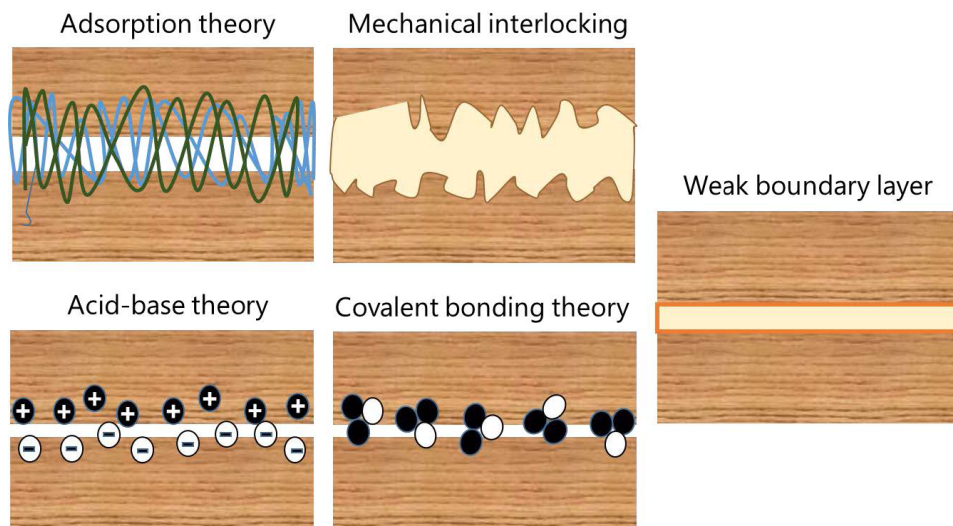
Fig. 4.2: Illustration of accepted models of wood adhesion. Image courtesy of Rene Herrera.

the adhesive is very viscous, it becomes more difficult to be applied besides not penetrating properly into the wood. Then, a thick layer is formed between the substrates, and consequently, there is no good diffusion of the adhesive in the pores of wood. On the other hand, a poor line glue is obtained when the adhesive has a very low viscosity. Absorption, mechanical interlocking, and weak boundary theories are influenced by adhesive viscosity.

On the other hand, some aspects of the substrate (wood) must also be taken into account. The wood is formed by elements such as rays, tracheids/vessels, and resin channels that chance in size and quantity from one species to another,[200][201] as shown in Fig. 4.3. In addition, the surface of the wood must be cleaned to prevent the adhesive from attaching to any type of dirt that may result in a weak boundary layer. As well as, the roughness on wood can hinder the adhesion between wood and adhesive.
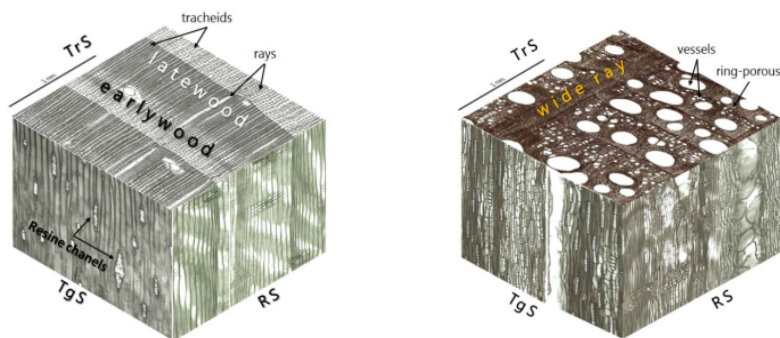
(a) Softwood   (b) Hardtwood

Fig. 4.3: Three-dimensional design of the wood microscopic structure a) Pine sylvestris, b) Quercus robur. The scheme shows transverse section (TrS), radial section (RS), and tangencial section (TgS) of each specie.[202]

4.2 Objectives

The main purpose of this chapter was evaluate the possibility of partially replacing the aromatic OH with biopolyol to produce wood adhesive with similar standard properties. For this, the following specific objectives are highlighted.

- Asses the effect of different reaction conditions using an experimental design being the biopolyol, formaldehyde and catalyst concentrations the main variables;

- Characterization of bioresins obtained from experimental design;

- Characterization of optimized bioresins;

- Evaluation of optimized bioresins as a wood adhesive;

4.3   Experimental procedure

4.3.1   Materials

The obtained biopolyol in the Chapter 3 were used to partially substitute the phenol in the resol formulations. Besides, phenol, formaldehyde, NaOH, propan-2-ol, hydroxylamin hydrochloride and HCl were used. Technical information about these reagents are listed in Appendix C.

4.3.2   Procedure

The bioresin was prepared in a 500 mL neck glass flask reactor with magnetic stirrer, temperature control and condenser. A desired amount of biopolyol, phenol, formaldehyde and NaOH pellets (Table 4.1) were charged together into the reactor. When the temperature reached 80 °C it was kept for 3:30 h. The bioresin was cooled in a water-ice bath and kept in a refrigerator for futures analysis.

Under optimized reaction conditions, the bioresins were produced in large quantities for subsequent applications as wood adhesive.

4.3.3   Experimental design

A CCD experimental design was used to establish optimum conditions for the production of bioresin. The weight ratio of polyol:phenol (p:Ph), molar ratio of formaldehyde:phenol (F:Ph) and NaOH:Ph were chosen as independent variables and were coded by equation A.11. On the other hand, FFC, pH, SC and viscosity were selected as dependent variables (response). The 16 runs, including two central points (with factors at level zero), were performed in a completely random order, according to the experimental design. The reaction
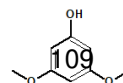
conditions and the results obtained for the dependent variables are summarized in Table 4.1. Response surface method (RSM) was used to establish a statistical relationship between experimental variables and responses.

Table 4.1: Reaction conditions of bioresins and basic properties.

Sample	p/Ph (w/w %)	F/Ph (molar ratio)	NaOH/Ph (molar ratio)	SC (%)	FFC (%)	Viscosity mPa.s	pH
LPF1	60	2.5	1.1	53.69 [a] (0.22)	2.31 [c d] (0.36)	59.2	11.96
LPF2	50	2.0	1.3	65.86 [d] (0.03)	1.17 [a b] (0.46)	651.9	14.01
LPF3*	60	2.5	0.5	-	-	-	-
LPF4	66.82	1.5	0.8	58.48 [b c] (0.68)	1.94 [c d] (0.10)	103.9	11.55
LPF5	66.82	2.0	0.8	56.12 [a b] (0.08)	1.16 [a b] (0.81)	90.0	11.37
LPF6*	33.18	2.0	0.8	-	-	-	-
LPF7*	40	2.5	0.5	-	-	-	-
LPF8	50	2.0	0.8	59.18 [c] (1.26)	1.77 [b c] (0.32)	248.8	11.45
LPF9	60	1.5	0.5	64.26 [d] (1.31)	0.73 [a] (0.01)	1555.6	11.39
LPF10	50	1.16	0.8	69.61 [e] (0.23)	1.60 [b c] (0.22)	1262.1	13.40
LPF11	40	1.5	1.1	65.09 [d] (0.55)	1.96 [c d] (0.17)	1481.6	13.14
LPF12	40	2.5	1.1	74.59 [f] (4.73)	2.52 [d] (0.13)	6252.2	12.34
LPF13	50	2.0	0.8	64.34 [d] (0.07)	1.69 [b c] (0.06)	304.3	12.05
LPF14*	50	2.0	0.3	-	-	-	-
LPF15*	50	2.84	0.8	-	-	-	-
LPF16	60	1.5	1.1	66.75 [d] (0.64)	1.88 [b c d] (0.05)	436.6	13.16

Coded variables: p/Ph (w/w%) (-1.628 = 33.18, -1 = 40, 0 = 50, +1 = 60, +1.628 = 66.82); F/Ph molar ratio (-1.682 = 1.16, -1 = 1.5, 0 = 2.0, +1 = 2.5, +1.682 = 2.84); and NaOH/Ph molar ratio (-1.682 = 0.3, -1 = 0.5, 0 = 0.8, +1 = 1.1, +1.682 = 1.3). * These experiments were not characterized because solid formation during the reaction. The values in parentheses are the standard deviation. The values followed by the same superscript letter in the same column are not statistically different at 95% significance, $p < 0.05$.

110
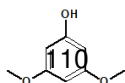
Statistical analysis was performed using STATGRAPHICS Centurion XV software. The data were analyzed by the analysis of variance (ANOVA) to determine the variables that are significant in the properties of bioresins. In addition, the overall contribution of each variable in the bioresins properties was analyzed using the Pareto chart and RSM, which shows the interaction between the variables.
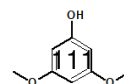
4.3.3.1   Characterization of bioresin

The obtained bioresins from experimental design were characterized as basic properties, such as solid content (SC) following the standard ASTM D4426[203] and free formaldehyde content (FFC) in accordance to EN ISO 9397[204]. These procedures are reported in Appendix A.0.3.1 and A.0.3.2, respectively. The viscosity was performed at 25 °C using a rotational viscosimeter (Appendix B.5.3) and the pH values were measured with a pH meter at room temperature. The molecular distribution of the bioresins was measured by gel permeation chromatography (GPC) following the procedure described in Appendix B.

The water resistance test is a useful method to predict the quality of the obtained bioresins. About 1 g of pre-cured resin (125 °C for 105 min) was submerged in the flask with 100 mL of distilled water for one month and visually evaluated.

4.3.3.2   Characterization of bioresin-based adhesive

Pine wood samples with dimensions of 105 X 25.4 X 8 mm were (Fig. 4.4) prepared for the lap shear strength test based on ASTM D5868-14[205] using a MTS Insight 10 equipment (see Section B.4.1). About 220 g.cm^{-1} (± 0.1375 g) of each adhesive formulation were applied in an area of 25 mm^2 of the final section of only one ve-

neer. The two veneers were pressed at 10 bars, at 125 °C for 4 min. Five replicate of each different adhesives were tested and the results were reported by average arithmetic as maximum shear strength.
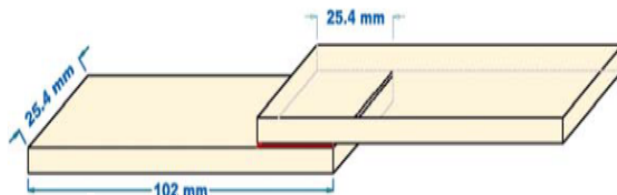

Fig. 4.4: Shear and dimension of test piece.

The three-ply plywood with dimensions of 25.0 X 25.0 X 1.5 mm for pine wood and 15.0 X 15.0 X 1.9 for beech wood were produced to evaluated the tensile shear strength according to ASTM D906-98.[206] The three-ply-plywood was coated with single glue-line with 180 g.cm^{-1} and then hot-pressed at 125 °C, 10 bars of pressure for 4 min. Then the plywood was cut as shown in Fig. 4.5. Five specimens of each three-ply plywood were tested and the results were reported by average arithmetic

For both mechanical characterization, the wood failure percentage for each specimen was checked visually and assessed in accordance with EN-314-2 standard.
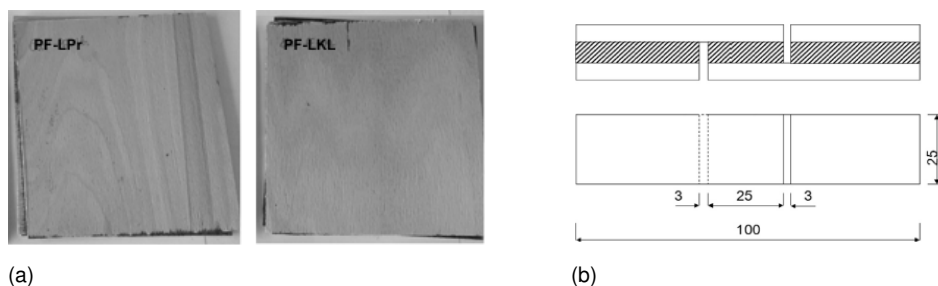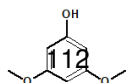

(a) (b)

Fig. 4.5: Three-layer plywood (a); scheme and dimension of the specimen obtained from plywood (b).

# 4.4   Results and discussion

4.4.1   Experimental design

To investigate the potential of biopolyol as an alternative to partial substitution of phenol in a resol resin, a CCD design was performed by varying the mass ratio of biopolyol (LHKL), and molar ratio of both formaldehyde, and NaOH relative to phenol. Thus, the basic properties of the obtained bioresins were evaluated.

4.4.1.1   Influence of independent variables on the solid content of bioresins

The solid content of bioresins ranged from 53.69% to 74.59% (Table 4.1). Fig. 4.6 shows the solid content of pre-cured bioresins at 125 °C for 105 min, considering the amount of biopolyol as a substitute for phenol. As can be observed, the minimum values of SC (about 50%) were found mainly in the presence of higher concentration of biopolyol. This can be explained by the fact that biopolyol is less reactive than phenol, therefore in large amounts (above 60%) during pre-cure, most of the unreacted compounds have resulted in its volatilization. In contrast, higher values of SC were verified with moderate or low percentage of biopolyol (50 or 40%, respectively). Hussin *et al.*,[185] studied the resinification of Kraft and organosolv lignin reported inverse trends to those found in this investigation. The authors observed an increase in SC with the increase in the percentage of lignin (for both Kraft and organosolv) increased.

The solid content relative to the different formaldehyde/phenol molar ratio (2.5, 2.0, 1.5, and 1.16) is shown in Fig. 4.7. The lowest and highest SC values (LPF1 and LPF12, respectively) were verified at a proportion of F/Ph of 2.5. However, in the LPF12 sample, poly-
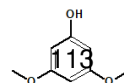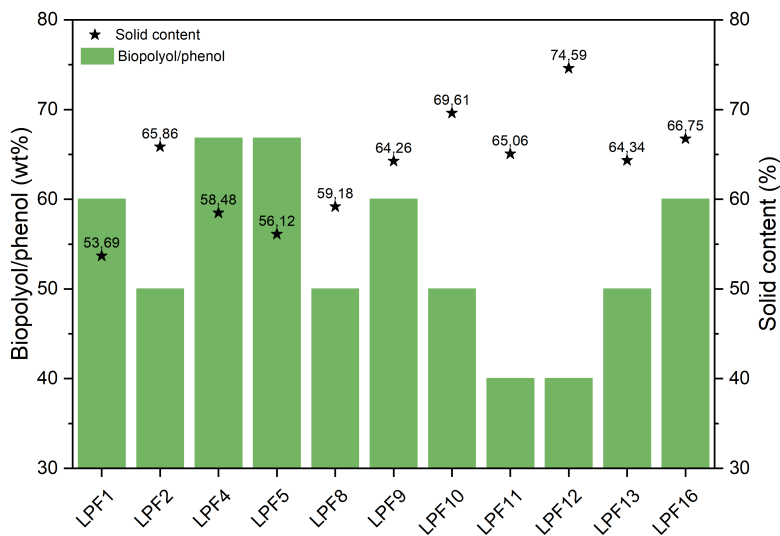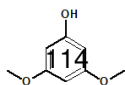
Fig. 4.6: Solid content of the bioresins as a function of the percentage weight of biopolyol used to partially replace the phenol.

merization reactions was observed as can be confirmed by its high molecular weight. In counterpoint, the low SC value in LPF1 can be explained by the large percentage of monomers presents in this sample. As shown in the GPC analysis, more than 63% of the compounds were of low molecular weight, about 270 g.mol^{-1} (reaction time over 25 min, Fig. 4.19).
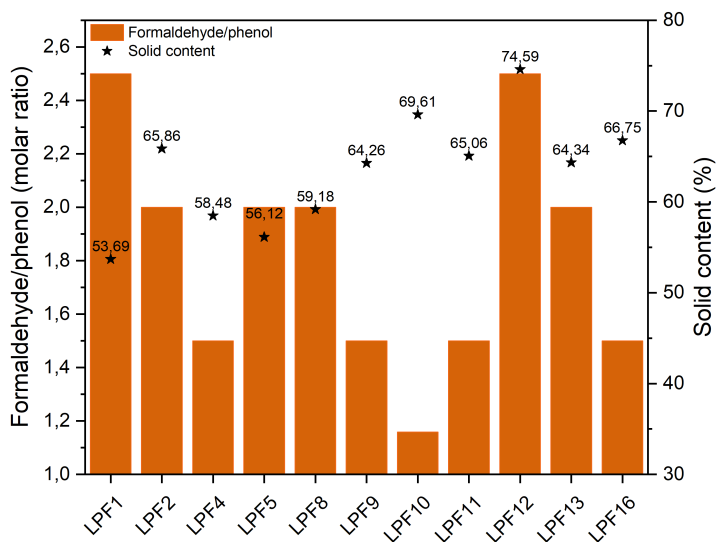
114

Fig. 4.7: Solid content of the bioresins in terms of the F/Ph molar ratio.

Fig. 4.8 shows the solid content of the bioresins considering the different NaOH/phenol molar ratios (0.5, 0.8, 1.1, and 1.3) used. Most of the minimum SC values, around 50%, were displayed using the molar ratio catalyst of 0.8. However, it was observed that the lowest solid content of 53.69% (LPF1 sample) and also the highest with 74.59% (LPF12 sample) were found in formulations with molar ratio of 1.1 NaOH.
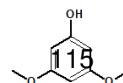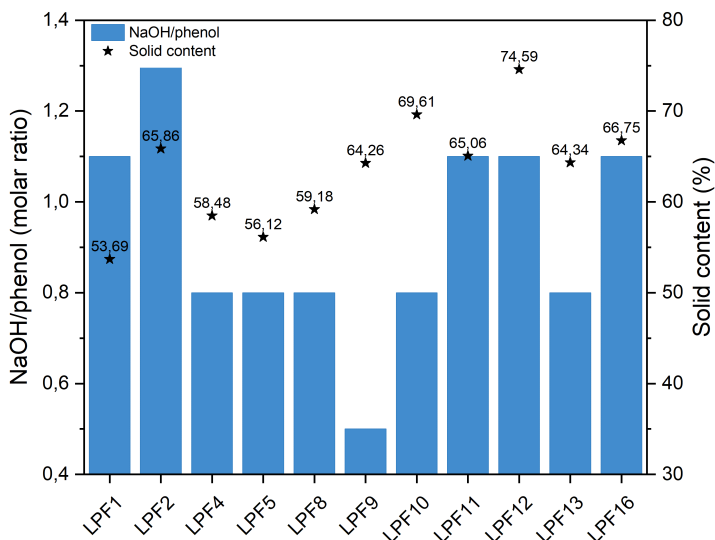
Fig. 4.8: Solid content of the bioresins in terms of the NaOH/Ph molar ratio.

The independent variables and their interactions did not statistically influence ($p > 0.05$) the solids content of the bioresins, as presented in the Table A.11. The contribution of each variable and its interactions can be clearly observed through a standardized Pareto chart based on a second-order model (Fig. 4.9).
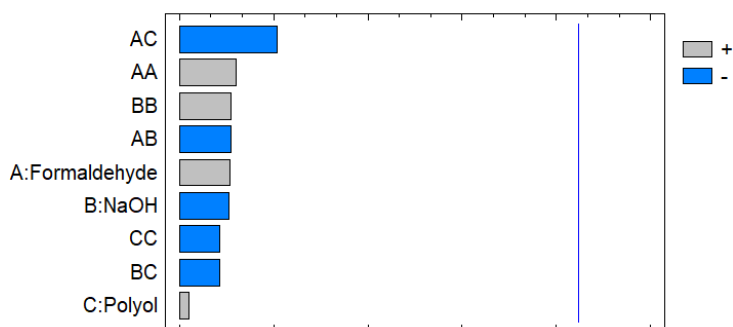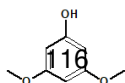

Fig. 4.9: Pareto chart shows the contribution of each independent variable (A: formaldehyde, B: NaOH, and C: biopolyol) and their interactions on the solid content of the bioresins. The vertical line represents the p-value ($p < 0.05$).

4.4.1.2 Influence of independent variables on the free formaldehyde content of bioresins

Table 4.1 displays the free formaldehyde content (FFC), which range from 0.73% to 2.52%, as a function of the independent variables. From Fig. 4.10, it can be observed the obtained FFC regarding to the amount of biopolyol (40, 50, 60, and 66.82) used as substitute to phenol. The samples LPF9 and LPF12 were formulated with 40% of biopolyol. In addition, in both samples a certain degree of polymerization occurred as displayed in Table 4.2. However, the formaldehyde was much more consumed in LPF9 than in LPF12. The last, has larger molecular weight and polydispersity than LPF9. This could explain the less formaldehyde consumption in LPF12 since 43% of its molecular distribution is compost of very low molecular weight. Results similar to that obtained in the LPF9 sample (0.73%) were reported by Qiao *et al.*[207] using 60% bioethanol production residue. However, the authors modified the residue by phenolation method before use.
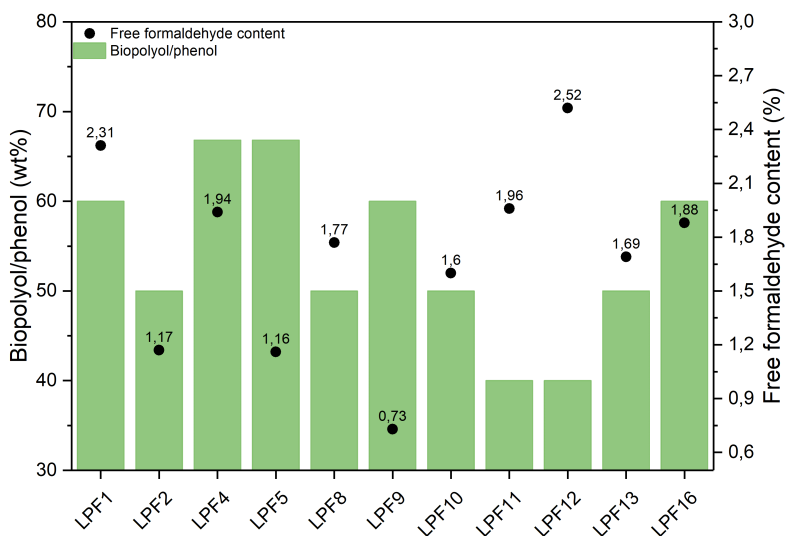

Fig. 4.10: Free formaldehyde content of the bioresins considering the different amount (wt%) of biopolyol to replace phenol.
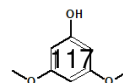
Fig. 4.11 shows the free formaldehyde content of the resins based on the different molar ratios of formaldehyde/phenol used. As can be seen, the lower formaldehyde consumption occurred in the samples (LPF1 and LPF12) carried out with a large amount of formaldehyde (2.5 molar ratio). Similar results were found by Han and collaborators[119] using modified spent liquor with phenol to prepare phenolic resin. On the other hand, lower FFC value was verified using 40% formaldehyde, as observed in the LPF9 sample.
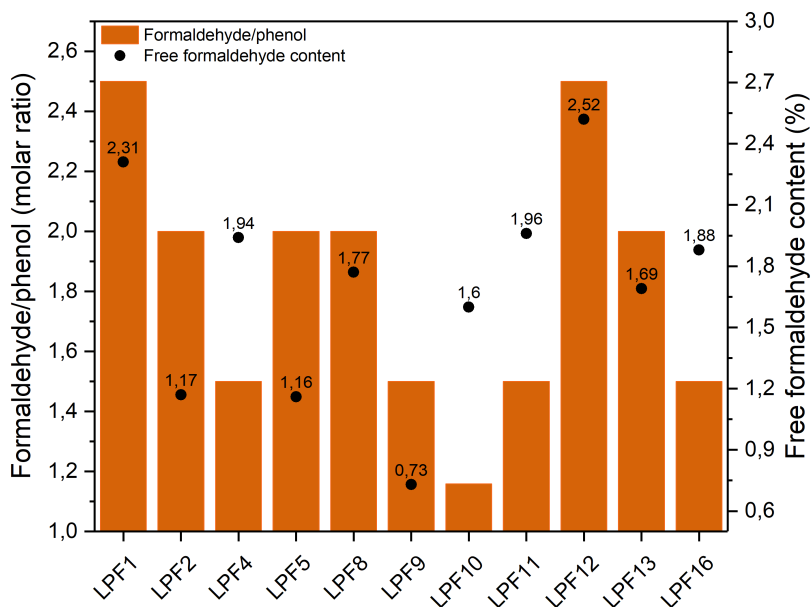
Fig. 4.11: Free formaldehyde content of the bioresins respect to the variation of formaldehyde/phenol molar ratio.

The results of the free formaldehyde content as a function of the molar ratio of the catalyst to phenol (0.5, 0.8, 1.1, and 1.3) are shown in Fig. 4.12. The main consumption of formaldehyde was revealed in presence of ow catalyst loading (molar ratio of 0.5). However, maximum FFC values were observed in samples run with a molar ratio catalyst of 0.8.

118
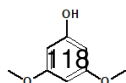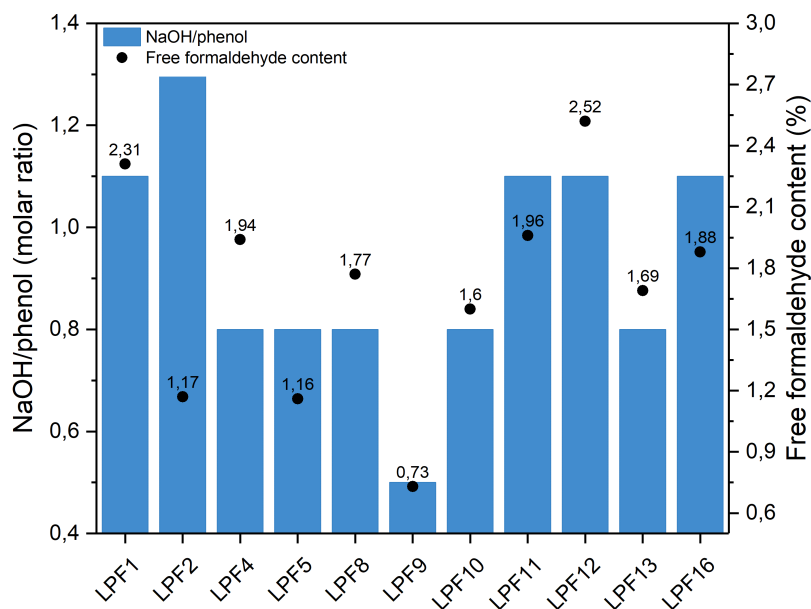
Fig. 4.12: Free formaldehyde content of the bioresins respect to the variation of NAOH/phenol molar ratio.

Fig. 4.13 presents the statistical analysis of the variables on the FFC. Based on the data, the ANOVA analysis showed that although the catalytic variable has an important contribution in the FFC, as shown in Fig. 4.13a, only the biopolyol variable was significant in the consumption of formaldehyde ($p < 0.05$, Table A.13). The adjusted mathematical model may explain 98.83% of the results as follows Eq. A.21. In addition, the response surface method (RSM) was used to predict optimum experimental conditions for optimum performance.

Fig. 4.13: Pareto chart and response surface plot showing the influence of the variables on the free formaldehyde content of the resins. The vertical line in Pareto chart (a) represents the p-value (p<0.05).
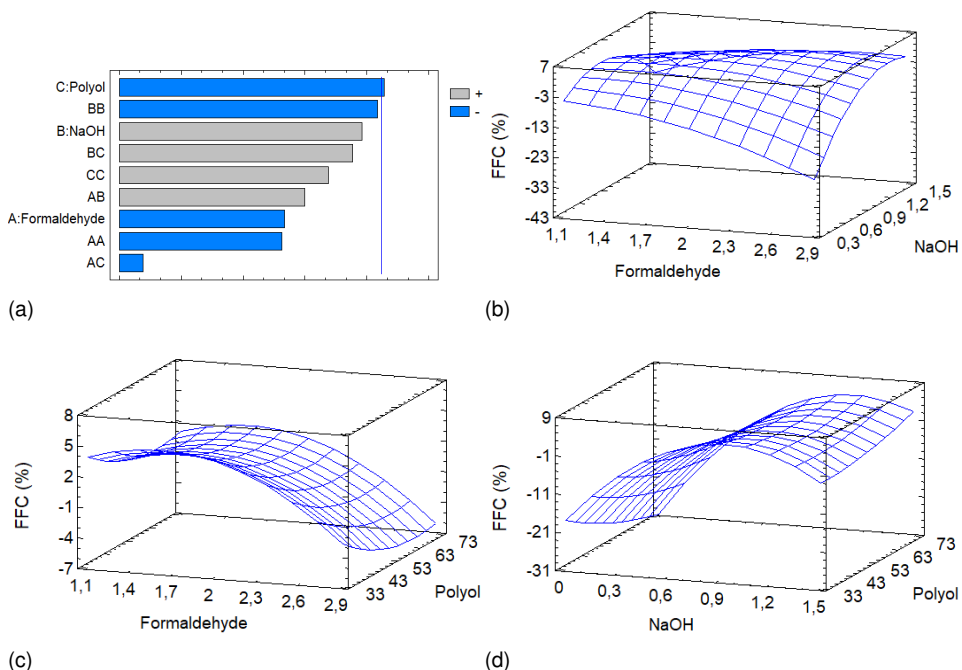
4.4.1.3 Influence of independent variables on the viscosity of bioresins

The bioresins presented a wide range of viscosity values as shown in Table 4.1. Fig. 4.14 displays the viscosities obtained, taking into account the weight ratio of the biopolyol used to replace the phenol. The lowest viscosity was found in the LPF1 formulation made with 60% biopolyol (sample LPF1). This sample is formed by compounds of low molecular weight (Table 4.2), which could explain the low viscosity. In contrast, the higher viscosity was obtained using 40% biopolyol (sample LPF12). The high viscosity value of this sample suggest large-scale polymerization. This result is in accordance with the molecular weight shown in Table 4.2.
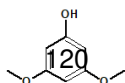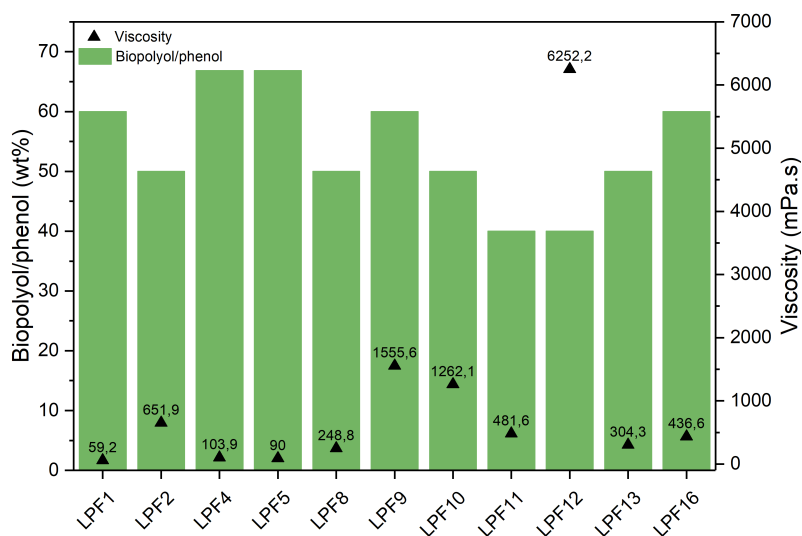
Fig. 4.14: The viscosity of the resins obtained as a function of the substitution of the biopolyol by phenol.

Fig. 4.15 shows the viscosity values of the resins in terms of molar ratio formaldehyde/phenol. The minimum and maximum viscosity values were verified in the formulations (LPF1 and KPF12, respectively) with large amount of formaldehyde (molar ratio of 2.5). As mentioned above, there were no polymerization reactions in the LPF1 sample resulting in low viscosity. In contrast, in the LPF12 sample, the same amount of formaldehyde resulted in a high crosslinking.

The viscosity of the resins taking into account the molar ratio of catalyst to phenol is shown in Fig. 4.16. Regarding to the catalyst variable, the viscosity presented the same trend observed for the formaldehyde variable in terms of minimum and maximum viscosity values. That is, both viscosity values were obtained in formulations (LPF1 and LPF12, respectively) with molar ratio of 1.1 NaOH.

121
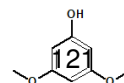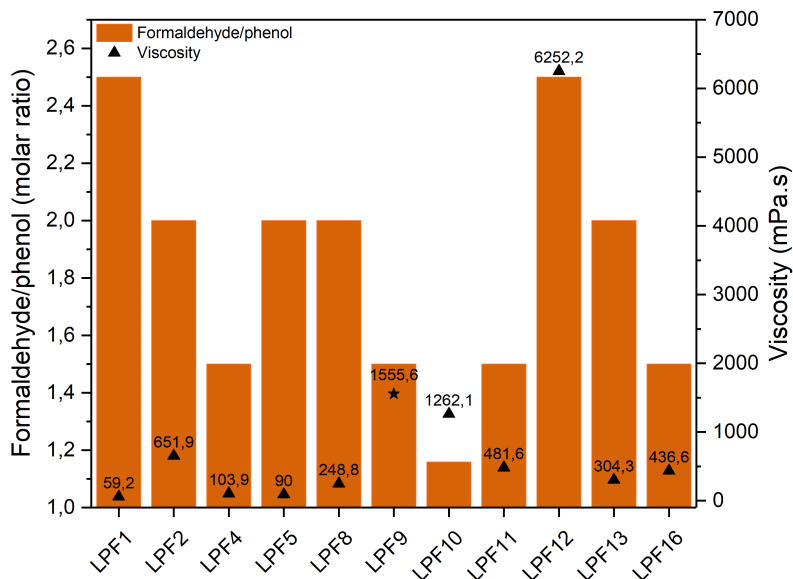
Fig. 4.15: The viscosity of the resins obtained as a function of the formaldehyde/phenol molar ratio.

Among the basic properties evaluated, the viscosity was the most influenced by the independent variables ($p < 0.05$, Table A.14, and Fig. 4.17). The overall contribution of each variable and their interactions for viscosity of bioresins are shown in Fig. 4.17a, in addition, Fig. 4.17b-4.17d show the behavior of the adjusted model which can account for 99.95% of the viscosity variability through Eq. A.22.
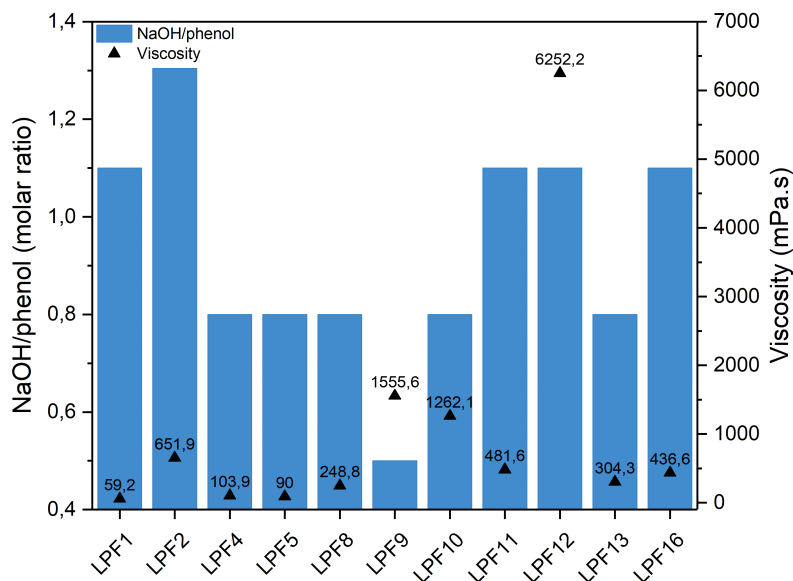
Fig. 4.16: The viscosity of the resins obtained as a function of the NaOH/phenol molar ratio.

4.4.1.4   Effec of independent variables on the pH of bioresins

Table 4.1 exhibited the pH values of bioresins formulated. The bioresin with a high percentage of biopolyol (66.82%) and moderate NaOH/Ph molar ratio (0.8) had the lowest pH (11.37, LPF5), while the highest pH of 14.01 was observed in the LPF2 with 50% biopolyol and high amount of catalyst (molar ratio of 1.3). In these formulations, the F/Ph molar ratio of 2.5 was used. The independent variables and their interactions also did not affect the pH of resins ($p > 0.05$, Table A.12 and Fig. 4.18).

The optimization of the experimental design of the resins was determined by the analysis of multiple responses using the STAT-GRAPHICS Centurio XV software. The results showed that the optimal reaction condition to prepare bioresin based on the biopolyol (LHKL) is: biopolyol/phenol = 60/40 (w/w), molar ratio of formalde-
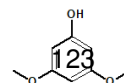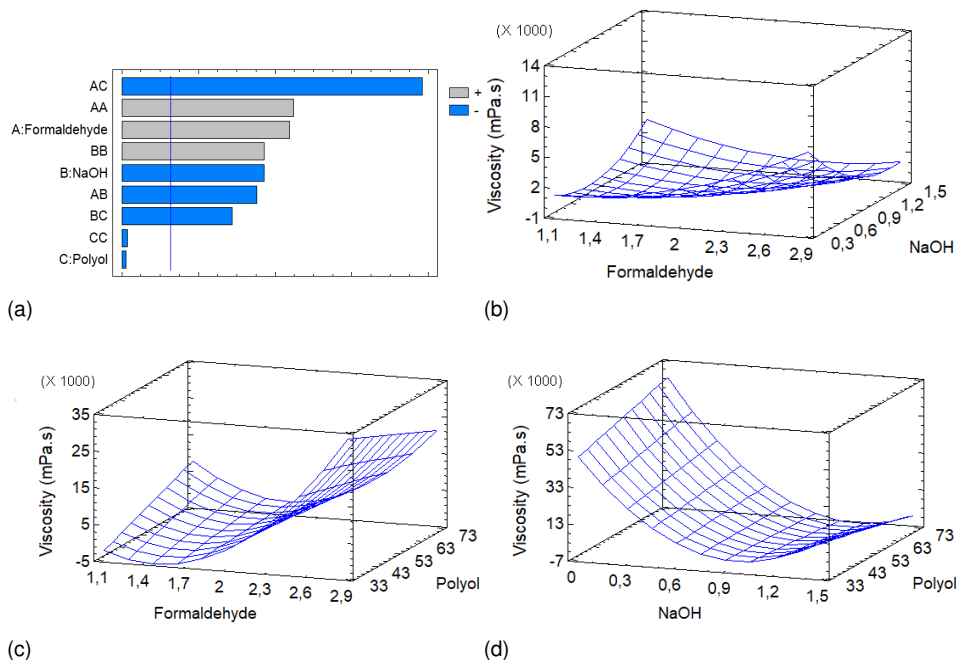
Fig. 4.17: Pareto chart and response surface plot showing the influence of the variables on the viscosity of the resins. The vertical line in Pareto chart (a) represents the p-value ($p<0.05$).

hyde/phenol = 1.5, and NaOH/phenol molar ratio = 0.5.
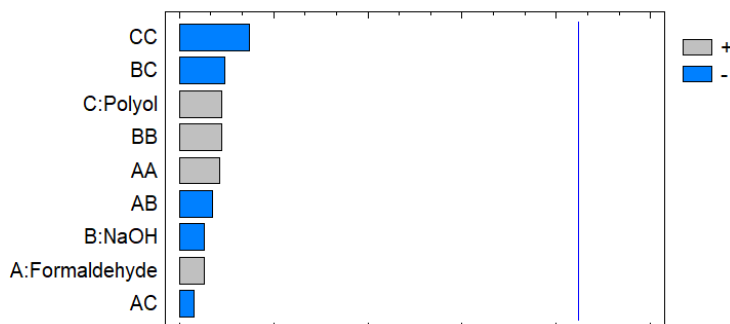
Fig. 4.18: Pareto chart shows the contribution of each independent variable (A: formaldehyde, B: NaOH, and C: biopolyol) and their interactions on the pH of the bioresins. The vertical line in Pareto chart (a) represents the p-value (p<0.05).

4.4.1.5   Molecular mass distribution

Fig. 4.19 shows the GPC chromatograms and the corresponding $\overline{M}$n, $\overline{M}$w, and polydispersity ($\overline{M}$n/$\overline{M}$w) values are summarized in Table 4.2.

As can be seen, most of the bioresins presented a very low molecular weight, suggesting that the addition reactions were dominant to form intermediates such as mono, di-, tri-hydroxymetyl phenol. Low molecular weight resins were found in the literature.[208] Furthermore, it appears that there was a depolymerization of the biopolyol, since its initial $\overline{M}$w was 1416 g.mol^{-1}. However, in the LPF9, LPF10, LPF11, and LPF12 samples, where the molecular weight ranged from 2745 g.mol^{-1} to 93111 g.mol^{-1}, besides the addition reactions, the condensation reactions were dominant, allowing some degree of cross-linking.
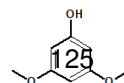
Table 4.2: Molecular mass distribution of bioresins.

Sample	$\overline{M}n$	$\overline{M}w$	PDI	Sample	$\overline{M}n$	$\overline{M}w$	PDI
LPF1	296	344	1.16	LPF10	661	2745	4.15
LPF2	253	270	1.06	LPF11	819	3194	3.90
LPF4	344	563	1.63	LPF12	731	93111	127.45
LPF5	318	415	1.30	LPF13	277	312	1.12
LPF8	293	342	1.16	LPF16	207	261	1.26
LPF9	626	69039	110.36				
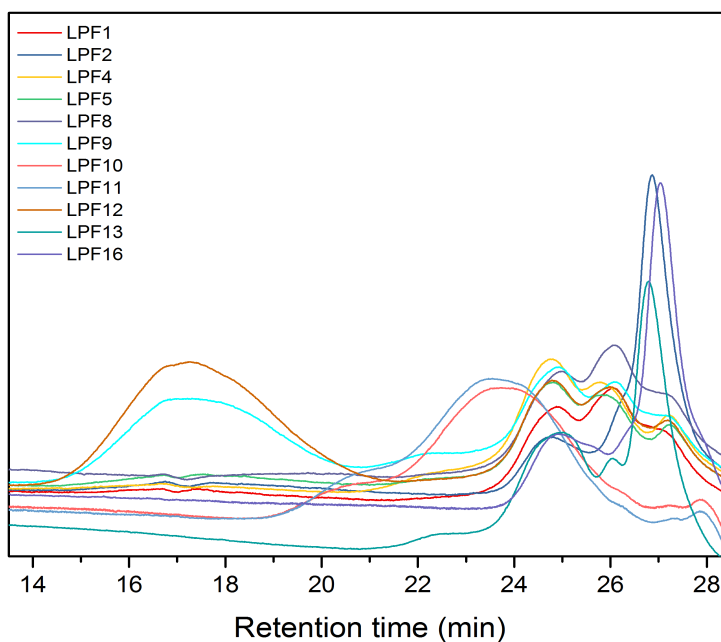
Fig. 4.19: Molecular mass distribution of bioresins.

4.4.1.6 Water resistance performance

In general, pre-cured bioresins when immersed in water were immediately dissolved (partially or totally). With the exception of the bioresins LPF10, LPF11, and LPF12, which took a few days and LPF9, which was the only one that showed resistance even after one month. This confirms a very high degree of polymerization of LPF9

126

bioresin, as demonstrated previously by GPC chromatography.

4.4.2   Optimized biopolyol-based bioresins

Under optimum conditions (p/Ph = 60/40 w/w, F/Ph = 1.5 molar ratio, and NaOH/Ph = 0.5 molar ratio), as determined previously, the biopolyols obtained from Kraft lignin (LHKL), almond shells (LA), bagasse (LB), and pine sawdust (LPr) were used to produce the bioresins named, respectively, PF-LKL, PF-LA, PF-LB, and PF-LPr.

4.4.2.1   Properties of the bioresins

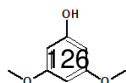Table 4.3 shows the basic properties of the bioresins synthesized using different biopolyols as a partial substituted for the phenol. The bioresins showed solid content lower than the control resin (PF-Ctrl) except the resin PF-LA. This may be explained by the high molecular weight and polydispersity of the biopolyol LA which must have contributed to the highest SC of 75.43% in this bioresin. These values are similar to those found by Zhao *et al.*,[209] who used phenolate lignin as a partial substitute for phenol. However, higher than the values obtained in another study where alkaline lignin was liquefied with phenol under acid conditions.[210]

The different biopolyols used to prepare the resins were significant in the free formaldehyde content results (p<0.05). The PF-LB and PF-LKL resin have lower FFC values than PF-Ctrl. In fact, PF-LKL resin exhibited the best FFC consumption (0.77%). Qiao *et al.*[207] reported similar free formaldehyde content using phenolated bio-ethanol residue to replace 60% phenol. On the other hand, PF-LA and PF-PLr exhibited large FFC values. On the other hand, PF-LA and PF-LPr exhibited large FFC values. The large amount of formaldehyde observed in these samples can be explained by the
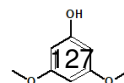
high molecular weight and polydispersity of the biopolyols (Table 3.6) used in these syntheses. This way, few active sites were available to react with formaldehyde due to the presence of large molecules and steric hindrance.[122]

As in FFC, the biopolyol type had a significant influence on resin viscosity ($p<0.05$). The PF-LB and PF-LPr resins presented lower viscosity values than the PF-Ctrl resin, while the PF-LKL resin had the highest viscosity at 574.2 mPa.s. Regarding pH variable, all the resins presented pH around 9, except the PF-LKL with pH = 10.05. Similar results are found in literature.[121][122][209]

In general, the optimized resins exhibited basic properties that meet the standard requirements, except for FFC values that were higher than the standard (GB/T 14732-2006). However, this issue can be controlled by the use of some additive that absorbs formaldehyde.

Table 4.3: Basic properties of optimized bioresins.

Sample	Solid content (%)	FFC (%)	Viscosity (mPa.s)	pH
PF-Ctrl	70.63 (16.97) [a]	1.75 (0.38) [b]	195.5 [a]	9.36
PF-LKL	65.99 (1.53) [a b]	0.77 (0.03) [a]	574.2 [b]	10.05
PF-LA	75.43 (1.18) [a b c]	3.15 (0.59) [c]	218.9 [c]	9.36
PF-LB	57.66 (0.04) [b c]	1.57 (0.19) [b]	173.9 [d]	9.36
PF-LPr	54.14 (0.18) [c]	5.55 (0.01) [d]	109.1 [e]	9.70
GB/T 14732-06	≥ 35.0	≤ 0.3	≥ 60.0	≥ 7.0

Optimized condition: p/PH = 60:40 (w/w), F/Ph = 1.5 molar ratio, and NaOH/Ph = 0.5 molar ratio, at 80 °C, for 3 h 30 min. Values in parentheses are standard deviation. The values followed by the same superscript letter in the same column are not statistically different at 95% significance, $p<0.05$.

4.4.2.2 Water resistance performance

Resins synthesized with part of phenol substituted by different biopolyols under optimum conditions were undergo to the water re-

sistance test and assess visually. The results showed that all resins exhibited excellent resistance to water even after two month of immersion
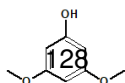
4.4.3 Bio-adhesive performance

4.4.3.1 Mechanical properties

The mechanical performance of bioresins-based adhesives was evaluated. For this, samples of pine wood were glued with 220 g.cm^{-1} in a single glue line in an area of 25 mm^2 at the final section of the specimen. Samples were pressed at 10 bar for 4 min at 125 °C. Table 4.4 shows the performance of the PF-LKL resin-based adhesive as compared to the laboratory control resin.

The results showed that the PF-LKL had a shear strength of 1.37 MPa, which was higher than the PF-Ctrl with 0.75 MPa. Kalamil *et al.*[211] used the same kind of test to evaluated their adhesives and they obtained low shear strength (0.65 MPa) using 100% lignin-based resin. The wood failure occurred for both resins, however, the PF-LKL had a better performance (73%) compared to the control.

Table 4.4: Lap shear strength and wood failure of the bio-adhesives.

Sample	Adhesive amount (g)	Shear strength (Mpa)	Wood failure (%)
PF-Ctrl	0.1486 (0.01)	0.75 (0.18)	35
PF-LKL	0.1390 (0.13)	1.37 (0.52)	73
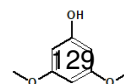
Three-ply plywood panels of pine and beech wood were produced using PF-LKL and PF-LPr as a bio-adhesive, as described in section 4.3.3.2. After, the machined panels (Fig. 4.5b) were tested for shear stress. The results are shown in Table 4.5. Regarding the type of resin, it was observed that the panels coated with PF-LKL resin presented higher shear strength than those glued with PF-LPr resin, regardless of the type of wood. The results showed that type resin was significant on the shear strength (p<0.05). This may be attributed to the fact that in the synthesis of PF-LPr the consumption of formaldehyde was much lower than in PF-LKL (Table 4.3). In addition, PF-LPr resin has higher polydispersity than than PF-LKL resin, which suggests a great presence of low molecular weight species in the former than in PF-LKL resin. Therefore, these small molecules can volatilize during the adhesion process, causing a slightly weaker reticulation network. The adhesives showed shear performance data according to the literature.[121][209]

In addition, it was observed that the shear strength of both resins was affected by the type of wood (p<0.05). This can be attributed to intrinsic characteristics of each species. The pine is more resinous, which makes the chemical interaction (acid-based and covalent theories) with the adhesive more difficult and time consuming. On the other hand, the beech is more porous than the pine wood, facilitating the penetration of the adhesive to promote a better mechanical interlocking. However, in the combination of adhesive and wood type only the pine wood coated with PF-LPr resin was different (p<0.05).

The bio-adhesives presented acceptable percentage of wood failure according to standard, except for the three-ply plywood from pine wood glued with PF-LPr bioresin (Table 4.5) and PF-Ctrl resin in Table 4.4.
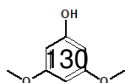
Table 4.5: Bonding strength and wood failure in three-ply plywood.

Sample	Adhesive amount (g)	Shear strength (MPa)	Wood failure (%)
	Pine wood		
PF-LKL	5.185 (0.49)	1.38 (0.95) [b]	5
PF-LPr	3.850 (0.07)	0.62 (0.19) [a]	0
	Beech wood		
PF-LKL	3.865 (0.05)	1.82 (0.33) [b]	0
PF-LPr	3.675 (0.19)	1.33 (0.31) [b]	0

The values followed by the same superscript letter in the same column are not statistically different at 95% significance, $p < 0.05$.

Further mechanical test varying the temperature of the press and the time will be investigated in future works. However, the data demonstrate that the performance of bioadhesives shows that biopolyols are a promising alternative as partial substitutes (60%) of phenol.

4.5   Conclusion

Based on the results of the CCD design, it was concluded that viscosity is the property most influenced by reaction conditions and the free formaldehyde content is influenced only by the polyol content.

Under optimal conditions, all pre-cured bioresins had excellent water resistance.

Biopolyol obtained from different lignocellulosic biomasses (Kraft lignin, sugarcane bagasse, almond shells and pine sawdust) can be used for the synthesis of bioresins with 60% phenol substitution, presenting SC, viscosity and pH properties that meet the requirement standard. FFC property requires some additive to absorb formaldehyde.
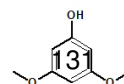
The bioresin, synthesized with biopolyol from Kraft lignin showed better mechanical performance than the bioresin using liquefied pine.

The bioadhesives presented acceptable percentage of wood failure according to standard, except for the three-ply plywood glued with PF-LPr bioresin.
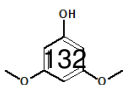
Chapter 5

General conclusions, future research
and published works

5.1   General conclusions

In this thesis, different lignocellulosic residues were liquefied and the possibility of being used as partial substitutes of the phenol in phenolic resins was studied. For this, Kraft lignin precipitated from industrial black liquor was liquefied and extensively studied in Chapter 2, while liquefied agricultural and forest residues were investigated in Chapter 3. Moreover, the synthesis of biophenolic resins was studied in Chapter 4.

In Chapter 2, initially, Kraft lignin was precipitated using some organic acids (acetic acid, lactic acid, and citric acid), apart from the traditional sulfuric acid. Lignin precipitated with organic acids showed higher purity than with sulfuric acid. In addition, a correlation was observed between the ionic strength of the organic acids and the molecular characteristics, such as functional groups, monomers composition and molecular weight of lignin. Moreover, the use of strong organic acid makes the lignin less thermal stable, however, for all acids, the decomposition temperatures were above 200 °C.

Then, Kraft lignin (precipitated with sulfuric acid) was liquefied using two different heat sources, reflux and microwave. For each technique, an experimental design (varying reaction time, mass, and catalyst concentration) was adopted and the optimized conditions were determined as a function of yield, acid and hydroxyl number and viscosity of the polyols. At reflux, the experimental design revealed that the catalyst variable was significant ($p<0.05$) in the yield and the reaction time was significant in the hydroxyl groups. While the viscosity was influenced ($p<0.05$) by the reaction time and catalyst variables. Regarding microwave liquefaction, the yield was influenced by the reaction time and by the catalyst. The number of acids was affected by the catalyst and mass variables, while the viscosity was influenced by all the variables.
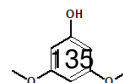
Optimized conditions under reflux were determined as 15% lignin, in absence of catalyst at 60 min, and under microwave heating was 20% lignin, 5 min and 3% catalyst.

The synthesis of optimized polyols under reflux with some lignocellulosic residues was developed in Chapter 3. The lignin precipitated with organic acids was liquefied and their properties compared to the polyol obtained from lignin precipitated with sulfuric acid. In this sense, lignin precipitated with SA gave with higher yield, OH number and viscosity values than those precipitated with organic acids. While the precipitation with acetic acid resulted in a polyol with the highest acid number. LHKL and LKLL polyols (precipitated with SA and lactic acid, respectively), showed similar molecular weight and polydispersity, as did LKLA and LKLC polyol (precipitated with acetic acid and citric acid, respectively). This demonstrates that organic acid precipitated lignin has a great potential for producing polyol with properties similar to those using SA precipitated lignin.

In addition, the organic acids were evaluated as liquefying catalysts. For this, the liquefied lignin was produced using three different concentrations of catalyst (3, 6 and 9%) for each organic acid. The polyols showed a similar yield and the higher formation of acidic substances was found in the polyol produced with citric acid. In fact, a trend of increasing the number of acids with increased ionic strength (acetic acid <lactic acid <citric acid) and catalyst concentration was observed. The minimum OH values were found in 6% of the catalyst, regardless to the type of organic acid used, while higher viscosity was found in the presence of 6 and 9% citric acid. The chemical structure and volatile compounds showed traces of lignin derivatives and some intermediate solvent products. The organic acids studied showed great potential to be used as catalysts in the liquefaction process, being renewable and ecologically correct reagents.

Apart from Kraft lignin, almond shells, cane bagasse, pecan shells,
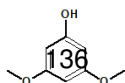
pine and Oak sawdust were studied as a raw material for the production of polyols. Higher yield, viscosity and molecular weight were found in the liquefied oak sawdust. Conversely, low conversion, acid substances and hydroxyl groups were found in liquefied pecan (LPS) shells. The chemical structure showed that the polyols are rich in hydroxyl groups, in addition to characteristic peaks of lignin.

Finally, the synthesis of biophenolic resins using some of the polyols obtained in the previous chapter to partially replace the phenol was investigated in Chapter 4. For this, an experimental design was carried out and the independent variables were polyol / phenol (w / w), formaldehyde / phenol (molar ratio) and NaOH / phenol (molar ratio). The optimum conditions were determined in terms of solid content, free formaldehyde content, viscosity and pH. Experimental design with EFS precipitated lignin to replace part of the phenol revealed that FFC was influenced ($p < 0.05$) by the amount of polyol and viscosity was influenced by all variables. Under optimum conditions, the biophenolic resins were synthesized using different polyols (lignin, almond, bagasse and pine) to replace 60% of the phenol. The properties of the bioresins, such as SC, viscosity and pH, showed that they meet the requirement standard. However, in the case of FFC requires some additive to absorb formaldehyde. All pre-cured bioresins presented excellent water resistance. In addition, bioresins using liquefied lignin and liquefied pine sawdust were evaluated as wood adhesive. The bioresin, synthesized with biopolyol from Kraft lignin showed better mechanical performance than the bioresin using liquefied pine. The bioadhesives presented acceptable percentage of wood failure according to standard, except for the three-ply plywood glued with PF-LPr bioresin.
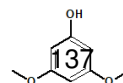
5.2 Future research

Taking into account the initial results and conclusions obtained in the present thesis, the following future research lines are proposed:

- To produce modified biopolyols.

- To produce plywood with bioresinas using different temperatures and time.

- To evaluate the mechanical properties of plywood.

- To use the bioresin as impregnation for the production of external panels.

- To explore the application of biopolyol in other field.

5.3 Published works

Publications in scientific journals

During this doctoral thesis, the following publications in scientific journals related to the topic of the thesis have been produced:

1. **Authors: Silva S H F**, Santos P S B, Silva D T, Briones R, Gatto D A, Labidi J
   Title: Kraft lignin-based polyols by microwave: Optimizing reaction conditions
   Journal: Journal of Wood Chemistry and Technology
   DOI: 10.1080/02773813.2017.1303513
   **Volume:** 37(5)
   Pages: 343 - 358
   Year: 2017
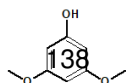
2. **Authors: Silva S H F**, Santos P S B, Gatto D A, Andres M A, Egües I
   Title: Liquefaction of Kraft Lignin at Atmospheric Pressure
   Journal: Journal of Renewable Materials
   DOI: 10.32604/jrm.2019.04291
   ISSN: 2164.6341
   Volume: 7 (6)
   Pages: 527-534
   Year: 2019

3. **Authors: Silva S H F**, Egües I, Labidi J
   Title: Liquefaction of Kraft Lignin using polyhydric alcohols and organic acids as catalysts for sustainable polyol production
   Journal: Industrial Crops and Products
   DOI: 10.1016/j.indcrop.2019.05.075
   Volume: 137
   Pages: 687-693
   Year: 2019

Contributions in scientific conferences

The following works related to this doctoral thesis were presented in international scientific conferences:

1. **Authors:** Itziar Egües, Arantxa Olasagasti, Xabier Erdocia, Pedro Luis de Hoyos, **Silvia H. Fuentes**, Jalel Labidi
   Title: Lignin-based resol resins: effect of lignin fractionation
   Conference: 14th European Workshop on Lignocellulosics and Pulp
   Presentation: Oral
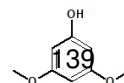
Place: Autrans, France
Date: 28 June - 1st July, 2016

2. **Authors:** <u>**Silvia H. Fuentes da Silva**</u>, Patricia S. Bilhalva dos Santos, Darci Alberto Gatto, Jalel Labidi
   Title: Influence of reaction conditions of liquefaction in the viscosity of Kraft lignin-based polyols
   Conference: Hygrothermal Performance of Buildings and their Materials
   Presentation: Oral
   Place: Poznan, Poland
   Date: 30-31 August, 2016

3. **Authors:** Patricia S. Bilhalva dos Santos, <u>**Silvia H. Fuentes da Silva**</u>, Darci Alberto Gatto, Jalel Labidi
   Title: Solid residue characterization occurred from organosolv black liquor depolymerization
   Conference: Hygrothermal Performance of Buildings and their Materials
   Presentation: Oral
   Place: Poznan, Poland
   Date: 30-31 August, 2016

4. **Authors:** <u>**Silvia H. Fuentes da Silva**</u>, Patricia S. Bilhalva dos Santos, Darci Alberto Gatto, Jalel Labidi
   Title: Liquefaction of Kraft lignin using different solvents
   Conference: Innovative production technologies and increased wood products recycling and reuse
   Presentation: Oral
   Place: Brno, Czech Republic

Date: 29-30 September, 2016

5. **Authors:** <u>**Silvia H. Fuentes da Silva**</u>, Patricia S. Bilhalva dos Santos, Rodrigo Brione, Darci Alberto Gatto, Jalel Labidi
   Title: Kraft lignin based on polyol - Optimized liquefaction reaction
   Conference: XXIII TECNICELPA International Forest, Pulp and Paper Conference
   Presentation: Oral
   Place: Porto, Portugal
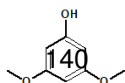   **Date:** 12-14 October, 2016

6. **Authors:** <u>**Silvia H. Fuentes da Silva**</u>, Patricia S. Bilhalva dos Santos, Darci Alberto Gatto, Jalel Labidi
   Title: Liquefaction of Kraft lignin at atmospheric pressure
   Conference: International Conference on Materials and Energy
   Presentation: Oral
   Place: Donostia - San Sebastián, Spain
   Date: 30 Abril to 4 May, 2018

7. **Authors: Silvia H. Fuentes**, Itziar Egüés, Jalel Labidi
   Title: Polyols from lignin and sawdust of oak wood
   Conference: 8th Hardwood Conference
   Presentation: oral
   Place: Sopron, Hungary
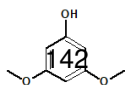   **Date:** 25-26 October
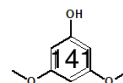
Assistance to training related to the thesis

1. **Title:** Characterization of plywood modified by compressed veneer woods using phenolic resins based on biopolymers
   **Place:** Poznan University of Life Sciences, Poznan, Poland
   Date: 16-26 February, 2019

Bibliography

[1] **Fund, U. N. P.**, *State of world population 2011: people and possibilities in a world of 7 billion*, Tech. Rep. 2011 UNPF Rep, 2011.

[2] **World Health Organization - WHO**, *IARC: DIESEL ENGINE EXHAUST CARCINOGENIC*, *International Agency for Research on Cancer - I.A.R. on Cancer*, edited by I.A.R.C., Press Release Nº 213, Jun. 2012.

[3] **Ministério do Meio Ambiente - MMA**, *Protocolo de Quito*, 2008, http://www.mma.gov.br/clima/convencao-das-nacoes-unidas/protocolo-de-quioto - Last checked: 12.11.2018.

[4] **Generalitat de Catalunya**, *Ratificación del Protocolo de Kioto por España*, 2010, http://www.mma.gov.br/clima/convencao-das-nacoes-unidas/protocolo-de-quioto - Last checked: 12.11.2018.

[5] **World Health Organization - WHO**, *Rio+20 declares health key to sustainable development goals*, Public Health and Environment e-News, 2012.

[6] **Brundtland Report**, *World Commission on Environment and Development. Our Common Future, published as an-*
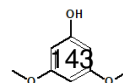
nex to General Assembly document A/42/427, August 1987, http://www.un-documents.net/wced-ocf.htm - Last checked: 01.11.2018.

[7] **IEA Bioenergy - Task 42**, *Broschure of IEA Bioenergy Task 42, Biorefining*, 2009, https://www.iea-bioenergy.task42-biorefineries.com/en/ieabiorefinery.htm - Last checked: 13.11.2018.

[8] **Kohlhepp, G.**, *Análise da situação da produção de etanol e biodiesel no Brasil*, Estudos avançados, Vol. 24, No. 68, pp. 223–253, 2010.

[9] **Unica, U. d. I. d. C.-d.-a.**, *BIOCOMBUSTÍVEIS TERÃO PAPEL RELEVANTE PARA CUMPRIMENTO DAS METAS DE PARIS*, 2018, http://www.unica.com.br/noticia/19187063920326811142/ biocombustiveis-terao-papel-relevante-para-cumprimento-das-metas-de-paris/ - Last checked: 10.12.2018.

[10] **for Research, D.-G.** and **Innovation**, *European Bioeconomy Strategy 2012: "Innovating for Sustainable Growth: A Bioeconomy for Europe"*, Publications Office of the European Union, 2012.

[11] **Hassan, S. S., Williams, G. A.** and **Jaiswal, A. K.**, *Lignocellulosic Biorefineries in Europe: Current State and Prospects*, Trends in biotechnology, 2018.

[12] **based Industries Consortium, B. et al.**, *The Bio-based Industries: Mapping European Biorefineries*, 2012, https://biconsortium.eu/news/mapping-european-biorefineries - Last checked: 25.11.2018.

[13] **Cherubini, F.**, *The biorefinery concept: using biomass instead*

of oil for producing energy and chemicals, Energy conversion and management, Vol. 51, No. 7, pp. 1412–1421, 2010.

[14] **Nali, E. C., Ribeiro, L. B. N. M.** and **Hora, A. B. d.**, *Biorrefinaria integrada a industria de celulose no Brasil: oportunidade ou necessidade?*, 2016.

[15] **Unica, U. d. I. d. C.-d.-a.**, *INDÚSTRIA QUÍMICA AVANÇA EM TECNOLOGIAS ENZIMÁTICAS PARA PRODUÇÃO DE ETANOL 2G*, 2016, http://www.unica.com.br/noticia/3102159920315624493/ industria-quimica-avanca-em-tecnologias-enzimaticas-para- producao-de-etanol-2g/ - Last checked: 10.12.2018.

[16] **Statista**, *Fuel ethanol production worlwide*, 2017, https://www.statista.com/statistics/281606/ethanol- production-in-selected-countries/ - Last checked: 26.11.2018.

[17] **MAPA**, *Projeções do Agronegócio : Brasil 2017/18 a 2027/28*, 2018.

[18] **de Pesquisa Energética, E.-E.**, *Plano nacional de energia 2030*, Rio de Janeiro: EPE, pp. 1970–2010, 2007.

[19] **Özdenkçi, K., De Blasio, C., Muddassar, H. R., Melin, K., Oinas, P., Koskinen, J., Sarwar, G.** and **Järvinen, M.**, *A novel biorefinery integration concept for lignocellulosic biomass*, Energy Conversion and Management, Vol. 149, pp. 974–987, 2017.

[20] **Mongkhonsiri, G., Gani, R., Malakul, P.** and **Assabumrungrat, S.**, *Integration of the biorefinery concept for the development of sustainable processes for pulp and paper industry*, Computers & Chemical Engineering, Vol. 119, pp. 70–84, 2018.

[21] **Foelkel, C.**, *O processo de impregnação dos cavacos de madeira de eucalipto pelo licor Kraft de cozimento*, Porto Alegre: Eucaliptus Online Book, 2009.

[22] **Lee, R. A.** and **Lavoie, J.-M.**, *From first-to third-generation biofuels: Challenges of producing a commodity from a biomass of increasing complexity*, Animal Frontiers, Vol. 3, No. 2, pp. 6–11, 2013.

[23] **Chen, H.**, *Lignocellulose biorefinery engineering: principles and applications*, , No. 74, 2015.

[24] **Bilal, M., Asgher, M., Iqbal, H. M., Hu, H.** and **Zhang, X.**, *Biotransformation of lignocellulosic materials into value-added products—A review*, International journal of biological macromolecules, Vol. 98, pp. 447–458, 2017.

[25] **Anwar, Z., Gulfraz, M.** and **Irshad, M.**, *Agro-industrial lignocellulosic biomass a key to unlock the future bio-energy: a brief review*, Journal of radiation research and applied sciences, Vol. 7, No. 2, pp. 163–173, 2014.

[26] **Menon, V.** and **Rao, M.**, *Trends in bioconversion of lignocellulose: biofuels, platform chemicals & biorefinery concept*, Progress in energy and combustion science, Vol. 38, No. 4, pp. 522–550, 2012.

[27] **Pettersen, R. C.**, *The chemical composition of wood*, The chemistry of solid wood, Vol. 207, pp. 57–126, 1984.

[28] **Pereira, H.**, *Variability in the chemical composition of plantation eucalypts (Eucalyptus globulus Labill.)*, Wood and Fiber Science, Vol. 20, No. 1, pp. 82–90, 2007.

[29] **McKendry, P.**, *Energy production from biomass (part 1):*

overview of biomass, Bioresource technology, Vol. 83, No. 1, pp. 37–46, 2002.

[30] **Kim, M.** and **Day, D. F.**, *Composition of sugar cane, energy cane, and sweet sorghum suitable for ethanol production at Louisiana sugar mills*, Journal of industrial microbiology & biotechnology, Vol. 38, No. 7, pp. 803–807, 2011.

[31] **Yao, S., Nie, S., Yuan, Y., Wang, S.** and **Qin, C.**, *Efficient extraction of bagasse hemicelluloses and characterization of solid remainder*, Bioresource technology, Vol. 185, pp. 21–27, 2015.

[32] **de Moraes Rocha, G. J., Nascimento, V. M., Goncalves, A. R., Silva, V. F. N.** and **Martín, C.**, *Influence of mixed sugarcane bagasse samples evaluated by elemental and physical–chemical composition*, Industrial Crops and Products, Vol. 64, pp. 52–58, 2015.

[33] **Littlefield, B.**, Characterization of pecan shells for value-added applications, Ph.D. thesis, 2010.

[34] **Foelkel, C.**, *As biorrefinarias integradas no setor brasileiro de fabricação de celulose e papel de eucalitpo*, Eucalyptus Online Book & Newsletter, pp. 1–270, 2012.

[35] **Habibi, Y., Lucia, L. A.** and **Rojas, O. J.**, *Cellulose nanocrystals: chemistry, self-assembly, and applications*, Chemical reviews, Vol. 110, No. 6, pp. 3479–3500, 2010.

[36] **Varshney, V.** and **Naithani, S.**, *Chemical functionalization of cellulose derived from nonconventional sources*, *Cellulose Fibers: Bio-and Nano-Polymer Composites*, pp. 43–60, Springer, 2011.

[37] **Hu, Y., Acharya, S.** and **Abidi, N.**, *Cellulose porosity improves its dissolution by facilitating solvent diffusion*, International journal of biological macromolecules, 2018.

[38] **Hansen, C.** and **Björkman, A.**, *The ultrastructure of wood from a solubility parameter point of view*, Holzforschung-International Journal of the Biology, Chemistry, Physics and Technology of Wood, Vol. 52, No. 4, pp. 335–344, 1998.

[39] **Timell, T. E.**, *Recent progress in the chemistry of wood hemicelluloses*, Wood Science and Technology, Vol. 1, No. 1, pp. 45–70, 1967.

[40] **Ponnusamy, V. K., Nguyen, D. D., Dharmaraja, J., Shobana, S., Banu, R., Saratale, R. G., Chang, S. W.** and **Kumar, G.**, *A review on lignin structure, pretreatments, fermentation reactions and biorefinery potential*, Bioresource technology, 2018.

[41] **Adler, E.**, *Lignin chemistry—past, present and future*, Wood science and technology, Vol. 11, No. 3, pp. 169–218, 1977.

[42] **Smolarski, N.**, *High-value opportunities for lignin: unlocking its potential*, Frost & Sullivan, Vol. 1, 2012.

[43] **Bruijnincx, P., Weckhuysen, B., Gruter, G.-J.** and **Engelen-Smeets, E.**, Lignin Valorisation: The Importance of a Full Value Chain Approach, Utrecht University, 2016.

[44] **Boerjan, W., Ralph, J.** and **Baucher, M.**, *Lignin biosynthesis*, Annual review of plant biology, Vol. 54, No. 1, pp. 519–546, 2003.

[45] **Gellerstedt, G.** and **Henriksson, G.**, *Lignins: major sources, structure and properties*, *Monomers, Polymers and Composites from Renewable Resources*, pp. 201–224, Elsevier, 2008.

[46] **Donaldson, L. A.**, *Lignification and lignin topochemistry—an ultrastructural view*, Phytochemistry, Vol. 57, No. 6, pp. 859–873, 2001.

[47] **Tobimatsu, Y.** and **Schuetz, M.**, *Lignin polymerization: how do plants manage the chemistry so well?*, Current Opinion in Biotechnology, Vol. 56, pp. 75–81, 2019.

[48] **Sjostrom, E.**, Wood chemistry: fundamentals and applications, Elsevier, 2013.

[49] **Rinaldi, R., Jastrzebski, R., Clough, M. T., Ralph, J., Kennema, M., Bruijnincx, P. C.** and **Weckhuysen, B. M.**, *Paving the way for lignin valorisation: recent advances in bioengineering, biorefining and catalysis*, Angewandte Chemie International Edition, Vol. 55, No. 29, pp. 8164–8215, 2016.

[50] **Macfarlane, A., Mai, M.** and **Kadla, J.**, *Bio-based chemicals from biorefining: Lignin conversion and utilisation*, *Advances in Biorefineries*, pp. 659–692, Elsevier, 2014.

[51] **Pandey, M. P.** and **Kim, C. S.**, *Lignin depolymerization and conversion: a review of thermochemical methods*, Chemical Engineering & Technology, Vol. 34, No. 1, pp. 29–41, 2011.

[52] **Vanholme, R., Demedts, B., Morreel, K., Ralph, J.** and **Boerjan, W.**, *Lignin biosynthesis and structure*, Plant physiology, Vol. 153, No. 3, pp. 895–905, 2010.

[53] **Derkacheva, O. Y.**, *Estimation of aromatic structure contents in hardwood lignins from IR absorption spectra*, Journal of Applied Spectroscopy, Vol. 80, No. 5, pp. 670–676, 2013.

[54] **Gao, L., Chen, S.** and **Zhang, D.**, *Advances in modifying lignin structures for largely enhancing high-lignin biomass sac-*

charification, Process Biochemistry, Vol. 57, pp. 175–180, 2017.

[55] **Zhang, M., Lapierre, C., Nouxman, N. L., Nieuwoudt, M. K., Smith, B. G., Chavan, R. R., McArdle, B. H.** and **Harris, P. J.**, *Location and characterization of lignin in tracheid cell walls of radiata pine (Pinus radiata D. Don) compression woods*, Plant physiology and biochemistry, Vol. 118, pp. 187–198, 2017.

[56] **Laurichesse, S.** and **Avérous, L.**, *Chemical modification of lignins: Towards biobased polymers*, Progress in polymer science, Vol. 39, No. 7, pp. 1266–1290, 2014.

[57] **Admin**, *The chemical reactions in Kraft pulping process*, 2015, http://www.pulppapermill.com/the-chemical-reactions-in-kraft-pulping-process/ - Last checked: 15.11.2018.

[58] **Berlin, A.** and **Balakshin, M.**, *Industrial lignins: analysis, properties, and applications*, *Bioenergy Research: Advances and Applications*, pp. 315–336, Elsevier, 2014.

[59] **Valmet**, *First LignoBoost plants producing large volumes of kraft lignin to the market place*, 2016, https://www.valmet.com/media/articles/up-and-running/new-technology/PEERS1stLignoBoostPlants/ - Last checked: 01.12.2018.

[60] **Lora, J.**, *Industrial commercial lignins: sources, properties and applications*, *Monomers, polymers and composites from renewable resources*, pp. 225–241, Elsevier, 2008.

[61] **Demirbaş, A.**, *Biomass resource facilities and biomass conversion processing for fuels and chemicals*, Energy conversion and Management, Vol. 42, No. 11, pp. 1357–1378, 2001.

[62] **Isa, K. M., Abdullah, T. A. T.** and **Ali, U. F. M.**, *Hydrogen donor solvents in liquefaction of biomass: A review*, Renewable and Sustainable Energy Reviews, 2017.

[63] **Kleerebezem, R.**, *Biochemical conversion: anaerobic digestion*, W. d. J. a. JR v. Ommen, ed. Biomass as a Sustainable Energy Source for the Future: Fundamentals of Conversion Processes. New jersey: Wiley, pp. 441–461, 2014.

[64] **Haverly, M. R.**, *An experimental study on solvent liquefaction*, 2016.

[65] **Dhyani, V.** and **Bhaskar, T.**, *A comprehensive review on the pyrolysis of lignocellulosic biomass*, Renewable Energy, Vol. 129, pp. 695–716, 2018.

[66] **Kim, J. W., Lee, H. W., Lee, I.-G., Jeon, J.-K., Ryu, C., Park, S. H., Jung, S.-C.** and **Park, Y.-K.**, *Influence of reaction conditions on bio-oil production from pyrolysis of construction waste wood*, Renewable energy, Vol. 65, pp. 41–48, 2014.

[67] **Wielgosiński, G., Łechtańska, P.** and **Namiecińska, O.**, *Emission of some pollutants from biomass combustion in comparison to hard coal combustion*, Journal of the Energy Institute, Vol. 90, No. 5, pp. 787–796, 2017.

[68] **Gu, H., Tang, Y., Yao, J.** and **Chen, F.**, *Study on biomass gasification under various operating conditions*, Journal of the Energy Institute, 2018.

[69] **de Caprariis, B., De Filippis, P., Petrullo, A.** and **Scarsella, M.**, *Hydrothermal liquefaction of biomass: influence of temperature and biomass composition on the bio-oil production*, Fuel, Vol. 208, pp. 618–625, 2017.

[70] **Alma, M. H.** and **Karaoğul, T. S.-E. A.-E.**, *Liquefaction Processes of Biomass for the Production of Valuable Chemicals and Biofuels: A Review*, 2013.

[71] **Jiang, W., Kumar, A.** and **Adamopoulos, S.**, *Liquefaction of lignocellulosic materials and its applications in wood adhesives—A review*, Industrial Crops and Products, Vol. 124, pp. 325–342, 2018.

[72] **Huang, X.-Y., Li, F., Xie, J.-L., Cornelis, F., Hse, C.-Y., Qi, J.-Q.** and **Xiao, H.**, *Microwave-assisted Liquefaction of Rape Straw for the Production of Bio-oils*, BioResources, Vol. 12, No. 1, pp. 1968–1981, 2017.

[73] **Jasiukaitytė-Grojzdek, E., Kunaver, M.** and **Crestini, C.**, *Lignin structural changes during liquefaction in acidified ethylene glycol*, Journal of wood chemistry and technology, Vol. 32, No. 4, pp. 342–360, 2012.

[74] **Zheng, Z., Pan, H., Huang, Y., Chung, Y., Zhang, X., Feng, H. et al.**, *Rapid liquefaction of wood in polyhydric alcohols under microwave heating and its liquefied products for preparation of rigid polyurethane foam*, Open Materials Science Journal, Vol. 5, pp. 1–8, 2011.

[75] **Lidström, P., Tierney, J., Watheyb, B.** and **Westmana, J.**, *Microwave assisted organic synthesisÐa review*, Tetrahedron, Vol. 57, pp. 9225–9283, 2001.

[76] **Xue, B.-L., Wen, J.-L.** and **Sun, R.-C.**, *Producing lignin-based polyols through microwave-assisted liquefaction for rigid polyurethane foam production*, Materials, Vol. 8, No. 2, pp. 586–599, 2015.

[77] **Zhuang, Y., Guo, J., Chen, L., Li, D., Liu, J.** and **Ye, N.**, *Microwave-assisted direct liquefaction of Ulva prolifera for*

bio-oil production by acid catalysis, Bioresource technology, Vol. 116, pp. 133–139, 2012.

[78] **Lee, Y.** and **Lee, E. Y.**, *Liquefaction of Red Pine Wood, Pinus densiflora, Biomass Using Peg-400-Blended Crude Glycerol for Biopolyol and Biopolyurethane Production*, Journal of Wood Chemistry and Technology, Vol. 36, No. 5, pp. 353–364, 2016.

[79] **Kim, K. H., Jo, Y. J., Lee, C. G.** and **Lee, E.**, *Solvothermal liquefaction of microalgal Tetraselmis sp. biomass to prepare biopolyols by using PEG# 400-blended glycerol*, Algal Research, Vol. 12, pp. 539–544, 2015.

[80] **Nasar, M., Emam, A., Sultan, M.** and **Hakim, A. A.**, *Optimization and characterization of sugar-cane bagasse liquefaction process*, Indian Journal of Science and Technology, Vol. 3, No. 2, pp. 207–212, 2010.

[81] **Kržan, A.** and **Žagar, E.**, *Microwave driven wood liquefaction with glycols*, Bioresource Technology, Vol. 100, No. 12, pp. 3143–3146, 2009.

[82] **Kumar, A., Vlach, T., Ryparovà, P., Škapin, A. S., Kovač, J., Adamopoulos, S., Hajek, P.** and **Petrič, M.**, *Influence of liquefied wood polyol on the physical-mechanical and thermal properties of epoxy based polymer*, Polymer Testing, Vol. 64, pp. 207–216, 2017.

[83] **Zhang, H., Pang, H., Shi, J., Fu, T.** and **Liao, B.**, *Investigation of liquefied wood residues based on cellulose, hemicellulose, and lignin*, Journal of Applied Polymer Science, Vol. 123, No. 2, pp. 850–856, 2012.

[84] **Hu, S., Wan, C.** and **Li, Y.**, *Production and characterization of biopolyols and polyurethane foams from crude glycerol*

based liquefaction of soybean straw, Bioresource technology, Vol. 103, No. 1, pp. 227–233, 2012.

[85] **Yu, F., Liu, Y., Pan, X., Lin, X., Liu, C., Chen, P.** and **Ruan, R.**, *Liquefaction of corn stover and preparation of polyester from the liquefied polyol*, *Twenty-Seventh Symposium on Biotechnology for Fuels and Chemicals*, pp. 574–585, Springer, 2006.

[86] **Yona, A. M. C., Budija, F., Kričej, B., Kutnar, A., Pavlič, M., Pori, P., Tavzes, Č.** and **Petrič, M.**, *Production of biomaterials from cork: Liquefaction in polyhydric alcohols at moderate temperatures*, Industrial Crops and Products, Vol. 54, pp. 296–301, 2014.

[87] **El-barbary, M. H.** and **Shukry, N.**, *Polyhydric alcohol liquefaction of some lignocellulosic agricultural residues*, Industrial Crops and Products, Vol. 27, No. 1, pp. 33–38, 2008.

[88] **Gama, N. V., Soares, B., Freire, C. S., Silva, R., Neto, C. P., Barros-Timmons, A.** and **Ferreira, A.**, *Bio-based polyurethane foams toward applications beyond thermal insulation*, Materials & Design, Vol. 76, pp. 77–85, 2015.

[89] **Jin, Y., Ruan, X., Cheng, X.** and **Lü, Q.**, *Liquefaction of lignin by polyethyleneglycol and glycerol*, Bioresource technology, Vol. 102, No. 3, pp. 3581–3583, 2011.

[90] **Gosz, K., Kosmela, P., Hejna, A., Gajowiec, G.** and **Piszczyk, Ł.**, *Biopolyols obtained via microwave-assisted liquefaction of lignin: structure, rheological, physical and thermal properties*, Wood Science and Technology, Vol. 52, No. 3, pp. 599–617, 2018.

[91] **Mahmood, N., Yuan, Z., Schmidt, J.** and **Xu, C. C.**, *Production of polyols via direct hydrolysis of kraft lignin: Effect of pro-*

cess parameters, Bioresource technology, Vol. 139, pp. 13–20, 2013.

[92] **The Essential Chemical Industry**, *Sulfuric acid*, 2016, http://www.essentialchemicalindustry.org/chemicals/sulfuric-acid.html - Last checked: 10.01.2019.

[93] **Khan, M. A., Ashraf, S. M.** and **Malhotra, V. P.**, *Eucalyptus bark lignin substituted phenol formaldehyde adhesives: A study on optimization of reaction parameters and characterization*, Journal of applied polymer science, Vol. 92, No. 6, pp. 3514–3523, 2004.

[94] **IARC**, *Occupational exposures to mists and vapours from strong inorganic acids and other industrial chemicals*, IARC Monogr Eval Carcinog Risks Hum, Vol. 54, pp. 1–310, 1992.

[95] **Shi, Y., Xia, X., Li, J., Wang, J., Zhao, T., Yang, H., Jiang, J.** and **Jiang, X.**, *Solvolysis kinetics of three components of biomass using polyhydric alcohols as solvents*, Bioresource technology, Vol. 221, pp. 102–110, 2016.

[96] **Jo, Y. J., Ly, H. V., Kim, J., Kim, S.-S.** and **Lee, E.**, *Preparation of biopolyol by liquefaction of palm kernel cake using PEG# 400 blended glycerol*, Journal of Industrial and Engineering Chemistry, Vol. 29, pp. 304–313, 2015.

[97] **Chen, F.** and **Lu, Z.**, *Liquefaction of wheat straw and preparation of rigid polyurethane foam from the liquefaction products*, Journal of Applied Polymer Science, Vol. 111, No. 1, pp. 508–516, 2009.

[98] **Budija, F., Tavzes, Č., Zupančič-Kralj, L.** and **Petrič, M.**, *Self-crosslinking and film formation ability of liquefied black poplar*, Bioresource technology, Vol. 100, No. 13, pp. 3316–3323, 2009.

[99] **Pavier, C.** and **Gandini, A.**, *Oxypropylation of sugar beet pulp. 2. Separation of the grafted pulp from the propylene oxide homopolymer*, Carbohydrate polymers, Vol. 42, No. 1, pp. 13–17, 2000.

[100] **Nadji, H., Bruzzèse, C., Belgacem, M. N., Benaboura, A.** and **Gandini, A.**, *Oxypropylation of lignins and preparation of rigid polyurethane foams from the ensuing polyols*, Macromolecular Materials and Engineering, Vol. 290, No. 10, pp. 1009–1016, 2005.

[101] **Cateto, C. A., Barreiro, M. F., Rodrigues, A. E.** and **Belgacem, M. N.**, *Optimization sdudy of lignin oxypropylation in view of the preparation of polyurethane rigid foams*, Industrial and Engineering Chemistry Research, Vol. 48, No. 5, pp. 2583–2589, 2009.

[102] **Mateus, M. M., Acero, N. F., Bordado, J. C.** and **dos Santos, R. G.**, *Sonication as a foremost tool to improve cork liquefaction*, Industrial Crops and Products, Vol. 74, pp. 9–13, 2015.

[103] **Shin, H. J., Kim, C.-J.** and **Kim, S. B.**, *Kinetic study of recycled newspaper liquefaction in polyol solvent*, Biotechnology and Bioprocess Engineering, Vol. 14, No. 3, pp. 349, 2009.

[104] **Xu, J., Jiang, J., Hse, C.** and **Shupe, T. F.**, *Renewable chemical feedstocks from integrated liquefaction processing of lignocellulosic materials using microwave energy*, Green Chemistry, Vol. 14, No. 10, pp. 2821–2830, 2012.

[105] **Jasiukaitytė, E., Kunaver, M.** and **Crestini, C.**, *Lignin behaviour during wood liquefaction—Characterization by quantitative 31P, 13C NMR and size-exclusion chromatography*, Catalysis today, Vol. 156, No. 1-2, pp. 23–30, 2010.

[106] **Lu, Z., Fan, L., Wu, Z., Zhang, H., Liao, Y., Zheng, D.** and **Wang, S.**, *Efficient liquefaction of woody biomass in polyhydric alcohol with acidic ionic liquid as a green catalyst*, Biomass and Bioenergy, Vol. 81, pp. 154–161, 2015.

[107] **Ross, A., Biller, P., Kubacki, M., Li, H., Lea-Langton, A.** and **Jones, J.**, *Hydrothermal processing of microalgae using alkali and organic acids*, Fuel, Vol. 89, No. 9, pp. 2234–2243, 2010.

[108] **Li, H., Feng, S., Yuan, Z., Wei, Q.** and **Xu, C. C.**, *Highly efficient liquefaction of wheat straw for the production of bio-polyols and bio-based polyurethane foams*, Industrial crops and products, Vol. 109, pp. 426–433, 2017.

[109] **Philipp, C.** and **Eschig, S.**, *Waterborne polyurethane wood coatings based on rapeseed fatty acid methyl esters*, Progress in Organic Coatings, Vol. 74, No. 4, pp. 705–711, 2012.

[110] **Patil, C. K., Rajput, S. D., Marathe, R. J., Kulkarni, R. D., Phadnis, H., Sohn, D., Mahulikar, P. P.** and **Gite, V. V.**, *Synthesis of bio-based polyurethane coatings from vegetable oil and dicarboxylic acids*, Progress in Organic Coatings, Vol. 106, pp. 87–95, 2017.

[111] **Fridrihsone-Girone, A., Stirna, U., Misāne, M., Lazdiņa, B.** and **Deme, L.**, *Spray-applied 100% volatile organic compounds free two component polyurethane coatings based on rapeseed oil polyols*, Progress in Organic Coatings, Vol. 94, pp. 90–97, 2016.

[112] **Rajput, S. D., Mahulikar, P. P.** and **Gite, V. V.**, *Biobased dimer fatty acid containing two pack polyurethane for wood finished coatings*, Progress in Organic Coatings, Vol. 77, No. 1, pp. 38–46, 2014.

[113] **Lee, S.-H., Teramoto, Y.** and **Shiraishi, N.**, *Biodegradable polyurethane foam from liquefied waste paper and its thermal stability, biodegradability, and genotoxicity*, Journal of Applied Polymer Science, Vol. 83, No. 7, pp. 1482–1489, 2002.

[114] **Kurimoto, Y., Takeda, M., Doi, S., Tamura, Y.** and **Ono, H.**, *Network structures and thermal properties of polyurethane films prepared from liquefied wood*, Bioresource technology, Vol. 77, No. 1, pp. 33–40, 2001.

[115] **ACC - American Chemistry Council**, *Heterochain polymers*, 2019.

[116] *Em uma síntese de oxialcoóis aromáticos*, Relatórios da Sociedade Alemã de Química, Vol. 27.

[117] **Pilato, L.**, Phenolic resins: a century of progress, Vol. 11, Springer, 2010.

[118] **Gardziella, A., Pilato, L. A.** and **Knop, A.**, Phenolic resins: chemistry, applications, standardization, safety and ecology, Springer Science & Business Media, 2013.

[119] **Han, Q., Li, D., Li, X., Peng, X.** and **Zhang, D.**, *Preparing phenolic resins using pulping spent liquor*, International Journal of Adhesion and Adhesives, Vol. 77, pp. 72–77, 2017.

[120] **Lee, W.-J.** and **Liu, C.-T.**, *Preparation of liquefied bark-based resol resin and its application to particle board*, Journal of applied polymer science, Vol. 87, No. 11, pp. 1837–1841, 2003.

[121] **Zhang, W., Ma, Y., Xu, Y., Wang, C.** and **Chu, F.**, *Lignocellulosic ethanol residue-based lignin–phenol–formaldehyde resin adhesive*, International Journal of Adhesion and Adhesives, Vol. 40, pp. 11–18, 2013.

[122] **Yang, S., Zhang, Y., Yuan, T.-Q.** and **Sun, R.-C.**, *Lignin–phenol–formaldehyde resin adhesives prepared with biorefinery technical lignins*, Journal of Applied Polymer Science, Vol. 132, No. 36, 2015.

[123] **Hussin, M. H., Samad, N. A., Latif, N. H. A., Rozuli, N. A., Yusoff, S. B., Gambier, F.** and **Brosse, N.**, *Production of oil palm (Elaeis guineensis) fronds lignin-derived non-toxic aldehyde for eco-friendly wood adhesive*, International journal of biological macromolecules, Vol. 113, pp. 1266–1272, 2018.

[124] **Wang, G.** and **Chen, H.**, *Carbohydrate elimination of alkaline-extracted lignin liquor by steam explosion and its methylolation for substitution of phenolic adhesive*, Industrial Crops and Products, Vol. 53, pp. 93–101, 2014.

[125] **Gellerstedt, G.**, *Chemistry of chemical pulping*, Pulping chemistry and technology, Vol. 2, pp. 91–120, 2009.

[126] **Virkutyte, J.**, *Aerobic Treatment of Effluents From Pulp and Paper Industries*, *Current Developments in Biotechnology and Bioengineering*, pp. 103–130, Elsevier, 2017.

[127] **Boeriu, C. G., Bravo, D., Gosselink, R. J.** and **van Dam, J. E.**, *Characterisation of structure-dependent functional properties of lignin with infrared spectroscopy*, Industrial crops and products, Vol. 20, No. 2, pp. 205–218, 2004.

[128] **Domínguez-Robles, J., Tamminen, T., Liitiä, T., Peresin, M. S., Rodríguez, A.** and **Jääskeläinen, A.-S.**, *Aqueous acetone fractionation of kraft, organosolv and soda lignins*, International journal of biological macromolecules, Vol. 106, pp. 979–987, 2018.

[129] **Li, H.** and **McDonald, A. G.**, *Fractionation and characterization of industrial lignins*, Industrial crops and products, Vol. 62, pp. 67–76, 2014.

[130] **Gordobil, O., Moriana, R., Zhang, L., Labidi, J.** and **Sevastyanova, O.**, *Assesment of technical lignins for uses in biofuels and biomaterials: Structure-related properties, proximate analysis and chemical modification*, Industrial crops and products, Vol. 83, pp. 155–165, 2016.

[131] **Gordobil, O., Delucis, R., Egüés, I.** and **Labidi, J.**, *Kraft lignin as filler in PLA to improve ductility and thermal properties*, Industrial Crops and Products, Vol. 72, pp. 46–53, 2015.

[132] **Namane, M., Garcia-Mateos, F. J., Sithole, B., Ramjugernath, D., Rodriguez-Mirasol, J.** and **Cordero, T.**, *Characteristics of lignin precipitated with organic acids as a source for valorisation of carbon products*, Cellulose Chem. Technol, Vol. 50, No. 3-4, pp. 355–360, 2016.

[133] **Dang, B. T., Theliander, H., Brelid, H.** and **Köhnke, T.**, *Effect of sodium ion concentration profile during softwood kraft pulping on delignification rate, xylan retention and reactions of hexenuronic acids*, Nordic Pulp & Paper Research Journal, Vol. 29, No. 4, pp. 604–611, 2014.

[134] **Zhu, W.** and **Theliander, H.**, *Equilibrium of lignin precipitation, 16th International Symposium on Wood, Fiber and Pulping Chemistry-Proceedings, ISWFPC, Tianjin; 8 June 2011 through 10 June 2011*, Vol. 1, pp. 195–199, 2011.

[135] **Chakar, F. S.** and **Ragauskas, A. J.**, *Review of current and future softwood kraft lignin process chemistry*, Industrial Crops and Products, Vol. 20, No. 2, pp. 131–141, 2004.

[136] **Zhu, W.** and **Theliander, H.**, *Precipitation of lignin from softwood black liquor: an investigation of the equilibrium and molecular properties of lignin*, BioResources, Vol. 10, No. 1, pp. 1696–1714, 2015.

[137] **Dodd, A. P., Kadla, J. F.** and **Straus, S. K.**, *Characterization of fractions obtained from two industrial softwood kraft lignins*, ACS Sustainable Chemistry & Engineering, Vol. 3, No. 1, pp. 103–110, 2014.

[138] **Yuan, T.-Q., He, J., Xu, F.** and **Sun, R.-C.**, *Fractionation and physico-chemical analysis of degraded lignins from the black liquor of Eucalyptus pellita KP-AQ pulping*, Polymer degradation and stability, Vol. 94, No. 7, pp. 1142–1150, 2009.

[139] **Zhu, W.**, *Equilibrium of lignin precipitation: the effects of ph, temperature, ion strength and wood origins*, 2013.

[140] **Liu, Z., Luo, X. G., Li, Y., Li, L.** and **Huang, Y.**, *Extraction of Lignin from Pulping Black Liquor by Organic Acid*, *Materials Science Forum*, Vol. 620, pp. 571–574, Trans Tech Publ, 2009.

[141] **Sathawong, S., Sridach, W.** and **Techato, K.-a.**, *Lignin: Isolation and preparing the lignin based hydrogel*, Journal of environmental chemical engineering, Vol. 6, No. 5, pp. 5879–5888, 2018.

[142] **Cachet, N., Camy, S., Benjelloun-Mlayah, B., Condoret, J.-S.** and **Delmas, M.**, *Esterification of organosolv lignin under supercritical conditions*, Industrial Crops and Products, Vol. 58, pp. 287–297, 2014.

[143] **Hu, J., Xiao, R., Shen, D.** and **Zhang, H.**, *Structural analysis of lignin residue from black liquor and its thermal performance in thermogravimetric-Fourier transform infrared spectroscopy*, Bioresource technology, Vol. 128, pp. 633–639, 2013.

[144] **Martín-Sampedro, R., Santos, J. I., Fillat, Ú., Wicklein, B., Eugenio, M. E.** and **Ibarra, D.**, *Characterization of lignins from Populus alba L. generated as by-products in different transformation processes: Kraft pulping, organosolv and acid hydrolysis*, International journal of biological macromolecules, Vol. 126, pp. 18–29, 2019.

[145] **Holtman, K. M., Chang, H.-m., Jameel, H.** and **Kadla, J. F.**, *Quantitative 13C NMR characterization of milled wood lignins isolated by different milling techniques*, Journal of Wood Chemistry and Technology, Vol. 26, No. 1, pp. 21–34, 2006.

[146] **Constant, S., Wienk, H. L., Frissen, A. E., de Peinder, P., Boelens, R., Van Es, D. S., Grisel, R. J., Weckhuysen, B. M., Huijgen, W. J., Gosselink, R. J. et al.**, *New insights into the structure and composition of technical lignins: a comparative characterisation study*, Green Chemistry, Vol. 18, No. 9, pp. 2651–2665, 2016.

[147] **Huijgen, W. J., Reith, J. H.** and **den Uil, H.**, *Pretreatment and fractionation of wheat straw by an acetone-based organosolv process*, Industrial & Engineering Chemistry Research, Vol. 49, No. 20, pp. 10132–10140, 2010.

[148] **Ponomarenko, J., Dizhbite, T., Lauberts, M., Viksna, A., Dobele, G., Bikovens, O.** and **Telysheva, G.**, *Characterization of softwood and hardwood LignoBoost kraft lignins with emphasis on their antioxidant activity*, BioResources, Vol. 9, No. 2, pp. 2051–2068, 2014.

[149] **Lin, X., Sui, S., Tan, S., Pittman, C., Sun, J.** and **Zhang, Z.**, *Fast pyrolysis of four lignins from different isolation processes using Py-GC/MS*, Energies, Vol. 8, No. 6, pp. 5107–5121, 2015.

[150] **Ray, S.** and **Cooney, R. P.**, *Thermal degradation of polymer and polymer composites*, *Handbook of Environmental Degradation of Materials (Third Edition)*, pp. 185–206, Elsevier, 2018.

[151] **Monteil-Rivera, F., Phuong, M., Ye, M., Halasz, A.** and **Hawari, J.**, *Isolation and characterization of herbaceous lignins for applications in biomaterials*, Industrial Crops and Products, Vol. 41, pp. 356–364, 2013.

[152] **Bertini, F., Canetti, M., Cacciamani, A., Elegir, G., Orlandi, M.** and **Zoia, L.**, *Effect of ligno-derivatives on thermal properties and degradation behavior of poly (3-hydroxybutyrate)-based biocomposites*, Polymer degradation and stability, Vol. 97, No. 10, pp. 1979–1987, 2012.

[153] **Park, S. Y., Kim, J.-Y., Youn, H. J.** and **Choi, J. W.**, *Fractionation of lignin macromolecules by sequential organic solvents systems and their characterization for further valuable applications*, International journal of biological macromolecules, Vol. 106, pp. 793–802, 2018.

[154] **Guo, J., Zhuang, Y., Chen, L., Liu, J., Li, D.** and **Ye, N.**, *Process optimization for microwave-assisted direct liquefaction of Sargassum polycystum C. Agardh using response surface methodology*, Bioresource technology, Vol. 120, pp. 19–25, 2012.

[155] **Li, J., Dai, J., Liu, G., Zhang, H., Gao, Z., Fu, J., He, Y.** and **Huang, Y.**, *Biochar from microwave pyrolysis of biomass: A review*, Biomass and Bioenergy, Vol. 94, pp. 228–244, 2016.

[156] **Barbanera, M., Pelosi, C., Taddei, A.** and **Cotana, F.**, *Optimization of bio-oil production from solid digestate by*

microwave-assisted liquefaction, Energy conversion and management, Vol. 171, pp. 1263–1272, 2018.

[157] **Behr, A., Eilting, J., Irawadi, K., Leschinski, J.** and **Lindner, F.**, *Improved utilisation of renewable resources: new important derivatives of glycerol*, Green Chemistry, Vol. 10, No. 1, pp. 13–30, 2008.

[158] **Xiao, W., Han, L.** and **Zhao, Y.**, *Comparative study of conventional and microwave-assisted liquefaction of corn stover in ethylene glycol*, Industrial Crops and Products, Vol. 34, No. 3, pp. 1602–1606, 2011.

[159] **Mushtaq, F., Mat, R.** and **Ani, F. N.**, *A review on microwave assisted pyrolysis of coal and biomass for fuel production*, Renewable and Sustainable Energy Reviews, Vol. 39, pp. 555–574, 2014.

[160] **Agarwal, A., Rana, M.** and **Park, J.-H.**, *Advancement in technologies for the depolymerization of lignin*, Fuel Processing Technology, Vol. 181, pp. 115–132, 2018.

[161] **Pan, H., Zheng, Z.** and **Hse, C. Y.**, *Microwave-assisted liquefaction of wood with polyhydric alcohols and its application in preparation of polyurethane (PU) foams*, European Journal of Wood and Wood Products, Vol. 70, No. 4, pp. 461–470, 2012.

[162] **Kunaver, M., Medved, S., Čuk, N., Jasiukaitytė, E., Poljanšek, I.** and **Strnad, T.**, *Application of liquefied wood as a new particle board adhesive system*, Bioresource technology, Vol. 101, No. 4, pp. 1361–1368, 2010.

[163] **INC**, *International Nut&DriedFruit*, 2018, https://www.nutfruit.org/industry/statisticsl - Last checked: 21.12.2018.

[164] **Miarnau, X., Torguet, L., Zazurca, L., Maldonado, M., Girabet, R., Batlle, I.** and **Rovira, M.**, *El futuro del almendro en España: ¿Será posible producir 4.000 kg de grano/ha?*, 2018, https://www.interempresas.net/Horticola/Articulos/223521-El-futuro-del-almendro-en-Espana-Sera-posible-producir-4000-kg-de-grano-ha.html - Last checked: 21.12.2018.

[165] **Pecans, U.**, *History of Pecans*, 2018, https://uspecans.org/history-of-pecans/ - Last checked: 30.12.2018.

[166] **Villarreal-Lozoya, J. E., Lombardini, L.** and **Cisneros-Zevallos, L.**, *Electron-beam irradiation effects on phytochemical constituents and antioxidant capacity of pecan kernels [Carya illinoinensis (Wangenh.) K. Koch] during storage*, Journal of agricultural and food chemistry, Vol. 57, No. 22, pp. 10732–10739, 2009.

[167] **Rosa, J. R., da Silva, I. S. V., de Lima, C. S. M.** and **Pasquini, D.**, *Production of polyols and new biphasic mono-component materials from soy hulls by oxypropylation*, Industrial Crops and Products, Vol. 72, pp. 152–158, 2015.

[168] **Ortiz, E.**, *Histórico da nogueira-pecã no Brasil*, 2016, https://www.divinut.com.br/blog/84/historico-da-nogueira-peca-no-brasil - Last checked: 30.12.2018.

[169] **Raseira, A.**, *A cultura da nogueira peçã (Carya illinoensis).*, Embrapa Clima Temperado-Comunicado Técnico (INFOTECA-E), 1990.

[170] **History, S.**, *Sugarcane History and Facts*, 2015, http://www.sugarhistory.net/sugar-making/sugarcane/ - Last checked: 29.12.2018.

[171] **Conab - Companhia Nacional de Abastecimento**, *Acompanhamento da Safra Brasileira Cana-de-açucar*, 2018, https://www.conab.gov.br - Last checked: 29.12.2018.

[172] **NovaCana**, *Como é feito o processamento da cana-de-açúcar nas usinas*, 2016, https://www.novacana.com/usina/como-e-feito-processamento-cana-de-acucar - Last checked: 01.12.2018.

[173] **Alcarde, A.**, *Árvore do Conhecimento cana-de-açucar*, 2015, http://www.agencia.cnptia.embrapa.br/gestor/cana-de-acucar/arvore/ - Last checked: 30.12.2018.

[174] **Forestry Corporation**, *Radiata pine the remarkable pine*, 2016, https://www.forestrycorporation.com.au/ - Last checked: 29.12.2018.

[175] **Earle, C.**, *The Gymnosperm Database*, 2018, https://www.conifers.org/pi/Pinusradiata.php - Last checked: 27.12.2018.

[176] **Barrón, E., Averyanova, A., Kvaček, Z., Momohara, A., Pigg, K. B., Popova, S., Postigo-Mijarra, J. M., Tiffney, B. H., Utescher, T.** and **Zhou, Z. K.**, *The Fossil History of Quercus*, *Oaks Physiological Ecology. Exploring the Functional Diversity of Genus Quercus L.*, pp. 39–105, Springer, 2017.

[177] **Nixon, K.**, *Global and neotropical distribution and diversity of oak (genus Quercus) and oak forests*, *Ecology and conservation of neotropical montane oak forests*, pp. 3–13, Springer, 2006.

[178] **Mooney, D. E.**, *Examining Possible Driftwood Use in Viking Age Icelandic Boats*, Norwegian Archaeological Review, Vol. 49, No. 2, pp. 156–176, 2016.

[179] **Martínez, J., García, S. O., Bretón, P. R., Cadahía, E.** and **de Simón Bermejo, M. B. F.**, *El roble español: una alternativa para la crianza en barrica de vinos de calidad*, Cuaderno de campo, , No. 37, pp. 35–39, 2007.

[180] **Choowang, R., Lin, J.** and **Zhao, G.**, *Effects of Liquefaction Temperature and Time on Characterization of Liquefied Oil Palm Trunk Residue in the Presence of Polyhydric Alcohols*, 2018.

[181] **Bui, N. Q., Fongarland, P., Rataboul, F., Dartiguelongue, C., Charon, N., Vallée, C.** and **Essayem, N.**, *FTIR as a simple tool to quantify unconverted lignin from chars in biomass liquefaction process: Application to SC ethanol liquefaction of pine wood*, Fuel Processing Technology, Vol. 134, pp. 378–386, 2015.

[182] **Li, Q., Liu, D., Song, L., Hou, X., Wu, C.** and **Yan, Z.**, *Efficient hydro-liquefaction of woody biomass over ionic liquid nickel based catalyst*, Industrial crops and products, Vol. 113, pp. 157–166, 2018.

[183] **Cruz, N., Bustos, C. A., Aguayo, M. G., Cloutier, A.** and **Castillo, R.**, *Impact of the chemical composition of Pinus radiata wood on its physical and mechanical properties following thermo-hygromechanical densification*, BioResources, Vol. 13, No. 2, pp. 2268–2282, 2018.

[184] **Cheng, S., D'cruz, I., Wang, M., Leitch, M.** and **Xu, C.**, *Highly efficient liquefaction of woody biomass in hot-compressed alcohol- water co-solvents*, Energy & Fuels, Vol. 24, No. 9, pp. 4659–4667, 2010.

[185] **Hussin, M. H., Zhang, H. H., Aziz, N. A., Samad, N. A., Faris, A. H., Ibrahim, M. N. M., Iqbal, A., Latip, A. F. A.** and

Haafiz, M. M., *Preparation of environmental friendly phenol-formaldehyde wood adhesive modified with kenaf lignin*, Beni-Suef University journal of basic and applied sciences, Vol. 6, No. 4, pp. 409–418, 2017.

[186] Kobayashi, M., Asano, T., Kajiyama, M. and Tomita, B., *Analysis on residue formation during wood liquefaction with polyhydric alcohol*, Journal of wood science, Vol. 50, No. 5, pp. 407–414, 2004.

[187] Islam, M. N., Beg, M. R. A. and Islam, M. R., *Pyrolytic oil from fixed bed pyrolysis of municipal solid waste and its characterization*, Renewable Energy, Vol. 30, No. 3, pp. 413–420, 2005.

[188] Barnés, M. C., de Visser, M., van Rossum, G., Kersten, S. and Lange, J.-P., *Liquefaction of wood and its model components*, Journal of analytical and applied pyrolysis, Vol. 125, pp. 136–143, 2017.

[189] Azadfar, M., Gao, A. H., Bule, M. V. and Chen, S., *Structural characterization of lignin: A potential source of antioxidants guaiacol and 4-vinylguaiacol*, International journal of biological macromolecules, Vol. 75, pp. 58–66, 2015.

[190] Jin, L., Li, W., Liu, Q., Wang, J., Zhu, Y., Xu, Z., Wei, X. and Zhang, Q., *Liquefaction of kraft lignin over the composite catalyst HTaMoO 6 and Rh/C in dioxane-water system*, Fuel Processing Technology, Vol. 178, pp. 62–70, 2018.

[191] Wang, J., Li, W., Wang, H., Ma, Q., Li, S., Chang, H.-m. and Jameel, H., *Liquefaction of kraft lignin by hydrocracking with simultaneous use of a novel dual acid-base catalyst and a hydrogenation catalyst*, Bioresource technology, Vol. 243, pp. 100–106, 2017.

[192] **Kurimoto, Y., Takeda, M., Koizumi, A., Yamauchi, S., Doi, S.** and **Tamura, Y.**, *Mechanical properties of polyurethane films prepared from liquefied wood with polymeric MDI*, Bioresource technology, Vol. 74, No. 2, pp. 151–157, 2000.

[193] **Luo, X., Hu, S., Zhang, X.** and **Li, Y.**, *Thermochemical conversion of crude glycerol to biopolyols for the production of polyurethane foams*, Bioresource technology, Vol. 139, pp. 323–329, 2013.

[194] **Tohmura, S.-I., Li, G.-Y.** and **Qin, T.-F.**, *Preparation and characterization of wood polyalcohol-based isocyanate adhesives*, Journal of applied polymer science, Vol. 98, No. 2, pp. 791–795, 2005.

[195] **Cinelli, P., Anguillesi, I.** and **Lazzeri, A.**, *Green synthesis of flexible polyurethane foams from liquefied lignin*, European Polymer Journal, Vol. 49, No. 6, pp. 1174–1184, 2013.

[196] **Briones, R., Torres, L., Saravia, Y., Serrano, L.** and **Labidi, J.**, *Liquefied agricultural residues for film elaboration*, Industrial Crops and Products, Vol. 78, pp. 19–28, 2015.

[197] **Esteves, B. M. D. M. L., Cruz-Lopes, L. P. V., Fernandes, A. P., Martins, J. M., Domingos, I. D. J., Ferreira, J. V., Silva, S. H. F.** and **Labidi, J.**, *Adhesives from liquefied eucalypt bark and branches*, Wood Research, Vol. 1, No. 64, pp. 105–116, 2019.

[198] **Ebnesajjad, S.**, *Material Surface Preparation Techniques*, *Handbook of Adhesives and Surface Preparation*, pp. 49–81, Elsevier, 2011.

[199] **Ebnesajjad, S.** and **Landrock, A. H.**, Adhesives technology handbook, William Andrew, 2014.

[200] **Ifju, G.**, *Quantitative wood anatomy certain geometrical-statistical relationships*, Wood and fiber science, Vol. 15, No. 4, pp. 326–337, 2007.

[201] **Carlquist, S.**, Comparative wood anatomy: systematic, ecological, and evolutionary aspects of dicotyledon wood, Springer Science & Business Media, 2013.

[202] **Schoch, W., Heller, I., Schweingruber, F. H.** and **Kienast, F.**, Wood anatomy of central European Species, Swiss Federal Institute for Forest, 2004.

[203] **ASTM D4426**, *Standard Test Method for Determination of Percent Nonvolatile Content of Liquid Phenolic Resins Used for Wood Laminating*, Annual Book of Standards, 2001.

[204] **EN ISO 9397**, *Determination of free-formaldehyde content by the hydroxylamine hydrochloride method*, Annual Book of Standards, 1997.

[205] **International, A.**, *Standard test method for lap shear adhesion for fiber reinforced plastic (FRP) bonding. ASTM D5868*, 2014.

[206] **International, A.**, *Standard test method for Strength properties of adhesives in plywood type construction in shear by tension loading. ASTM D906*, 1998.

[207] **Qiao, W., Li, S., Guo, G., Han, S., Ren, S.** and **Ma, Y.**, *Synthesis and characterization of phenol-formaldehyde resin using enzymatic hydrolysis lignin*, Journal of Industrial and Engineering Chemistry, Vol. 21, pp. 1417–1422, 2015.

[208] **Park, B.-D., Riedl, B., Kim, Y. S.** and **So, W. T.**, *Effect of synthesis parameters on thermal behavior of phenol–*

formaldehyde resol resin, Journal of applied polymer science, Vol. 83, No. 7, pp. 1415–1424, 2002.

[209] **Zhao, M., Jing, J., Zhu, Y., Yang, X., Wang, X.** and **Wang, Z.**, *Preparation and performance of lignin–phenol–formaldehyde adhesives*, International Journal of Adhesion and Adhesives, Vol. 64, pp. 163–167, 2016.

[210] **Lee, W.-J., Chang, K.-C.** and **Tseng, I.-M.**, *Properties of phenol-formaldehyde resins prepared from phenol-liquefied lignin*, Journal of Applied Polymer Science, Vol. 124, No. 6, pp. 4782–4788, 2012.

[211] **Kalami, S., Arefmanesh, M., Master, E.** and **Nejad, M.**, *Replacing 100% of phenol in phenolic adhesive formulations with lignin*, Journal of Applied Polymer Science, Vol. 134, No. 30, pp. 45124, 2017.

[212] **TAPPI T257 cm-85**, *Sampling and preparing wood for analysis*, TAPPI Testing Methods, TAPPI Press, 1985.

[213] **TAPPI T264 cm-97**, *Preparation of wood for chemical analysis*, TAPPI Testing Methods, TAPPI Press, 1997.

[214] **TAPPI T211 om-02**, *Ash in wood, pulp, paper and paperboard: combustion at 525 ºC*, TAPPI Testing Methods, TAPPI Press, 2002.

[215] **TAPPI T204 cm-07**, *Solvent extractives of wood and pulp*, TAPPI Testing Methods, TAPPI Press, 2007.

[216] **TAPPI T222 om-02**, *Acid-insoluble lignin in wood and pulp*, TAPPI Testing Methods, TAPPI Press, 2002.

[217] **Wise, L. E., Murphy, M.** and **D ADIECO, A.**, *A chlorite holocellulose, its fractionation and bearing on summative wood*

analysis and studies on the hemicelluloses, PAPER TRADE JOURNAL, 1946.

[218] **Rowell, R. et al.**, *The chemistry of solid wood.*, American Chemical Society, 1984.

[219] **ASTM D974**, *Standard Test Method for Acid and Base Number by Color-Indicator Titration*, Annual Book of Standards, 2008.

[220] **ASTM D4274**, *Standard Test Method for Testing Polyurethane Raw Materials: Determination of Hydroxyl Numbers of Polyols*, Annual Book of Standards, 2016.

[221] **Herrera, R., Erdocia, X., Llano-Ponte, R.** and **Labidi, J.**, *Characterization of hydrothermally treated wood in relation to changes on its chemical composition and physical properties*, Journal of analytical and Applied Pyrolysis, Vol. 107, pp. 256–266, 2014.

newpage

List of Abbreviations and acronyms

α	Alpha
β	Beta
μg	Micrograms
μL	Microliters
$\overline{M}$n	Average molecular number
$\overline{M}$w	Average molecular weight
$\pm$	More or less
m_f	Final weight of the sample
m_i	Initial weight of the sample
2G	Second generation
%	Percentage
G	Guaiacyl
H	*p*-coumaryl
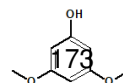
S	Syringil
M	Molarity
N	Newton
AD	Anno Domini
AIL	Acid insoluble lignin
Al	Alagoas
An	Acid number
ANOVA	Analysis of variance
ASL	Acid soluble lignin
ATR	Attenuated Total Reflectance
BC	Before Christ
CA	Catechol-type compound
CCD	Central composite design
DMF	*N,N*-Dimethylformamide
eV	Electrovolt
F	Formaldehyde
Fe	Iron
FFC	Free formaldehyde content
Fig.	Figure
FTIR	Fourier Transform Infrared
G	Glycerol

g	Grams
GC-MS	Gas Chromatography-Mass Spectrometry
GPC	Gel Permeation Chromatography
h	Hour
H_2SO_4	Sulfuric acid
HNO_3	Nitric acid
HPLC	High Performance Liquid Chromatography
K	Potassium
KL	Kraft lignin (precipitated with surfur acid)
KLA	Kraft lignin precipitated with acetic acid
KLC	Liquefied Kraft lignin precipitated with citric acid
KLL	Kraft lignin precipitated with lactic acid
KOH	Potassium hydroxide
kPa	KiloPascal
L	Liter
LAS	Liquefied almond shells
LB	Liquefied bagasse
LHKL	Liquefied hardwood Kraft lignin (precipitated with surfur acid)
LKLA	Liquefied Kraft lignin acetic (precipitated with acetic acid)
LKLAn	Liquefied Kraft lignin with acetic acid as catalyst, n is the acid concentration (precipitated with sulfur acid)

LKLC	Liquefied Kraft lignin citric (precipitated with citric acid)
LKLCn	Liquefied Kraft lignin with citric acid as catalyst, n is the acid concentration (precipitated with sulfur acid)
LKLL	Liquefied Kraft lignin lactic (precipitated with lactic acid)
LKLLn	Liquefied Kraft lignin with lactic cid as catalyst, n is the acid concentration (precipitated with sulfur acid)
LO	Liquefied oak sawdust
LPr	Liquefied pine sawdust
LPS	Liquefied pecan shells
m	Meters
MACL	Moderate acid-catalyzed liquefaction
mg	Milligrams
min	Minutes
mL	Milliliters
mm	Millimeters
mmol	Millimols
ms	Milliseconds
Na	Sodium
Na_2S	Sodium sulfide
NaOH	Sodium hydroxide
nº	Number
OH	Hydroxyl groups

OHn	Hydroxyl number
p	Polyol
Pa.s	Pascal second
PDI	Polydispersity
PEG	Polyethylene glycol 400
PF	phenol-formaldehyde
Ph	Phenol
pH	Potential of hydrogen
PU	polyurethane
Py-GC-MS	Pyrolysis-Gas Chromatography-Mass Spectrometry
RS	Radial section
RSM	Response surface method
s	Seconds
SA	sulfuric acid
Si	Silica
SO_3	Sulfonate group
SP	São Paulo
t	Tons
TAPPI	Technical Association of Pulp and Paper Industries
TGA	Thermogravimetric Analysis
TgS	Transverse section

Tmax$_1$ Temperatura maxima1

Tmax$_2$ Temperatura maxima2

TrS   Tangencial section

US   United States

UV   Ultraviolet

W   Weight

wt%   Weight percent

^{o}C   Degrees Celsius

List of Figures

List of Tables

List of Equations

Appendices

Appendix A

Procedures

A.0.1   Chemical Composition of Raw Materials

The raw materials composition was analyzed following standard methods. Each procedure was performed at least three times to obtain a representative average value of the results. Biomass characterization was reported on a dry weight basis.

A.0.1.1   Sample preparation (TAPPI T257 cm-85)

The raw material characterization was performed with particle size according to TAPPI T257[212].

A.0.1.2   Moisture content (TAPPI T264 cm-97)

TAPPI T264[213] procedure was used to determine the moisture content of the samples and the results were expressed by equação A.1.

$$Moisture\ (\%) = (\frac{m_i - m_f}{m_i}) * 100 \qquad (A.1)$$

where m_i = the initial weight of the sample and m_f = the moisture-free weight of the sample.

A.0.1.3 Determination of inorganic matter (TAPPI T211 om-02)

The composition and amount of ash in the sample may vary depending on source of raw material, treatment, metalic materials, pigments and chemicals used in its manufacture. In addition, it contains inorganic matter such as Na, K, Fe and Si, which are common in the composition of the lignocellulose. The ash content (AC), according to TAPPI T211[214], was expressed (AC% in dry basis) through the equation A.2.

$$Ash\ (\%) = (\frac{m_f}{m_i * (\frac{100-MC}{100})}) * 100 \tag{A.2}$$

A.0.1.4 Solvent extractives (TAPPI T204 cm-07)

This method describes a procedure for determining non-volatile compounds, which mainly consist of low molecular weight carbohydrates, waxes, salts, fats, resins and non-volatile hydrocarbons present in the sample. Although ethanol-benzene is mentioned in TAPPI T204[215] as extraction media, due to its highly hazardous nature, benzene was substituted by toluene. Equation A.3 was used to calculate the solvent extractable fraction (in dry basis) of the sample.

$$Extractives\ (\%) = (\frac{m_i * (\frac{100-MC}{100}) - m_f}{m_i * (\frac{100-MC}{100})}) * 100 \tag{A.3}$$

A.0.1.5   Acid-insoluble lignin (TAPPI T222 om-02)

Acid-insoluble lignin (AIL), also known as Klason lignin, is described by TAPI T222[216] standard was used to determine the AIL of agricultural and forest residues. In this procedure, in 72% sulfuric acid the carbohydrates (cellulose and hemicelluloses) are solubilized and the solid phase is recovered as acid-insoluble lignin (in dry basis and extractive-free) present in the sample (Eq. A.4).

The Kraft lignin samples were subjected to two acid hydrolysis step, the first with 72% H_2SO_4 for 1 h at 30 °C, and the second by diluting the samples in 12% (w/w) H_2SO_4 and autoclaving them for 1h at 121 °C.

$$Acid - insoluble\ lignin\ (\%) = (\frac{m_f}{m_i}) * 100 \tag{A.4}$$

A.0.1.6   Acid-soluble lignin

The filtrate obtained in Section A.0.1.5 was collected for determination of acid-soluble lignin (ASL) fraction by UV spectrophotometry (Appendix B.1.2). The result was expressed by equation A.5

$$LS\ (\%) = (\frac{A * V * df}{a * b * m_i}) \tag{A.5}$$

where *LS* = acid soluble lignin, *A* = absorbance at 205 nm, *V* = the filtrate volume (L), *df* = factor of dilution, *a* = is an averaged absorption coefficient (110 L.g^{-1}.cm^{-1}), *b* = is the width of the curvette (1 cm) and m_i = is the initial weight of the sample (g).

A.0.1.7   Holocellulose content (Wise et al., 1946)

This assay quantified the holocellulose fraction (Eq. A.6) which is the water insoluble carbohydrates fraction and comprises the sum of hemicellulose and cellulose. The holocellulose content (in dry basis and extractives-free) was determined according to the method proposed by Wise and co-workers[217].

$$Holocellulose\ (\%) = (\frac{m_f}{m_i}) * 100 \tag{A.6}$$

A.0.1.8 α-celulose content (Rowell et al., 1983)

Since the TAPPI T203 om-93 ("Determination of α, β and γ cellulose pulp") is defined only for paper pulp, and places special emphasis on it, it was decided to use the procedure referred to as "Rowell method"[218] from the book "The Chemistry of Solid Wood" of 1984, edited by Professor R. Rowell, to determine the content of α-cellulose and hemicelluloses in lignocellulosic tissues. The percentage of α-cellulose is determined as follows (Eq. A.7):

$$\alpha - cellulose\ (\%) = (\frac{m_f}{m_i}) * 100 \tag{A.7}$$

where m_i is the weight initial of moisture and extractives-free holocellulose (g) obtained in A.0.1.7 and m_f is the weight of dry solid residue obtained after filtration (g).

Hemicelluloses are calculated (Eq. A.8) by the difference of initial holocellulose weight (m_i) and obtained α-cellulose weight.

$$Hemicellulose\ (\%) = Holocellulose(\%) - \alpha cellulose(\%) \tag{A.8}$$

A.0.1.9　Carbohydrate content

Sugar content was determined injecting the obtained filtrate from acid-insoluble lignin analysis (Appendix A.0.1.6) into a HPLC equipment (Appendix B.2.2). The result was calculated as follows (Eq. A.9):

$$Sugar\ content\ (\%) = (\frac{A * B}{1000 * C}) * 100 \tag{A.9}$$

where A is the obtained concentration by HPLC (ppm); B is the filtrated volume from acid-insoluble lignin test (L) and C is the initial lignin weight (g)

A.0.2　Polyols

A.0.2.1　Determination of yield of the polyols

$$Yield\ (\%) = [1 - (\frac{m_f}{m_i})] * 100 \tag{A.10}$$

where m_f = is the solid residue of liquefaction (g) and m_i = is the initial feedstock used in the liquefaction (g).

A.0.2.2　Normalize the coded variable

$$X_n = 2 * \frac{X - \overline{X}}{\triangle X} \qquad n = -1, 0, 1 \tag{A.11}$$

where X_n is the coded independent variable, X represents studied non-coded independent variable, $\overline{X}$ represents the value of X at center point and $\triangle X$ represents the step-change value.

A.0.2.3 Acid and base number by titration (ASTM D974)

The acid or base number of the polyols was measured following the standards described in ASTM D974[219], The result is expressed in mg KOH.g^{-1} according the Equation A.12.

$$A_n = \frac{(C - B) * M * 56,1}{W}$$ (A.12)

where An = is the acid number (mg KOH.g^{-1}); B = is the volume of 0.1 M KOH solution in ethanol to titrate the blank (mL); C = is the volume of 0.1 M KOH solution in ethanol to titrated the sample (mL); M = molarity of the 0.1 M KOH solution in ethanol; 56.1 = molecular weight of KOH; and W = amount of sample (g).

A.0.2.4 Determination of hydroxyl number (ASTM D4274)

Polyol hydroxyl number was determined according Test Method C - Phthalic anhydridde reflux, described in the ASTM D4274[220]. The result is expressed in mg KOH.g^{-1} according the Equation A.13

$$I_{OH} = (\frac{(B - A) * N * 56,1}{W}) + An$$ (A.13)

where OHn = is the hydroxyl number (mg KOH.g^{-1}); B = is the volume of 2 M NaOH solution to titrate the blank (mL); A = is the volume of 2 M NaOH solution to titrated the sample (mL); M = molarity of the 2 M NaOH solution; 56.1 = molecular weight of KOH; An = is the acid number (mg KOH.g^{-1}) and W = amount of sample (g).

A.0.3 Phenolic resins

The phenolic resins were characterized following standard methods described in American Society of Testing Material (ASTM) and European standard.

A.0.3.1 Solid content (ASTM D4426)

The nonvolatile content of the resins was carried out according to ASTM D4426[203] as following: 1 g resin was weighted in an aluminum plate (previously dried and weighted) and dried in an oven at 125 °C for 105 min. The result was expressed by equation A.14.

$$Nonvolatile\ matter\ (\%) = (\frac{m_f}{m_i}) * 100 \qquad (A.14)$$

where m_i = the initial weight of the sample and m_f = the moisture-free weight of the sample.

A.0.3.2 Free formaldehyde content (EN ISO 9397)

Free formaldehyde content was determined in accordance to EN ISO 9397[204] such as: an appropriate amount of resin was dissolved in 50 mL isopropanol:water (3:1, v/v) mixture in a beaker. The solution was acidified to pH 3.5 with 1 *M* hydrochloric acid solution, then 25 mL hydroxylamine hydrochloride solution (10 wt%) was added. After 10 min stirring, the solution was titrated rapidly using 0.1 *M* sodium hydroxide solution to pH 3.5. The black test was carried out the same way but without resin. The result was calculate following equation A.15.

$$FFC\ (\%) = 3c(\frac{V_1 - V_0}{m}) \qquad (A.15)$$

where c = is the concentration, in moles per liter, of the solution of sodium hydroxide, V_0 = is the volume, in milliliters, of the solution of sodium hydroxide utilized for the blank test, V_1 = is the volume of the solution of sodium hydroxide utilized for the sample (mL) and m = is the amount of resin (g).

A.0.4   Suplementary information)

Table A.1: Experimental reaction conditions for liquefied Kraft lignin under reflux.

Sample	Time (min)	Mass (wt%)	Catalyst (wt%)	Yield (%)	An (mg.KOH^{-1})	OHn (mg.KOH^{-1})	Viscosity (Pa.s)
1C	80	25	3	93.19	12.65	2354.60	0.386
2C	60	20	0	68.41	10.84	983.09	0.136
3C	60	25	6	79.79	28.30	1280.53	0.644
4C	60	20	3	98.88	23.17	924.97	0.202
5C	80	20	0	78.62	14.77	2314.11	0.260
6C	80	25	0	94.13	50.49	1363.59	0.291
7C	60	15	6	61.97	13.54	733.45	0.271
8C	60	15	0	68.32	18.28	402.43	0.183
9C	80	15	0	81.58	16.63	1827.66	0.190
10C	100	15	0	81.68	6.04	2556.47	0.195
11C	100	20	6	72.43	6.39	902.34	0.688
12C	60	25	3	95.40	12.48	1582.62	0.512
13C	100	20	0	67.78	7.57	904.61	0.237
14C	80	20	6	81.54	37.03	1716.15	0.869
15C	100	25	3	92.10	14.23	1672.99	0.605
16C	100	15	3	98.17	12.42	544.83	0.425
17C	80	15	6	81.67	26.31	1372.81	1.336
18C	80	15	3	97.90	24.25	2399.51	0.444
19C	100	15	6	72.24	44.44	1275.65	0.440
20C	60	25	0	96.70	10.06	1687.97	0.667
21C	80	20	3	97.26	13.95	2351.04	0.618
22C	100	25	0	70.30	11.96	1773.06	0.281
23C	60	15	3	95.70	17.29	2092.55	0.556
24C	60	20	6	95.88	33.35	2173.90	0.791
25C	100	25	6	84.63	15.85	558.74	0.699
26C	80	25	6	94.98	34.00	1550.40	1.845
27C	100	20	3	96.80	14.22	1731.10	0.328

Table A.2: Statistical analysis of the experimental design on the yield of polyols under reflux.

Source	Sum of squares	DI	Mean square	Ratio-F	Value-P
A:Catalyst	18.806	1	18.806	0.25	0.6226
B:Mass	206.769	1	206.769	2.76	0.1148
C:Time	34.541	1	34.54	0.46	0.5061
AA	1633.15	1	1633.15	21.82	0.0002*
AB	13.9784	1	13.9784	0.09	0.6711
AC	2.36972	1	2.36972	0.03	0.8609
BB	12.4135	1	12.4135	0.17	0.6889
BC	216.292	1	216.292	2.89	0.1074
CC	211.922	1	211.922	2.83	0.1107
Total error	1272.54	17	74.8551		
Total (adjusted)	3622.78	26			

* Statistically different (95.0% significance, $p < 0.05$).

$$Yield_{Reflux} = (-60.2864 + 9.30798 * CAT + 1.55701 * MASS + 3.13486 * TIME - 1.83314 * CAT^2$$
$$+ 0.0719528 * CAT * MASS + 0.00740639 * CAT * TIME + 0.0575349 * MASS^2 \quad (A.16)$$
$$- 0.0424551 * MASS * TIME - 0.0148577 * TIME^2)$$

Table A.3: Statistical analysis of the acidic substances on the polyols under reflux.

Source	Sum of squares	Dl	Mean square	Ratio-F	Value-P
A:Catalyst	476.12	1	476.12	3.87	0.0656
B:Mass	6.49113	1	6.49113	0.05	0.8210
C:Time	64.9488	1	64.9488	0.53	0.4772
AA	172.549	1	172.549	1.40	0.2524
AB	118.38	1	118.38	0.96	0.3402
AC	2.18126	1	2.18126	0.02	0.8956
BB	40.289	1	40.289	0.33	0.5745
BC	42.5243	1	42.5243	0.35	0.5642
CC	472.426	1	472.426	3.84	0.0666
Total error	2089.88	17	122.934		
Total (adjusted)	3485.79	26			

Table A.4: Statistical analysis of the hydroxyl number of the polyols under reflux.

Source	Sum of squares	Dl	Mean square	Ratio-F	Value-P
A:Catalyst	281007.0	1	281007.0	0.82	0.3769
B:Mass	21295.9	1	21295.9	0.06	0.8057
C:Time	188.749	1	188.749	0.00	0.9815
AA	651517.0	1	651517.0	1.91	0.1850
AB	76.457	1	76.457	0.00	0.9882
AC	1.08708E6	1	1.08708E6	3.19	0.0922
BB	17523.3	1	17523.3	0.05	0.8234
BC	239372.0	1	239372.0	0.70	0.4139
CC	2.1275E6	1	2.1275E6	6.23	0.0231*
Total error	5.80195E6	17	341291.0		
Total (adjusted)	1.02275E7	26			

* Statistically different (95.0% significance, p<0.05).

$$Viscosity_{Reflux} = -2.9007 - 0.0476324 * CATALYST - 0.121866 * MASS + 0.110614 * TIME$$
$$+ 0.00905601 * CATALYST^2 + 0.00482054 * CATALYST * MASS - 0.00000550833 * CATALYST * TIME \quad (A.17)$$
$$+ 0.00290688 * MASS^2 + 0.0000964525 * MASS * TIME - 0.000697474 * TIME^2$$

Table A.5: Statistical analysis of the viscosity of the polyols under reflux.

Source	Sum of squares	DI	Mean square	Ratio-F	Value-P
A:Catalyst	1.70779	1	1.70779	22.28	0.0002*
B:Mass	0.123806	1	0.123806	1.61	0.2209
C:Time	0.0062399	1	0.0062399	0.08	0.7789
AA	0.0398575	1	0.0398575	0.52	0.4807
AB	0.0627415	1	0.0627415	0.82	0.3783
AC	0.00000131076	1	0.00000131076	0.00	0.9967
BB	0.0316874	1	0.0316874	0.41	0.5289
BC	0.00111637	1	0.001116370	0.01	0.9054
CC	0.467012	1	0.467012	6.09	0.0245*
Total error	1.30336	17	0.0766682		
Total (adjusted)	3.74361	26			

* Statistically different (95.0% significance, $p < 0.05$).

Table A.6: Experimental design of Kraft lignin-based polyol under microwave

Sample	Time (min)	Mass (wt%)	Catalyst (wt%)	Yield (%)	An (mg.KOH^{-1})	OHn (mg.KOH^{-1})	Viscosity (Pa.s)
01	30:00	0	20	63.79	18.64	188.96	0.090
02	5:00	3	15	93.27	33.43	220.15	0.073
03	17:30	0	20	64.94	21.70	424.52	0.061
04	30:00	6	20	81.67	36.33	609.12	0.189
05	30:00	6	15	73.72	59.58	467.13	0.093
06	17:30	3	15	94.82	34.49	1579.22	0.138
07	5:00	6	15	82.08	50.79	1189.87	0.178
08	30:00	0	25	66.61	11.05	671.53	0.087
09	5:00	0	20	84.16	9.39	1152.04	0.055
10	17:30	0	15	68.06	7.71	1401.66	0.116
11	5:00	3	20	95.27	17.83	537.95	0.524
12	5:00	3	25	97.69	27.09	1147.78	0.282
13	17:30	3	20	88.37	24.41	1150.76	0.126
14	5:00	6	25	91.90	16.93	265.60	0.529
15	30:00	0	15	69.97	4.72	333.05	0.070
16	30:00	3	20	95.74	20.37	973.31	0.115
17	5:00	0	25	74.19	15.85	1504.29	0.086
18	17:30	6	15	90.65	37.31	1196.10	0.148
19	17:30	3	25	92.11	15.80	1175.69	0.240
20	30:00	6	25	80.86	45.11	1390.89	0.081
21	17:30	6	25	71.49	37.28	623.58	0.612
22	30:00	3	25	94.22	21.59	1651.24	0.283
23	17:30	0	25	68.80	7.20	1314.84	0.168
24	5:00	0	15	75.75	10.17	1243.33	0.099
25	30:00	3	15	93.41	27.64	1302.71	0.220
26	17:30	6	20	86.03	44.44	1000.42	0.418
27	5:00	6	20	83.99	42.52	1425.13	0.546

$$Yield_{Micro} = 70.719 - 0.717711 * Time + 0.852433 * Mass + 12.8018 * Catalyst + 0.0169778 * Time^2$$

$$- 0.0107867 * Time * Mass + 0.0266889 * Time * Catalyst - 0.0184889 * Mass^2 \qquad \text{(A.18)}$$

$$+ 0.011 * Mass * Catalyst - 1.92062 * Catalyst^2$$

Table A.7: Statistical analysis of the yield of the polyols under microwave.

Source	Sum of squares	DI	Mean square	Ratio-F	Value-P
A:Time	188.892	1	188.892	6.39	0.0217*
B:Mass	0.827756	1	0.827756	0.03	0.8691
C:Catalyst	625.636	1	625.636	21.15	0.0003*
AA	42.2234	1	42.2234	1.43	0.2486
AB	5.45401	1	5.45401	0.18	0.6730
AC	12.02	1	12.02	0.41	0.5323
BB	1.2819	1	1.2819	0.04	0.8376
BC	0.3267	1	0.3267	0.01	0.9175
CC	1792.74	1	1792.74	60.90	0.0001*
Total error	502.913	17	29.5831		
Total (adjusted)	3172.26	26			

* Statistically different (95.0% significance, p<0.05).

Table A.8: Statistical analysis of the acidic substances of the polyols under microwave.

Source	Sum of squares	DI	Mean square	Ratio-F	Value-P
A:Time	45.9841	1	45.9841	0.56	0.4642
B:Mass	229.051	1	229.051	2.79	0.1130
C:Catalyst	3907,28	1	3907,28	47,64	0,0001*
AA	7,51894	1	7,51894	0,09	0,7657
AB	61,246	1	61,246	0,75	0,3995
AC	188,813	1	188,813	2,30	0,1476
BB	34,0023	1	34,0023	0,41	0,5282
BC	394,568	1	394,568	4,81	0,0425*
CC	21,9141	1	21,9141	0,27	0,6119
Total error	1394,26	17	82,0155		
Total (adjusted)	6284,64	26			

* Statistically different (95.0% significance, p<0.05).

$$An_{Micro} = -42.0686 + 0.282711 * Time + 4.87484 * Mass + 9.43148 * Catalyst + 0.00716444 * Time^2$$
$$- 0.0361467 * Time * Mass + 0.105778 * Time * Catalyst - 0.0952222 * Mass^2$$
$$- 0.382278 * Mass * Catalyst + 0.212346 * Catalyst^2$$

(A.19)

Table A.9: Statistical analysis of the hydroxyl groups of the polyols under microwave.

Source	Sum of squares	DI	Mean square	Ratio-F	Value-P
A:Time	103998,0	1	103998,0	0,47	0,5016
B:Mass	65066,7	1	65066,7	0,29	0,5942
C:Catalyst	244,795	1	244,795	0,00	0,9738
AA	257577,0	1	257577,0	1,17	0,2950
AB	217743,0	1	217743,0	0,99	0,3345
AC	438024,0	1	438024,0	1,99	0,1769
BB	224813,0	1	224813,0	1,02	0,3269
BC	98219,7	1	98219,7	0,45	0,5136
CC	119057,0	1	119057,0	0,54	0,4726
Total error	3,7511E6	17	220653,0		
Total (adjusted)	5,27584E6	26			

Table A.10: Statistical analysis of the viscosity of the polyols under microwave.

Source	Sum of squares	DI	Mean square	Ratio-F	Value-P
A:Time	0,0726626	1	0,0726626	5,65	0,0294*
B:Mass	0,0846172	1	0,0846172	6,58	0,0200*
C:Catalyst	0,213582	1	0,213582	16,62	0,0008*
AA	0,0038308	1	0,0038308	0,30	0,5922
AB	0,0191435	1	0,0191435	1,49	0,2389
AC	0,0671498	1	0,0671498	5,22	0,0354*
BB	0,0102431	1	0,0102431	0,80	0,3844
BC	0,0463719	1	0,0463719	3,61	0,0746
CC	0,00264711	1	0,00264711	0,21	0,6557
Total error	0,218478	17	220653,0		
Total (adjusted)	0,738726	26			

* Statistically different (95.0% significance, p<0.05).

$$
Viscosity_{Micro} = -0.838348 + 0.0193427 * Time + 0.0785724 * Mass + 0.00233699 * Catalyst
$$
$$
- 0.000161714 * Time^2 - 0.000639057 * Time * Mass - 0.0019948 * Time * Catalyst - 0.00165272 * Mass^2 \qquad \text{(A.20)}
$$
$$
+ 0.00414424 * Mass * Catalyst - 0.00233382 * Catalyst^2
$$

$$
FFC = 11.0805 + 3.88854 * Formaldehyde + 10.949 * NaOH - 0.653085 * Polyol
$$
$$
- 4.70895 * Formaldehyde^2 + 14.3339 * Formaldehyde * NaOH - 0.0065 * Formaldehyde * Polyol
$$
$$
- 26.0847 * NaOH^2 + 0.283393 * NaOH * Polyol + 0.00347103 * Polyol^2
$$
$$
\text{(A.21)}
$$

Table A.11: ANOVA analysis of SC of resin.

Source	Sum of squares	DI	Mean square	Ratio-*F*	Value-*P*
A:Formaldehyde	33,9503	1	33,9503	2,55	0,3562
B:NaOH	33,0182	1	33,0182	2,48	0,3602
C:Polyol	1,30541	1	1,30541	0,10	0,8068
AA	43,0497	1	43,0497	3,23	0,3231
AB	35,9351	1	35,9351	2,70	0,3481
AC	127,577	1	127,577	2,73	0,1989
BB	36,4007	1	36,4007	156,80	0,3463
BC	22,1801	1	22,1801	1,67	0,4196
CC	22,2955	1	22,2955	1,67	0,4188
Total error	13,31282	1	13,3128		
Total (adjusted)	374,7042	10			

Table A.12: ANOVA analysis of pH of resin.

Source	Sum of squares	DI	Mean square	Ratio-*F*	Value-*P*
A:Formaldehyde	0,112844	1	0,112844	0,63	0,5737
B:NaOH	0,11679	1	0,11679	0,65	0,5683
C:Polyol	0,330183	1	0,330183	1,83	0,4049
AA	0,290195	1	0,290195	1,61	0,4247
AB	0,204191	1	0,204191	1,13	0,4799
AC	0,04	1	0,04	0,22	0,7196
BB	0,329384	1	0,329384	1,83	0,4053
BC	0,38148	1	0,38148	2,12	0,3832
CC	0,882672	1	0,882672	4,90	0,2700
Total error	0,18	1	0,18		
Total (adjusted)	8,71242	10			

Table A.13: ANOVA analysis of FFC of resin.

Source	Sum of squares	DI	Mean square	Ratio-*F*	Value-*P*
A:Formaldehyde	0,20552	1	0,20552	0,20552	0,0790
B:NaOH	0,443593	1	0,443593	138,62	0,0539
C:Polyol	0,527056	1	0,527056	164,70	0,0495*
AA	0,198995	1	0,198995	62,19	0,0803
AB	0,2588	1	0,2588	80,87	0,0705
AC	0,004225	1	0,004225	1,32	0,4559
BB	0,501767	1	0,501767	156,80	0,0507
BC	0,409769	1	0,409769	128,05	0,0561
CC	0,328935	1	0,328935	102,79	0,0626
Total error	0,0032	1	0,0032		
Total (adjusted)	2,73042	10			

* Statistically different (95.0% significance, p<0.05).

$$Viscosity = -12817.3 - 13097.2 * Formaldehyde - 9013.56 * NaOH + 1042.36 * Polyol$$
$$+ 18521.7 * Formaldehyde^2 - 39020.9 * Formaldehyde * NaOH - 307.4 * Formaldehyde * Polyol$$
$$+ 53622.2 * NaOH^2 - 501.016 * NaOH * Polyol - 0.323886 * Polyol^2$$

(A.22)

Table A.14: ANOVA analysis of viscosity of resin.

Source	Sum of squares	DI	Mean square	Ratio-F	Value-P
A:Formaldehyde	2,94459E6	1	2,94459E6	1911,92	0,0146*
B:NaOH	2,11453E6	1	2,11453E6	1372,96	0,0172*
C:Polyol	1980,24	1	1980,24	1,29	0,4601
AA	3,07861E6	1	3,07861E6	1998,93	0,0142*
AB	1,91793E6	1	1,91793E6	1245,31	0,0180*
AC	9,44948E6	1	9,44948E6	6135,53	0,0081*
BB	2,12041E	1	2,12041E	1376,78	0,0172*
BC	1,28075E6	1	1,28075E6	831,59	0,0221*
CC	2864,03	1	2864,03	1,86	0,4028
Total error	1540,12	1	1540,12		
Total (adjusted)	3,22167E7	10			

* Statistically different (95.0% significance, p<0.05).

Appendix B

Instrumental techniques

B.1   Spectroscopic techniques

B.1.1   Infrared Spectroscopy (FTIR)

FTIR spectra was recorded on a Perkin Elmer spectrophotometer equipped with a Universal Attenuated Total Reflectance accessory (ATR) with the angle of incidence at 45º and internal reflection diamond crystal lens. The colected data were set up for 64 scans at 2 mm-s^{-1} in a range from 4000 to 400 cm^{-1} at a resolution of 4 cm^{-1}.

Initially, a background spectrum was collected to subtract from the sample spectrum. In the sequence, few milligrams of sample were analyzed and after scanning, the spectrum was treated with ATR and baseline correction. OriginPro 2017 software was used to normalize the scale of all spectra and to plot the graphs.

B.1.2 Ultraviolet Spectroscopy (UV)

The hydrolysate obtained in Section A.0.1.5 was used to determine the ASL by UV spectroscopy at 205 nm.

B.2 Chromatography techniques

B.2.1 Gel Permeation Chromatography (GPC)

The molecular distribution of the samples was performed using a Jasco Inc. chromatography provided with a LC-Net II/ACD interface equipped with a RI-2031Plus Intelligent refractive index detector. PolarGel-M column (300 mm x 7.5 mm) and PolarGel-M guard (50 mm x 7.5 mm). The column operated at 40 °C and eluted with *N,N*-Dimethylformamide (DMF) with 0.1% of lithium bromide at flow of 0.7 mL/min. The assay was performed with 0.25 mg of lignin sample dissolved in 5 mL of DMF with 0.1% of lithium bromide (mobile phase) and 20 μL of solution were injected. Calibration was made using polystyrene standards, ranging from 200 to 70.000 g.mol^{-1}.

B.2.2 High Performance Liquid Chromatography (HPLC)

An aliquot of the liquid filtrate from acid-insoluble lignin analysis (Appendix A.0.1.5 and A.0.1.6) was used to determine the sugar content of lignins. The degree of purity of lignin was analyzed using a Jasco chromatograph equipped with a LC Net II/ADC with an Aminex$^{®}$ HPX-87H column (BIO-RAD) (300 x 7.8 mm) equiped with a refractive index detector (RI-2031Plus) and a photodiode ar-

ray detector (MD-2018Plus). The column operated at 50 °C and the mobile phase (0.005 M H_2SO_4 prepared with 100% deionized water) pumped at a rate of 0.6 mL/min, the injection volume was 20 μL. High purity standards of D-(+)-glucose, D-(+)-xylose and D-(-)-arabinose were used for calibration. All samples were filtered through 0.22 μL nylon membrane before injection.

B.2.3   Gas Chromatography-Mass Spectrometry (GC-MS)

GC-MS analysis was carried out in split mode (10:1) on Agilent 7890A gas chromatograph coupled to a 5975C mass specrometer using helium as the carrier gas at a flow rate of 1 mL.min^{-1}. Separation was performed using a non-polar HP5-MS fused silica capillary column (30 m x 0.25 mm x 0.25 μm film thickness). Ionization voltage of mass spectrometer in the EI-mode was equal to 70 eV and ionizations source temperature was 250 °C.

The samples (4 g.L^{-1}) were diluted in ethyl acetate or methanol (HPLC grade). The temperature program started at 50 °C, held 2 min, then, the temperature is raised to 120 °C at 10 °C.min^{-1}, held 8 min, raided to 280 °C at 10 °C.min^{-1} and held 8 min. Finally, the temperature was elevated to 300 °C at 10 °C.min^{-1} and held for 10 min.

The identification of the obtained compounds was accomplished using a National Institute of Standards Library version 2.0 Mass Spectral Search Program (Agilent Techn.). Mass spectra and retention time of compounds were compared with available library data and the percentage of peaks was calculated by the area normalization method.

B.2.4   Pyrolysis/Gas Chromatography-Mass Spectrometry (Py/GC-MS)

Volatile compounds of raw materials were characterized by Py/GC-MS using a pyrolyzer (Pyroprobe model 5150, CDS Analytical Inc., Oxford, PA). The identification of the pyrolysis products was performed using a GC-MS instrument (Agilent Techs. Inc. 6890 GC/5973 MDS). The Py/GC-MS was carried out following the method described by Herrera.[221] A quantity between 400-800 mg was pyrolyzed in a quartz boat at 600 °C for 15 s with a heating rate of 20 °C/ms (ramp-off) with the interface kept at 260 °C. The pyrolyzates were purged from the pyrolysis interface into the GC injector under inert conditions using helium gas. The fused-silica capillary column used was an Equity-1701 (30 m x 0.20 mm x 0.25 μm). The GC oven program was held at 50 °C and for 2 min. Then it was raised to 120 °C at 10 °C/min (5 min), after that it was raised to 280 °C at 10 °C/min (8 min) and finally raised to 300 °C at 10 °C/min (10 min). The compounds were identified by comparing their mass spectra with the National Institute of Standards Library (NIST) and with compounds reported in the literature.

B.3   Thermal techniques

B.3.1   Thermogravimetric Analysis (TGA)

Thermal decomposition characteristics of samples were determined by thermogravimetric analysis (TGA) using Mettler Toledo TGA/SDTA 851 analyzer. About 5-10 mg of sample were tested under nitrogen atmosphere (50 mL/min) at a heating rate of 10 °C/min from 25 °C to 800 °C.

B.4   Mechanical characterization techniques

B.4.1   Mechanical tests

MTS Insight 10 equipment provided with pneumatic clamps (Advantage Pneumatic Grips) and with a loading cell of 250 *N* with a spped of 10 mm.min^{-1} mechanically tested elaborated materials.

B.5   Other

B.5.1   Elemental Analysis

The contents of carbon, hydrogen, nitroge and sulfur were analyzed using an EURO EA 3000 series elemental analyzer from EuroVector. The percentage of oxygen was calculated by difference.

B.5.2   Micrometer

A digital micrometer (ULTRA Germany) was used to measuring the dimension of the sample to evaluate some mechanical properties.

B.5.3   Viscosimeter

Viscosity was analyzed using a digital viscosimeter FUNGILAB (ALPHA SERIES). About 6 mL of sample was placed in the portable sample and the viscosity was measured using a suitable rotation rpm.

B.5.4 Rheology

Dynamic rheological behavior of the polyols was measured with a Rhoemetric Scientific Advanced Rheometric Expansion System (ARES), using parallel-plate geometry (25 mm diameter), and the upper plate was set at the separation distance (gap) of 0.5 mm. Frequency sweep measurements were carried out at 25 °C from 0.1 to 500 rad s^{-1} at a fixed strain.

Reagents used

√ 1,4-Dioxane Analytical reagent grade   ($C_4H_8O_2$)   CAS 123-91-1   Mw = 88.11   Fisher Chemical

√ 2-Propanol Analytical reagent grade   (C_3H_8O)   CAS 67-63-0   M = 60.10   d = 0.78 g.cm^{-3} Fisher Chemical

√ Acetic acid glacial, HPLC grade   (CH_3COOH)   CAS 64-19-7   Mw = 60.05   d = 1.05 g.cm^{-3} Scharlau

√ Acetone technical grade ($C_4H_8O_2$) CAS 67-64-1   Mw = 58.08   d = 0.79 g.cm^{-3} Scharlau

√ Citric acid monohydrate, Analytical reagent grade ($C_6H_8O_7.H_2O$)   CAS 5949-29-1   Mw = 210.15   Fisher Chemical

√ Dibutyltin dilaurate (DBTDL)   ($C_{32}H_{64}O_4Sn$)   CAS 77-58-7   Mw = 631.56   d = 1.066   Sigma Aldrich

√ Dimethylformamide (DMF) ⩾ 99.5%, HPLC grade   (C_3H_7NO) CAS 68-12-2   Mw = 73.09   Fischer Chemical

√ Dimethyl Sulfoxide (DMSO), HPLC grade   ($C_2H_6O_5$)   CAS 67-68-5   Mw = 78.13   d = 1.103   Scharlau

√ Ethanol absolute, synthesis grade   (C_2H_5OH)   CAS 64-17-5   Mw = 46.07   d = 0.79   Scharlau

√ Ethyl Acetate ⩾99.5%, HPLC grade   ($C_4H_8O_2$) CAS 141-78-6   Mw = 88.11   Fisher Chemical

√ Formaldehyde 37 - 38% w/w, ACS   (CH_2O)   CAS 50-00-0   Mw = 30.03   d = 1.08   PanReac AppliChem

√ Glycerol 99% for synthesis   ($C_3H_8O_3$)   CAS 56-81-5   Mw = 92.10   d = 1.259   PanReac AppliChem

√ Hydrochloric acid (37%) technical grade   (HCl)   CAS 7647-01-0   M = 36.46   d = 1.19 g.cm^{-3} PanReac AppliChem

√ Hydroxylamin hydrochloride 99%   NH2OH HCl   CAS 5470-1-1   Mw = 69.49   Sigma Aldrich

√ L(+)-Lactic acid, for analysis   ($C_3H_6O_3$)   CAS 79-33-4   Mw = 90.08   d = 1.20   Panreac AppliChem

√ Lithium bromide, PRS   (LiBr)   CAS 7550-35-8   M = 86,85   PanReac AppliChem (Germany)

√ Methanol HPLC grade   (CH$_4$O)   CAS 67-56-1   Mw = 32.04
   Fisher Chemical

√ Phenol crystalline for analysis, ACS   (C$_6$H$_6$O)   CAS 108-95-2
Mw = 94.11   PanReac AppliChem

√ Phthalic Anhydride 98% PS   (C$_8$H$_4$O$_3$)   CAS 85-44-9   Mw =
148.12   ACROS Organics

√ Potassium hydroxide Extra pure (Ph. Eur, BP NF)   (KOH)
CAS 1310-58-3   M = 56.11   Scharlau

√ Poly[(phenyl isocyanate)-co-formaldehyde] (pMDI)
[C$_6$H$_3$(NCO)CH$_2$]$_n$ CAS 9016-87-8   Mn = $\sim$ 340   d = 1.2 Sigma
Aldrich

√ Polyethylene glycol pure pharma grade   HO(C$_2$H$_4$O)$_n$H   CAS
25322-68-3   Mw = 400   d = 1.127   Panreac AppliChem

√ Pyridina Analytical reagent grade   (C$_5$H$_5$N)   CAS 110-86-1
Mw = 79.10   Fisher Chemical

√ Sodium hydroxide pellets for analysis   (NaOH)   CAS 1310-
73-2   M = 40.00   Panreac AppliChem

√ Sulfuric acid 96%, Technical grade   (H$_2$SO$_4$)   CAS 7664-93-9
Mw = 98.08   d = 1.84   PanReac AppliChem

√ Tolueno ⩾ 99% Reagent grade (C$_7$H$_8$)   CAS 108-88-3   Mw = 92.14   Fisher Chemical

The lignocellulosic residue has great potential, due to its structural composition, to be used in several applications. In this thesis, the production of polyols from agroforestry wastes was carried out and used partial replacement of the phenol in resol resin to obtain a greener wood adhesive.